UNIVERSITY OF NOVI SAD
FACULTY OF TECHNICAL SCIENCES
NOVI SAD

Design, Fabrication and Testing of Microfluidic Chips for Biomedical Application

PhD thesis

Candidate:
Sanja Kojić, MSc

Advisor:
Prof. Goran Stojaonvić, PhD

2021, Novi Sad

УНИВЕРЗИТЕТ У НОВОМ САДУ

ФАКУЛТЕТ ТЕХНИЧКИХ НАУКА У НОВОМ САДУ

Реализација и тестирање микрофлуидних чипова за примене у биомедицини

ДОКТОРСКА ДИСЕРТАЦИЈА

Кандидат:
Сања Којић

Ментор:
Проф. др Горан Стојановић

Нови Сад, 2021.

УНИВЕРЗИТЕТ У НОВОМ САДУ **ОБРАЗАЦ – 5а**
НАВЕСТИ НАЗИВ ФАКУЛТЕТА ИЛИ ЦЕНТРА

КЉУЧНА ДОКУМЕНТАЦИЈСКА ИНФОРМАЦИЈА[1]

Врста рада:	Докторска дисертација
Име и презиме аутора:	Сања Којић
Ментор:	Проф. др Горан Стојановић, редовни професор, Универзитет у Новом Саду, Факултет техничких наука
Наслов рада:	Реализација и тестирање микрофлуидних чипова за примене у биомедицини
Језик публикације (писмо):	Енглески језик
Физички опис рада:	Страница - 122 Поглавља - 8 Референци - 155 Табела - 11 Слика - 87
Научна област:	Електротехничко и рачунарско инжењерство
Ужа научна област:	Електроника
Кључне речи / предметна одредница:	микрофлуидика, чипови, фабрикациона технологија, микромиксер
Резиме на српском језику:	Микрофлуидика представља науку и технологију. Научни аспекат се бави понашањем флуида у каналима реда микрометра јер се понашање флуида на микроскали драстично разликује у односу на макроскалу. Технолошки аспекат се бави производњом и минијатуризацијом уређаја, који се састоје од микроканала или чак наноканала. За разлику од минијатуризације интегрисаних кола и микроелектромеханичких уређаја, код којих се цео уређај скалира, за микрофлуидику важно је само скалирање простора кроз који се флуид креће. Осетљивост уређаја је одређена најмањом количином микрофлуида који се може користити. Фабрикација микрофлуидних уређаја још је далеко од масовне производње за којом већ постоји потреба. Актуелне технологије фабрикације су прилагођене лабораторијским прототиповима или имају незадовољавајуће карактеристике за биомедицинску примену. Развој нове технологије која може да помири масовну производњу и биомедицинску компатибилност представља главну нит ове тезе. Примена микрофлуидних уређаја у биомедицини са акцентом на испитивање материјала као и персонализацију и прецизно дозирање терапије једна је од најактуелнијих тема данашњице. Код прецизног дозирања једну од важнијих улога игра микро мешач односно

[1] Аутор докторске дисертације потписао је и приложио следеће Обрасце:
5б – Изјава о ауторству;
5в – Изјава о истоветности штампане и електронске верзије и о личним подацима;
5г – Изјава о коришћењу.
Ове Изјаве се чувају на факултету у штампаном и електронском облику и не кориче се са тезом.

	микромиксер, јер од његове прецизности зависи прецизност и агилност читавог система. Конструкција микро мешача је актуелна тема у данашњим истраживачким лабораторијама.
Датум прихватања теме од стране надлежног већа:	27.06.2019.
Датум одбране: (Попуњава одговарајућа служба)	
Чланови комисије: (титула, име, презиме, звање, институција)	Председник: **проф. др Момир Миков**, редовни професор, Универзитет у Новом Саду, Медицински факултет Нови Сад Члан: **проф. др Бојан Петровић**, ванредни професор, Универзитет у Новом Саду, Медицински факултет Нови Сад Члан: **проф. др Зоран Прijић**, редовни професор, Универзитет у Нишу, Електронски факултет Члан: **др Милан Радовановић**, научни сарадник, Универзитет у Новом Саду, Факултет техничких наука Члан, ментор: **проф. др Горан Стојановић**, редовни професор, Универзитет у Новом Саду, Факултет техничких наука
Напомена:	

UNIVERSITY OF NOVI SAD
FACULTY OR CENTER

KEY WORD DOCUMENTATION[2]

Document type:	Doctoral dissertation
Author:	Sanja Kojić
Supervisor:	Prof. Dr Goran Stojanović, Full Professor, University of Novi Sad, Faculty of Technical Sciences
Thesis title:	Design, Fabrication and Testing of Microfluidic Chips for Biomedical Applications
Language of text:	English language
Physical description:	Pages - 122 Chapters - 8 References - 155 Tables - 11 Illustrations - 87
Scientific field:	Electrical and computer engineering
Scientific subfield:	Electronics
Subject, Key words:	microfluidics, chip, fabrication technology, micromixer
Abstract in English language:	Microfluidics is a science and technology. The scientific aspect deals with the behaviour of fluids in the channels of the micrometre order because the behaviour of fluids on the microscale differs drastically in relation to the macroscale. The technological aspect deals with the production and miniaturization of devices, which consist of microchannels or even nanochannels. Unlike the miniaturization of integrated circuits and microelectromechanical devices, in which the whole device is scaled, for microfluidics only the scaling of the space through which the fluid moves are important. The sensitivity of the device is determined by the minimum amount of microfluid that can be used. The fabrication of microfluidic devices is still far from mass production for which there is already a need. Current fabrication technologies are concentrated on the production of laboratory prototypes or have unsatisfactory characteristics for biomedical applications. The development of new technology that can reconcile mass production and biomedical compatibility is the main thread of this thesis. The use of microfluidic devices in biomedicine with an emphasis on material testing as well as personalization and precise dosing of therapy is one of the hot topics today. In precision dosing, one of the most important roles is played by the mixer or micromixer, because the precision and agility of the entire system depend on its precision. The construction of micromixers is a current topic in today's research laboratories.
Accepted on Scientific Board on:	27.06.2019.

[2] The author of doctoral dissertation has signed the following Statements:
5б – Statement on the authority,
5в – Statement that the printed and e-version of doctoral dissertation are identical and about personal data,
5г – Statement on copyright licenses.
The paper and e-versions of Statements are held at he faculty and are not included into the printed thesis.

Defended: (Filled by the faculty service)	
Thesis Defend Board:	President: Prof. Dr Momir Mikov, Full professor, University of Novi Sad, Faculty of Medicine Member: Prof. Dr Bojan Petrović, Associate professor, University of Novi Sad, Faculty of Medicine Member: Prof. Dr Zoran Prijić, Full professor, University of Niš, Faculty of Electronic Engineering Member: Dr Milan Radovanović, Full professor, University of Novi Sad, Faculty of Technical Sciences Member, Mentor: Prof. Dr Goran Stojanović, Full professor, University of Novi Sad, Faculty of Technical Sciences
Note:	

Zahvalnica

Doktorske studije su put koji se prelazi radoznalo, polako i pažljivo. Put na kome se uči i nauči mnogo više od onoga što na kraju ostane zapisano u doktorskoj disertaciji. Tako ova disertacija sadrži oko trećinu rezultata i zapažanja koja su pribavljena tokom trajanja doktorskih studija. Naravno u njoj nisu zapisane ni „životne" mudrosti naučene za to vreme.

Svega ovoga ne bi ni bilo da nije bilo mog mentora prof. dr Gorana Stojanovića koji me je još, sada davno, primio u svoju istraživačku grupu i otkrio za mene jedan sasvim novi svet. Svet istraživanja za koji nisam ranije ni pretpostavljala da će postati moj svet, mesto gde se osećam kao kod kuće. Hvala Vam za sve što ste, na ovom putu, učinili za mene.

Zahvaljujem se svim članovima komisije, bez kojih ovaj rad ne bi bio ono što sada jeste. Izdvojiću prof. dr Bojana Petrovića koji je uvek bio tu da na tom truckavom putu pruži podršku i pomoć.

Ideja o formiranju nove fabrikacione tehnologije nastala je u jednoj kancelariji u ulici dr Zorana Đinđića 1, jednog sasvim običnog dana kroz jedan sasvim običan razgovor. Ne, nije to bio običan razgovor, kada imate takvog kolegu, Vasu Radonjića. Vaso, da nije bilo tebe ova tehnologija možda nikada ne bi nastala. Ovoj doktorskoj tezi ti si bio pravi komentor. Nešto kasnije sam shvatila da ta kancelarija nikad nije bila nešto obično, već uvek, nešto izvanredno. Svaki dan proveden u njoj bio je inspirisan i nadahnut pravim istraživačkim duhom, onom dečijom radoznalošću koja vam brani da u 16h odete kući i kažete posao je gotov, već sa kolegama ostanete da čekate rezultate merenja, ne zato što je nešto hitno već zato što vi ne možete da dočekate rezultate. Poštovani V. C. i V. B. hvala vam što ste dopustili da budem tu.

Dragi prijatelji, hvala vam na podršci. Bojane, Sanja, Peđa, Tijana, Slobo, Bojana, Jovo, Jovana, Gorane, Ivana, Marko, Milane, Pal, Lazare i Zorane hvala vam što ste učinili da ne pokleknem, da izdržim i uspem.

Najveća zahvalnost ipak pripada mojoj porodici – majci Ljiljani, ocu Predragu, svekrvi Violeti, kumovima Verici i Jovanu, ali pre svega suprugu Aleksandru i ćerki Anđeli.

Doktorsku disertaciju posvećujem Anđeli - bez tebe sve ovo ne bi vredelo.

Prošireni izvod na srpskom jeziku

„Realizacija i testiranje mikrofluidnih čipova za primene u biomedicini“

Uvod

Mikrofluidika predstavlja nauku i tehnologiju. Naučni aspekat se bavi ponašanjem fluida u kanalima reda mikrometra jer se ponašanje fluida na mikroskali se drastično razlikuje u odnosu na makroskalu. Tehnološki aspekat se bavi proizvodnjom i minijaturizacijom uređaja, koji se sastoje od mikrokanala ili čak nanokanala. Za razliku od minijaturizacije integrisanih kola i mikroelektromehaničkih uređaja, kod kojih se ceo uređaj skalira, za mikrofluidiku važno je samo skaliranje prostora kroz koji se fluid kreće. Zarad sticanja osećaja o dimenzijama o kojima se ovde govori na slici 1 predstavljena je merna skala i na njoj su obeležene karakteristične dimenzije mikrofluidnih uređaja upoređene sa dimenzijama u svakodnevnoj upotrebi.

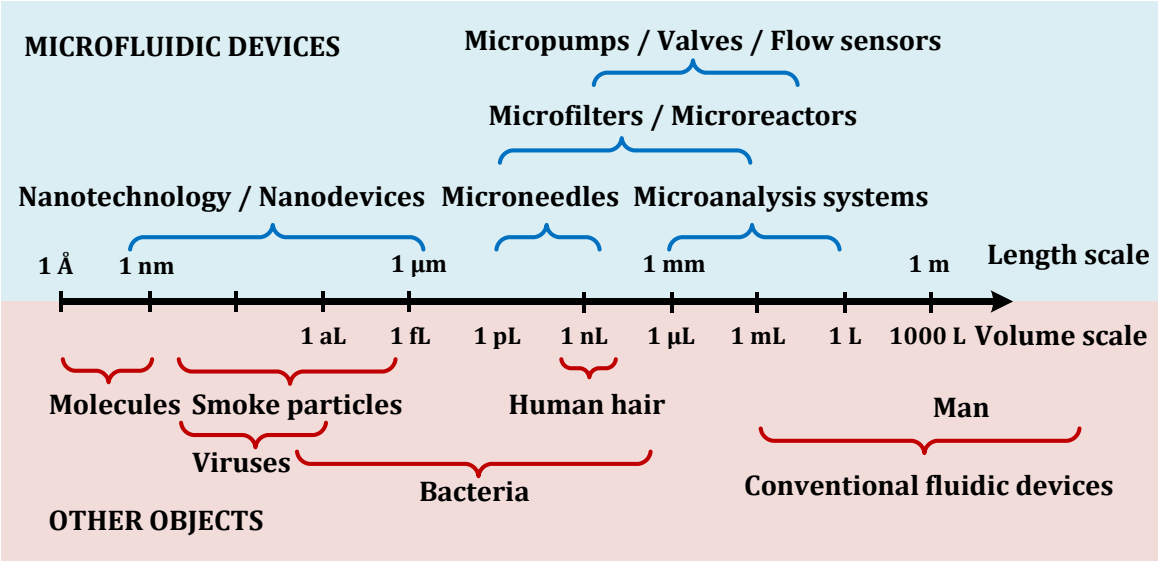

Slika 1 Karakteristične dimenzije mikrofluidnih uređaja upoređene sa dimenzijama u svakodnevnoj upotrebi

Osetljivost uređaja je određena najmanjom količinom mikrofluida koji se može koristiti. Mikrofluidni čip predstavlja set mikrokanala koji su izliveni, utisnuti ili ugravirani u materijale kao što su staklo, silicijum ili polimer – najčešće PDMS (polidimetilsiloksan). Mikrokanali su povezani unutar čipa i obezbeđuju jednu ili više željenih funkcionalnosti – mešanje, filtraciju, sortiranje, separaciju, kontorlu biohemijske okoline, itd. Povezanost sa makro okruženjem odvija se kroz otvore na čipu koji se nazivaju ulazima i izlazima. Tečnost se u čip može unositi aktivno ili pasivno. U slučaju aktivnog unosa tečnosti potrebni su nam eksterni uređaji kao kontrolor pritiska ili špric pumpa, dok se pasivan unos tečnosti odvija uz pomoć

hidrostatičkog pritiska odnosno kapilarnih sila. Raznolikost mikrofluidnih čipova prikazana je na slici 2.

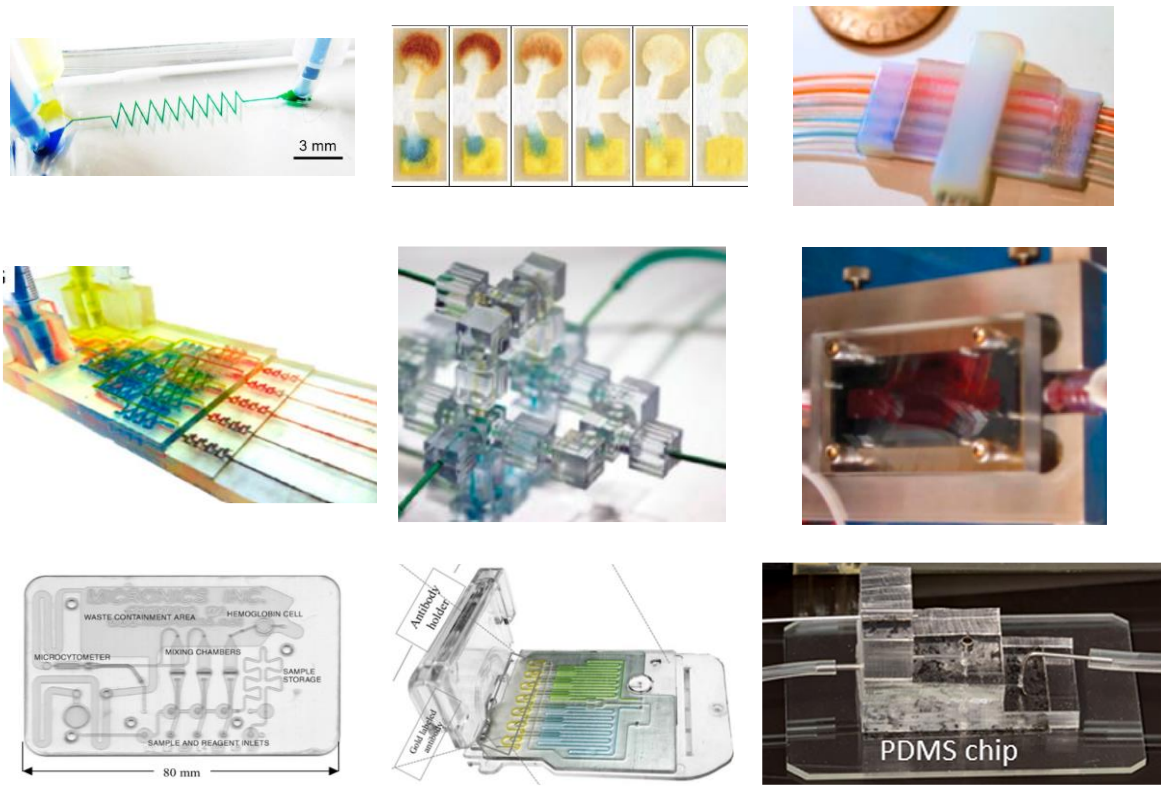

Slika 2 Raznolikost mikrofluidnih uređaja

Mikrofluidni čipovi mogu biti korišćeni kao simulacija okruženja. Ovo je odličan mehanizam za pojednostavljenje tranzicije eksperimenata koji su *in vitro* u eksperimente koji su *in vivo*. Osnovne komponente mikrofluidnih čipova su: mikrokanal, mikromešač, mikrokomore, mikropumpe i mikroventili.

Fabrikacija mikrofluidnih uređaja još je daleko od masovne proizvodnje za kojom već postoji potreba. Aktuelne tehnologije fabrikacije su prilagođene laboratorijskim prototipovima ili imaju nezadovoljavajuće karakteristike za biomedicinsku primenu. Razvoj nove tehnologije koja može da pomiri masovnu proizvodnju i biomedicinsku kompatibilnost predstavlja glavnu nit ove teze. Primena mikrofluidnih uređaja u biomedicini sa akcentom na ispitivanje materijala kao i personalizaciju i precizno doziranje terapije jedna je od najaktuelnijih tema današnjice. Kod preciznog doziranja jednu od važnijih uloga igra mikro mešač odnosno mikromešač, jer od njegove preciznosti zavisi preciznost i agilnost čitavog sistema. Konstrukcija mikro mešača je aktuelna tema u današnjim istraživačkim laboratorijama.

Dizajn

Dizajni karakterizaciju SAVA fabrikacione tehnologije predstavljeni su na slici 3(a), (b),(d) i (f) dok je na slici 3(c) i (e) predstavljen dizajn za fabrikaciju u PVC tehnologiji.

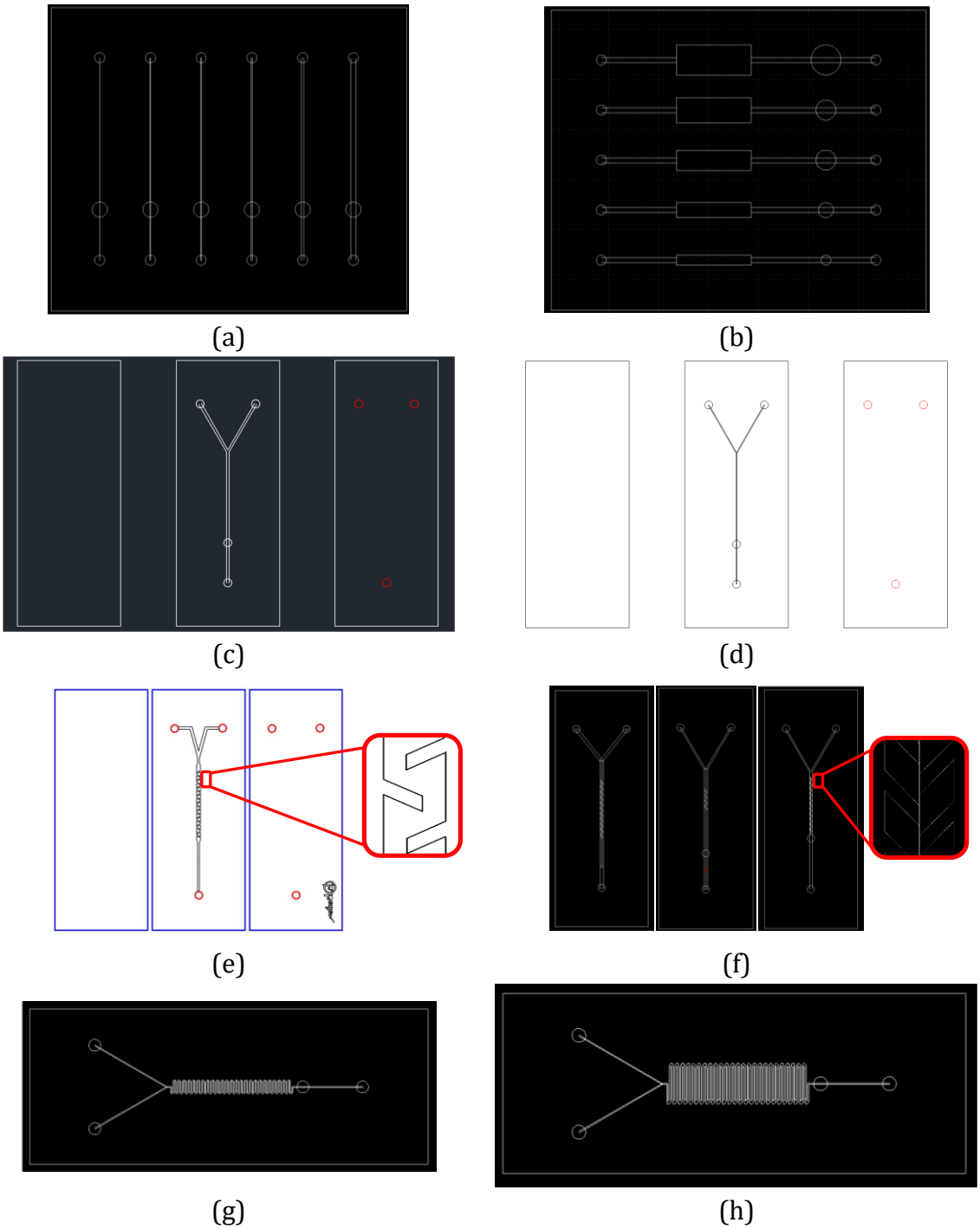

Slika 3 Dizajn čipova za fabrikaciju u PVC i SAVA tehnologiji

Kako je glavni element svakog mikrofluidnog čipa mikrofluidni kanal za karakterizaciju SAVA čipova smo napravili dizajn koji sadrži 6 kanala, svaki sa posebnim ulazom i izlazom i različite širine (50 μm – što je bila minimalna moguća dimenzija koju dozvoljava laser, 100 μm, 200 μm, 300 μm, 500 μm and 1000 μm). Svi kanali su bili funkcionalni. Uz kanale, najčešći element mikrofluidnog čipa su komore. Zato smo dizajnirali čip koji ima dve vrste komora – kružnu i pravougaonu i to u svaku vrstu u pet različitih veličina. Kružne imaju prečnike od 2 mm, 3 mm, 4 mm, 5 mm i 6 mm dok pravougaone imaju dužinu od 15 mm i širine od 2 mm, 3 mm, 4 mm, 5 mm i 6 mm.

Napravljen je i dizajn mikrofluidni čipovi sa Y kanalom bez prepreka u kojem je ugao ulaznih kalana 60° a širina kanala 800 μm - 1000 μm za PVC čipove dok je širina kanala 200 μm za SAVA čipove. Takođe su napravljeni i dizajni za mikromešače sa paralelogramskim barijerama za PVC i SAVA tehnologiju.

Inovativni dizajn sa polukružnim barijerama prikazan je na slici 4. Zbog svoje kompleksnosti (slobodnostojećih polukružnih barijera) ovaj dizajn je pogodan samo za fabrikaciju u PDMS tehnologiji, bar prema trenutnom statusu i mogućnostima koje ostale ovde predložene tehnologije imaju. U dizajnu možemo razlikovati 10 blokova, svaki sa po 5 polukružnih barijera postavljenih od konsekutivno od ulaza do izlaza. Fabrikovana struktura imala je ukupnu dužinu od 6 mm, širinu kanala sa barijerama od 2 mm dok je prečnik polukruga iznosio 0.5 mm.

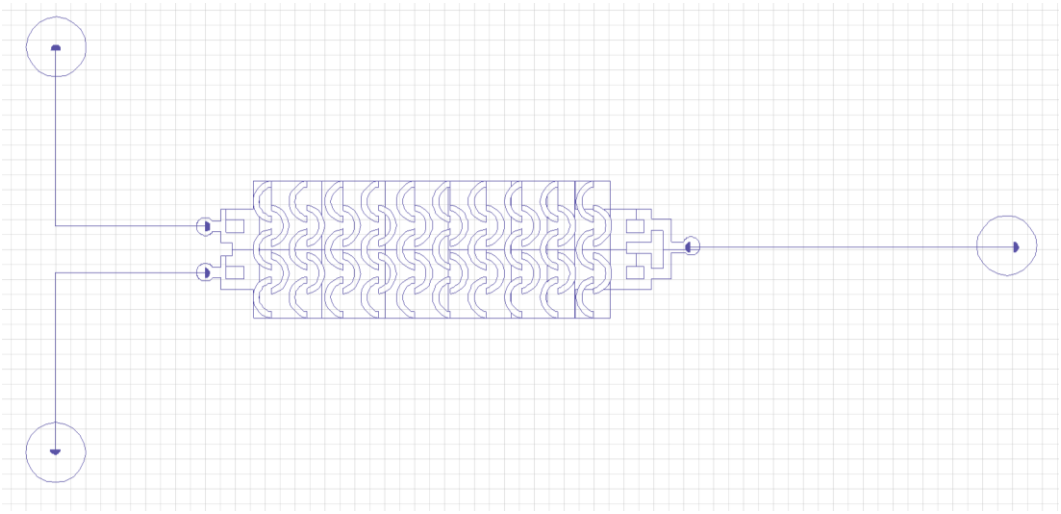

Na slici 3(g) i (h) prikazan je dizajn Y kanala sa serpentinom u dve varijante sa kratkom i dugom serpentinom.

Simulacija

Sve simulacije mikrofluidnih tokova u čipovima urađene su u programskom paketu Comsol Multiphysics®. Ovaj simulator odabran je zbog mogućnosti kombinacije fizičkih modela koji sami mogu biti definisani i zbog mogućnosti da izvrši simulacije bez dubokog ulazka u matematički model i računanje.

Za potrebe optimizacije dizajna mikromešača sa paralelogramskim barijerama za PVC tehnologiju simulirane su varijacije sa promenom broja barijera (5, 7 i 10 parova barijera) što je prikazano na slici 4.

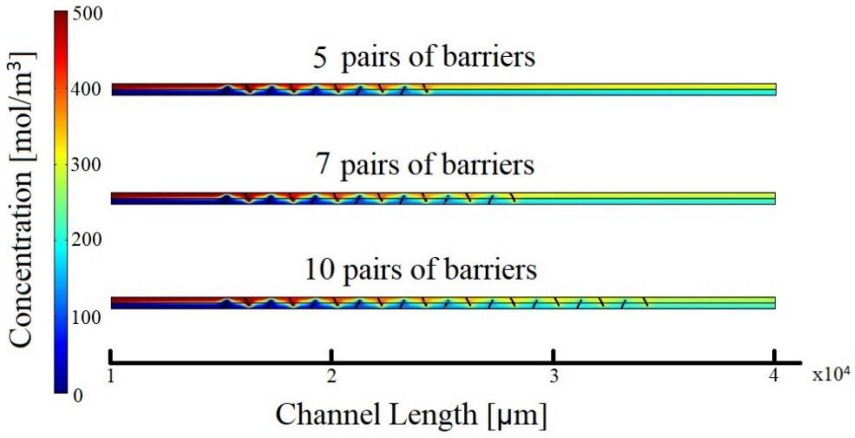

Slika 4 Comsol® simulacija broja paralelogramskih barijera

Za mikromešač inovativnog dizajna sa polukružnim barijerama urađene su simulacije u cilju optimizacije veličine polukružnih barijera što prikazuje slika 5.

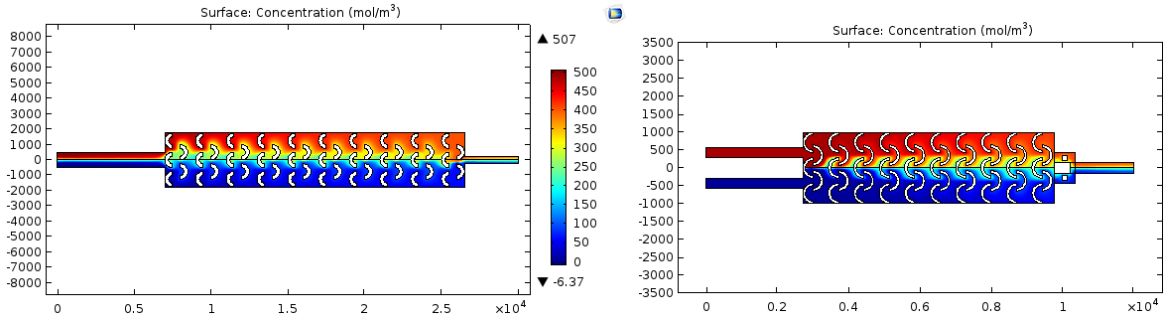

Slika 5 Simulacije dizajna sa cirkularnim barijerama.

Simulacije za mikromešača u SAVA tehnologiji su takođe izvedene. Simulirana je širina i ugao paralelogramskih barijera kao i razmak između istih. Osim prethodno

navedenog simuliran je i broj paralelogramskih barijera potreban za efikasno mešanje u zavisnosti od protoka. Zavisnost je prikazana na slici 6.

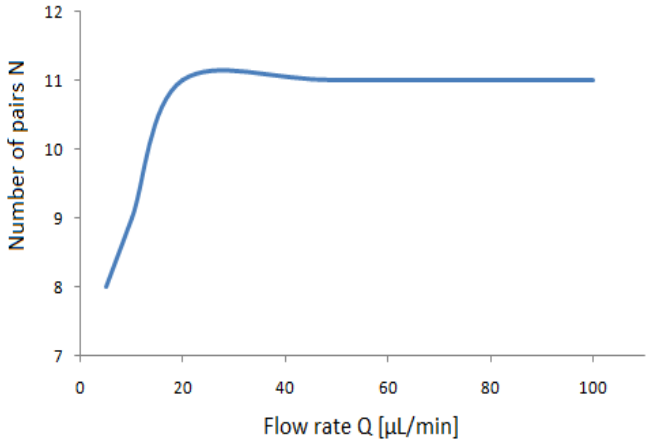

Slika 6 Uticaj protoka na optimalan broja pariva paralelogramskih barijera

Zatim je simuliran različiti protok. Naime, na ulaze u čip koji ima jednostavan Y dizajn i dimenzije koje odgovaraju fabrikaciji u SAVA tehnologiji, dovođene su tri vrste signala pritiska. Signali sinusoidalnog, pravougaonog i trougaonog oblika. Svaki od njih testiran je za tri nivoa amplitude. Na slici 7 prikazana je prikaz razlike između kontinualnog signala i sinusnog tipa signala pritiska prikazana na izlasku iz čipa. Dok slika 8 prikazuje detaljn prikaz razlika za sva tri tipa signala pri amplitudama pritiska od 10 mbar, 50 mbar i 100 mbara. Uočava se da pravougaoni signal daje najbolje mešanje

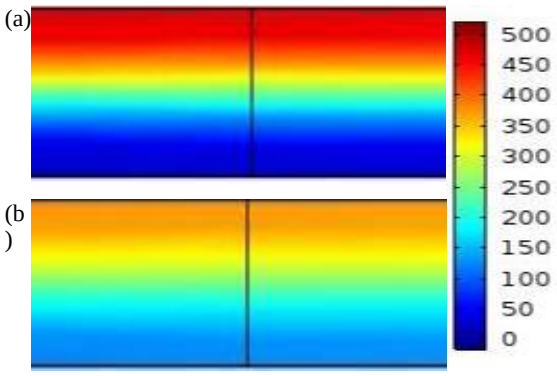

Slika 7 Prikaz razlike u kanalu

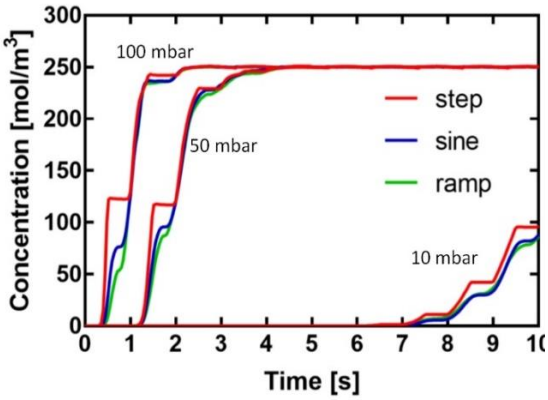

Slika 8 Prikaz svih razlika

Fabrikacija

Tri različita procesa fabrikacije korišćena su za pravljenje mikrofluidnih čipova korišćenih u ovoj tezi. To su izlivanje PDMSa iz kalupa, ksurografija i SAVA tehnologija.

Proizvodnja PDMS čipova zahtevala je skupe hemikalije i fabrikaciona postrojenja dok je PVC fabrikacija bila sa izrazito malim troškovima, bilo za materijal bilo za korišćenu opremu i laboratorijske uslove. Posledice ovih inicijalnih razlika su da su PDMS čipovi imali veliku preciznost izrade i veliku uspešnost u proizvodnji (95 % čipovaje uspešno napravljeno)* dok su PVC čipovi mnogo manje precizni i sa niskom stopom uspešnosti fabrikacije (manje od 10 % čipova je uspešno napravljeno)*.

Čipovi napravljeni u PDMS tehnologiji pratili su standardni protokol: mešalje PDMSa i očvršćivača u odnosu 10:1, izvučeni su mehurići vazduha, izliven je u kalup i pečen na 80 °C tokom 2 sata. Zatim je skinut sa kalupa isečen, izbušeni su otvori za ulaze i izlaz. PDMS i laboratorijsko staklo tretirani su plazmom i čip je spojen.

Čipovi proizvedeni u ksurografiji koristili su dva koraka, prvo je izvedeno sečenje svih slojeva, a zatim laminiranje istih tako što se u svakoj laminaciji dodaje po jedan sloj. Za sečenje i lanimiranje korišćeni su parametri iz tabele 1.

Tabela 1 Vrednosti parametara za sečenje i laminiranje

KORAK#1: Sečenje na ploteru

Parametar	**Vrednost**	**Komentar**
Brzina sečenja – ulaz/izlaz	30 [cm/s]	iz opsega: 1 – 60 [cm/s]
Brzina sečenja –konture	60 [cm/s]	iz opsega: 1 – 60 [cm/s]
Brzina sečenja – kanal	1 – 10 [cm/s]	iz opsega: 1 – 60 [cm/s]
Sila sečenja – 80 µm PVC	19	iz opsega: 1 – 38†
Sila sečenja – 125 µm PVC	26	iz opsega: 1 – 38*

KORAK#2: Laminacija

Parametar	**Vrednost**	**Komentar**
Temperatura	120 °C – 180 °C	150 °C ako nije drugačije naznačeno
Brzina	10 cm/min	iz opsega: 10 cm/min – 90 cm/min

* Proračun napravljen na osnovu svih pokušaja pravljenja čipova u okviru ove teze
† Sila sečenja je u opsegu od 0.2 N do 4.41 N (20 to 450 gf) kroz 38 koraka

Proizvodnja čipova u SAVA tehnologiji odvija se kroz 3 koraka. Prvi je sečenje keramičke trake laserom dok su drugi i treći su sečenje PVC slojeva i laminacija kao i u ksurografiji. Parametri fabrikacije za drugi i treći korak su isti kao u tabeli 1 a parametri prvog koraka dati su u tabeli 2.

Table 4.1 Hybrid fabrication technology parameters

KORAK#1a: Lasersko sečenje – bela keramička traka (debljina - 200 µm)		
Parametar	**Vrednost**	**Jedinica**
Struja	28	A
Frekvencija	10	kHz
Brzina	15	mm/s
Broj prolaza	1	Nije primenljivo
KORAK#1a: Lasersko sečenje – plava keramička traka (debljina - 300 µm)		
Parametar	**Vrednost**	**Jedinica**
Struja	28.6	A
Frekvencija	10	kHz
Brzina	30	mm/s
Broj prolaza	2	Nije primenljivo

Po jedan predstavnik fabrikovanih čipova u svakoj tehnologiji prikazan je na slici 9.

(a) (b) (c)

Slika 9 (a) PDMS čip, (b) PVC čip, (c) SAVA čip

Karakterizacija – rezultati i diskusija

Optička transmitansa mikrofluidnog čipa merena je u opsegu talasnih dužina od 300 nm do 1000 nm. Testirane su 4 različite konfiguracije – SAVA čipovi koji su imali jednu ili dve (sa svake strane keramičke trake po jednu) PVC foliju u dve debljine 80 μm i 125 μm. Na slici 10 prikazana je optička transmisija kao funkcija talasne dužine za sve četiri konfiguracije. Može se videti da je transmitansa veća od 80 % i da ima male varijacije iznad talasne dužine od 340 nm.

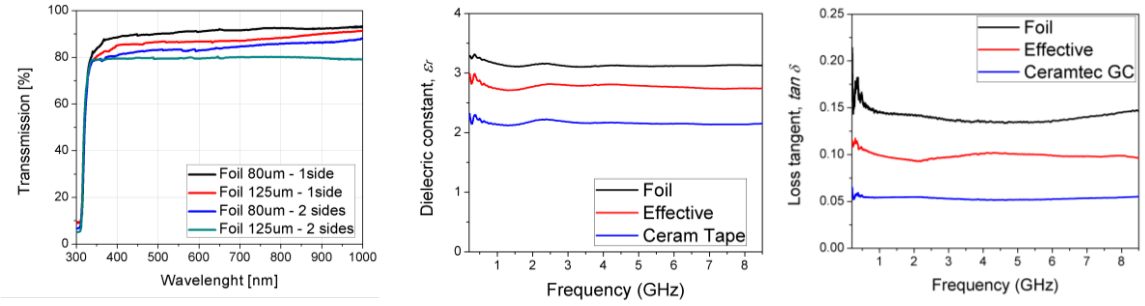

(a) (b) (c)

Slika 10 (a) Optička transmisija. Ekstrahovana vrednost: (b) efektivne permitivnosti, (c) tan δ.

Efektivna permitivnost konfiguracije predložene strukture, definisana je pomoću metoda promene faze – gde merenje faznog kašnjenja sinusoidalnog signala koji se prostire duž talasne linije. U ovu svrhu konstruisan je čip koji ima srednji sloj od keramičke trake, sa obe strane laminiran po jedan sloj PVC folije i zatim postavljene provodne linije od samolepljive aluminijumske trake preko PVC sloja. Napravljene su dve različite dužine linija i korišćene su dve debljine folije (80 μm i 125 μm). Poređenjem ovih konfiguracija izračunata je efektivna permitivnost kombinacije nehomogenih dielektričnih supstrata korišćenjem jednačine za efektivnu dielektričnu perimtivnost višeslojnih supstrata. Faza i amplituda mikrostrip linije određene su uređajem Agilent VNA E5071C u frekvensijskom opsegu od 500 MHz do 8.5 GHz. Slika 10(b) prikazuje egzaktne vrednosti efektivne permitivnosti višeslojne strukture i vrednosti pojedinačnih materijala. Dielektrični gubici su izračunati na amplitudi propagacionog signala i prikazani na slici 11(c).

SEM i optičkom profilometrijom proverena je funkcionalnost mikrofluidnih kanala i komora čipova proizvedenih u SAVA tehnologiji. Napravljena su četiri čipa po dva posebna dizajna za ove karakterizacije i svaki sa dve različite debljine folije (80 μm i 125 μm). Jedan sa kanalima širine 50 μm, 100 μm, 200 μm, 300 μm, 500 μm and 1000 μm a drugi sa komorama kružnog (prečnika 1 mm, 2 mm, 3 mm, 4 mm, i 5 mm) i pravougaonog oblika (širina 1 mm, 2 mm, 3 mm, 4 mm, i 5 mm i dužine 15mm) dok je širina kanala bila 200 μm. Slika 11 prikazuje SME mikrografove ivica kanala i optički

profil kanala u keramičkoj traci. Svaki kanal imao je poseban ulaz i izlaz. Svi kanali su funkcionalni dok su kružne komore bile nedeformisane za prečnike od 4 mm i manje, pravougaona komora za čip sa 80 μm PVC folijom za širine komore manje od 2 mm a sa 125 μm PVC folijama za širine komore od 2mm i manje.

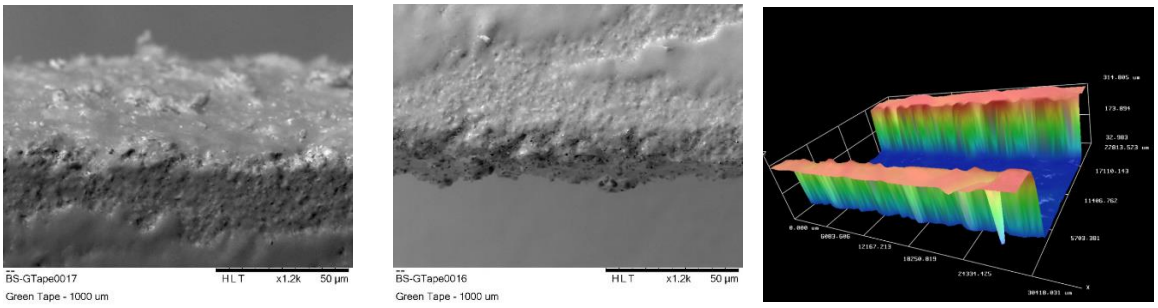

(a) (b) (c)

Slika 11 SEM mikrograf (a) leve i (b) desne ivice i (c) profil kanala keramičke trake

Mehaničkom karakterizacijom SAVA čipova utvrđeni su mehanički parametri nepečene keramičke trake, kojih nije bilo u literaturi, jer ona do sada nikada nije korišćena nesinterovana. Upoređene su karakteristike materijala - PDMS, PVC i keramičke trake i zaključeno je da kombinacija PVC i keramičkih slojeva ima zadovoljavajuće mehaničke performanse. Za svrhu mehaničkih testiranja napravljeno je 6 protokola nanoutiskivanja (nanoindentacije) i urađena su merenja u 300 hiljada mernih tačaka.

Krive koje prikazuju zavisnost dubine indentacije od opterećenja korišćene su za interpretaciju i komparaciju ponašanja ispitivanih materijala. Slika 12 prikazuje usrednjene krive za 100 mernih tačaka na kojima se vidi da je varijacija parametara između PVC folija različite debljine neznatna, dok promena nastala izlaganjem temperaturi usled laminacije menja parametre PVC folije.

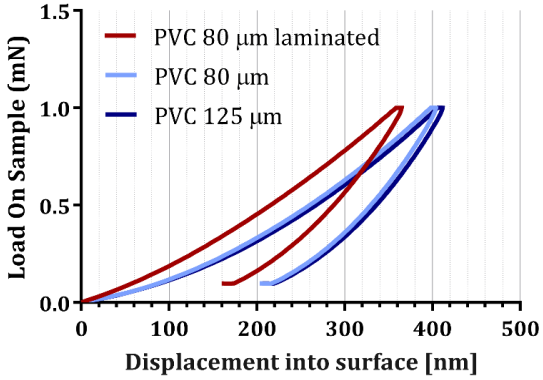

Slika 12 Usrednjena merenja za PVC

Krive PDMS materijala govore o njegovoj gotovo idealnoj elastičnosti i uniformnosti dok je PVC manje elastičan i manje uniforman kod tanjih slojeva i slojeva koji su termički tretirani.

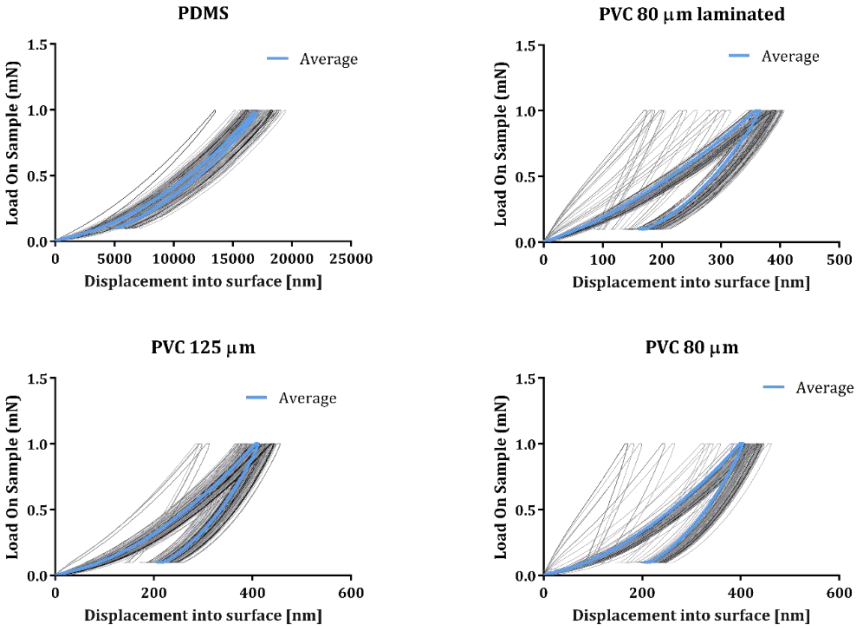

Slika 13 Krive zavisnosti dubine prodiranja od opterećenja za PDMS i PVC uzorke

Keramička traka je fleksibilan materijal koji sinterovanjem na 900 °C potpuno očvrsne. Za čipove u SAVA tehnologiji koristili smo nesinterovanu keramičku traku. Usrednjene krive opterećenja u zavisnosti od dubine indentacije, prikazane na slici 14, pokazuju da se keramička traka značajno mekša pre nego posle sinterovanja i da ta osobina ne zavisi od veličine sile, trend se održava.

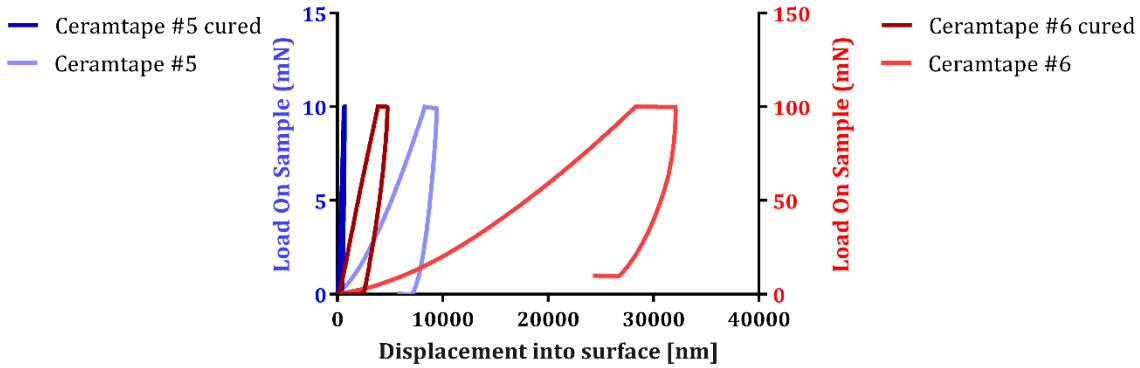

Slika 14 Usrednjene krive za keramičku traku

Zarad testiranja temperaturne stabilnosti čipova, oni su izlagani različitim temperaturama od 80 °C do 180 °C, sa korakom od 20 °C tokom 5 minuta. Pokazano je da su čipovi koji su zagrevani na 120 °C funkcionalni iako su imali male promene u dimenzijama kanala dok su čipovi na većim temperaturama nepovratno degradirani.

Maksimalan protok kroz SAVA čipove testiran je špric pumpom na dizajnu Y kanala. Za potrebe ovog eksperimenta razvijen je i poseban držač za čipove. Ulazi i izlazi su spojeni u držaču sa PTFE tubama pomoću samolepljivih silikonskih umetaka.

Opsežne i temeljene promene pritiska su testirane na SAVA čipovima i na PVC čipovima za komapraciju. Promena protoka prikazana je u tabeli 2.

Tabela 2 Opseg protoka za testiranje maksimuma istog kod PVC i SAVA čipova

	Opseg	*Od*	*Do*	*Korak*
PVC	I	0.1 µl/min	max	0.1 µl/min
SAVA	I	0.1 µl/min	1.0 µl/min	0.1 µl/min
	II	1 µl/min	10 µl/min	1 µl/min
	III	10 µl/min	100 µl/min	10 µl/min
	IV	100 µl/min	1 ml/min	100 µl/min
	V	1 ml/min	15 ml/min	1 ml/min

PVC čipovi mogli su da izdrže protoke od 5 µl/min bez curenja dok su čipovi u SAVA tehnologiji bez curenja podnosili protoke od 15 ml/min, što je 3000 puta više nego PVC čipovi.

Mešanje u mikrofluidnim čipovima testirano je za sve tri fabrikacione tehnologije. Eksperimentalne postavke sva tri mogu se videti na slici 15.

(a) (b) (c)

Slika 15 Eksperimentalne postavke za testiranje mešanja u (a) PDMS, (b) PVC i (c) SAVA čipovima

Za testiranje mikromešača proizvedenog u PDMS tehnologiji korišćena je eksperimentalna postavka sa kontrolom pritiska, gde je inkrementiran pritisak i praćena efikasnost mešanja. Mikroskopske slike ulaza, mikromešača i izlaza sa

različitim pritiscima, odnosno protocima prikazane su na slici 16. Ova struktura mikromiksera dala je dobre rezultate mešanja pri malim pritiscima, onim nižim od 40 mbar.

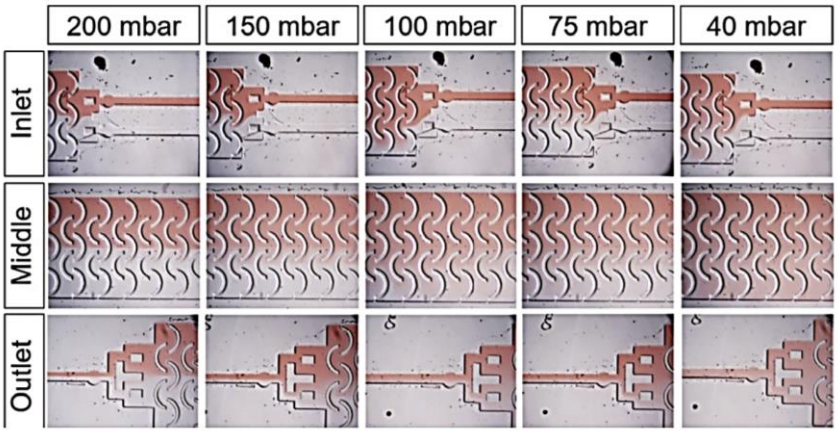

Slika 16 Mikroskopske slike na različitim pritiscima.

Za testiranje mikromešača sa paralelogramskim barijerama proizvedenim u PVCu koristili smo eksperimentalnu postavku sa špric pumpom. Za tečnosti koje su mešane korišćeni su rastvori za ispiranje usta . Rezultati mešanja očitavani su sa digitalnog mikroskopa a zatim obrađivani u Matlab®-u. Slika 17 pikazuje efikasnost mešanja pri različitim protocima i za različite dužine paralelogramskih barijera. Povećanje dužine barijere da zaprema samo 5 % više širine kanala povećava efikasnost mešanja pri niskim protocima.

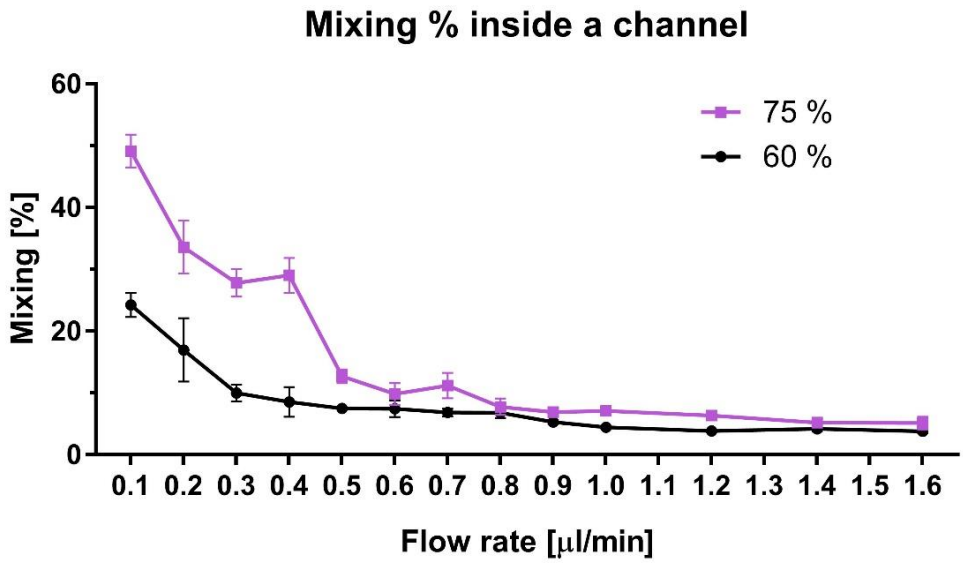

Slika 17 Efikasnost PVC mikromešača

Primeri upotrebe

Primer #1 – Analiza SAVA mikrofluidnih čipova za dostavu antibakterijskih rastvora u stomatologiji.

Za ovaj primer analizirane su osobine dva rastvora na bazi hlorheksidina. Eksperimentalna postavka sastojala se od kontrolora pritiska, držača, PVC čipa i mikroskopa, detalji postavke vide se na slici 18. Napravljeno je osam SAVA čipova sa Y kanalom, bez prepreka u kanalu i širine kanala od 500 – 700 μm. Analizirani su parametri prolaska, brzine i potrebnog pritiska za laminarni tok rastvora kroz čip. Zarad lakše vizualizacije, testirane tečnosti obojene su gencijanom.

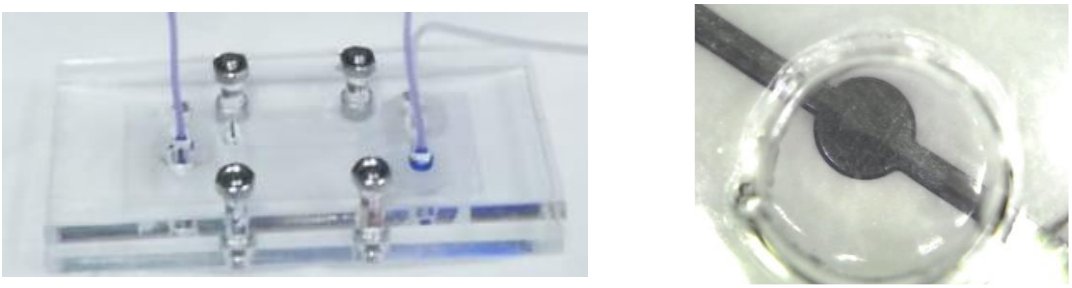

Slika 18 (a) držač mikrofluidnog čipa, (b) fotografija zumiranog opservacionog polja.

Ovaj primer primene je sproveden u cilju procene mogućnosti integracije dijagnostike pljuvačke u mikrofluidnim sistemima. Eksperiment istražuje mogućnosti projektovanja optimalnog mikrofluidnog sistema za teranostiku pljuvačke zasnovanog na ekonomičnoj i tehnološki jednostavnoj SAVA tehnologiji, prateći kriterijume postavljene za savremene medicinske uređaje, a definisane kao *ASSURED* Svetske zdravstvene organizacije. Ovi kriterijum sugerišu da aparati koji se koriste za rutinske procedure u opštem praćenju zdravlja moraju biti pristupačni, osetljivi, specifični, laki za korišćenje, brzi i robusni i bez upotrebe složene opreme.

Dobijeni podaci ukazuju da kontrolisana isporuka lekova za rutinsku primenu u stomatološkoj kliničkoj praksi korišćenjem mikrofluidnih podešavanja zahteva dodatnu pretkliničku potvrdu, kalibraciju svih relevantnih parametara i unapređenje spajanja postojećih medicinskih i inženjerskih tehnologija.

Primer #2 – Viskoznost i mešanje veštačke pljuvačke sa četiri tipa rastvora za ispiranje usta

U ovom primeru primene, analize veštačke pljuvačke na bazi karboksimetil celuloze (označene kao S) rađen po receptu Apotekarske ustanove Beograd, sa četiri rastvora

za ispiranje usta: 0,1% rastvor hlorheksidina (označen kao C); rastvor fluorida srednje koncentracije (2000 ppm) (označen kao F), cink-hidroksiapatit (označen kao ZM) i kazein-fosfopeptid amorfni kalcijum fosfat (označen kao CPP-ACP).

U cilju kontrole protoka i mešanja tokom eksperimenta korišćeni su mikrofluidni čipovi proizvedeni u SAVA tehnologiji. Dizajn čipa je jednostavni Y-kanal bez ikakvih prepreka, sa ulaznim kanalima postavljenim pod uglom od šezdeset stepeni, širine 600 nm i prečnika oba ulaza i izlaza od 2 mm.

Svi eksperimenti su izvedeni korišćenjem dva sistema – špric pumpe i kontrolera pritiska. Podešavanje špric pumpe je pripremljeno na sledeći način: na špric je vršen mehanički pritisak sa ispitivanim rastvorom što je rezultiralo promeni zapremine srazmerne primenjenom pritisku. Pre početka eksperimenta definisane su dimenzije (prečnik i zapremina) šprica, a brzina je automatski regulisana podešavanjem protoka pumpe. Regulator pritiska radi na veoma sličan način, sa malom razlikom – protok tečnosti je omogućen ubrizgavanjem vazduha kompresorm u komore koje sadrže tečnost. Na taj način se tečnost istiskuje pod jednakim pritiskom pod kojim se uvodi vazduh. Glavna razlika između ove dve metode je parametar koji želimo da pratimo, u eksperimentima sa špric pumpom uvek znamo tačan protok tečnosti kroz čip, dok u eksperimentima koji koriste kontroler pritiska znamo tačan pritisak. Vrednost korišćenog pritiska odgovara brzini protoka generisanom pomoću špric pumpe. U eksperimentu sa špric pumpom, korišćen je protok od 10 mL/min i pritisak od 80 mbar na regulatoru pritiska.

Za određivanje proporcije mešanja korišćen je algoritam za obradu slike u Matlab programu. Eksperimenti su prvo snimljeni mikroskopom opremljenim kamerom uz uvećanje do 10 puta. Veštačka pljuvačka je obojena plavom bojom radi jednostavnijeg praćenja procesa mešanja rastvora. Dobijene slike su zatim obrađene na sledeći način: za svako od dva rešenja definisane su vrednosti piksela pre mešanja tečnosti i broj piksela polja za posmatranje. Svaka boja je jedinstveno određena sa tri komponente, crvenom, zelenom i plavom. Nakon mešanja, slike polja posmatranja su obrađene MATLAB algoritmom da bi se definisao broj tečnih piksela čije vrednosti se uopšte nisu promenile tokom procesa mešanja. To je bio deo koji je ostao nepomešan što se vidi na slici 19. Zatim je ta vrednost oduzeta od ukupnog broja piksela i izračunat je kvantitativni deo ostalih, mešovitih rešenja.

Zbog gustine, CPP-ACP pasta je razređena u eksperimentalnim postavkama destilovanom vodom u odnosu 1:3.

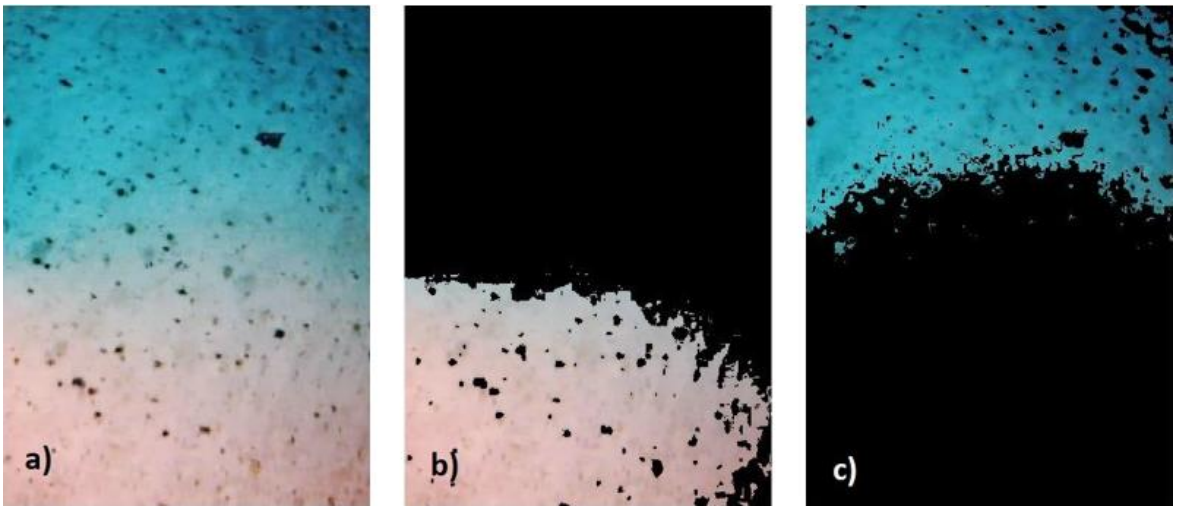

Slika 19 (a), (b), (c). Analysis of solution mixing using MATLAB

RheolabQC rotacioni viskozimetar je korišćen za merenje viskoziteta rastvora pojedinačno kao i mešavine sa veštačkom pljuvačkom.

Viskoznost je merena na dve temperature, sobnoj (25,0 °C) i telesnoj temperaturi (36,6 °C). Korišćena su i dva viskozimetarska alata, cilindrični (CC27) koji se preporučuje za viskozne rastvore i dvostruki zazor (DG42) koji se preporučuje za manje viskozne rastvore. Zbog svoje konzistencije, CPP-ACP pasta se mogla testirati samo cilindričnim alatom.

Rezultati mešanja dobijeni na slici 20 podržavaju nepotpuno mešanje svih rastvora sa veštačkom pljuvačkom, u opsegu od 23,29% za rastvore cink-hidroksiapatita do 43,65% za rastvore fluorida. Takođe, rezultati ukazuju na veći procenat mešanja pomoću regulatora pritiska u odnosu na špric pumpu.

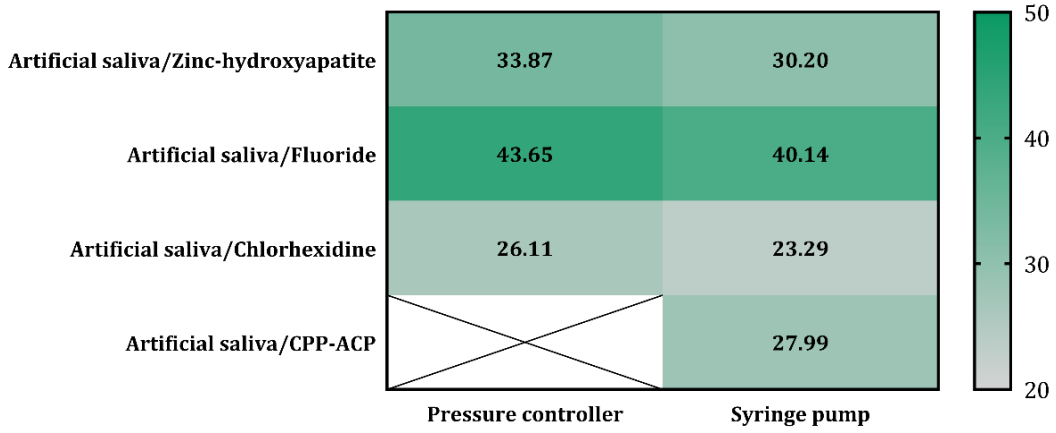

Slika 20 Proporcija mešanja tečnosti u dve eksperimentalne postavke

Primer #3 – Filtracija čestica polena

Da bi se prikazala raznovrsnost primene, predstavljeno je rešenje za brzu izradu prototipova mikrofluidnih elemenata primenom kombinacije laserske mikromašinske obrade i ksurografske tehnike, bez korišćenja skupe čiste sobe. Da bi se demonstrirala primenljivost predloženog koncepta tehnologije, 3D mikrofluidni čip za filtraciju polena koji kombinuje mikromikser, jedinicu za filtraciju i kanal sa serpentinom je proizveden i testiran.

3D višeslojni čip koji se sastoji od pet slojeva, prikazan na slici 21(a), proizveden je kombinacijom laserske mikromašinske obrade i procesa PVC laminacije. Slojevi 2-4 su realizovani korišćenjem keramičke trake, dok su sloj 1 i sloj 5 realizovani korišćenjem PVC folija. Proces laserske mikromašinske obrade je korišćen za pripremu keramičkih traka i sečenje mikrofluidnog kanala, mikromiksera, serpentina i filtera. Mikrofluidni kanali su široki 200 μm, dok su otvori za međusobnu vezu između slojeva i rupe za ulaz i izlaz realizovane prečnika 2 mm. U sledećem koraku, keramičke trake su naslagane i laminirane korišćenjem uniaksijalne prese pod pritiskom od 2200 kg i temperaturom od 80 °C, tokom 3 min. Vhatman® 1441-150 filter papir od 20 - 25 μm prethodno isečen laserom je ugrađen u sloj 3 tokom slaganja slojeva pre laminacije. Da bi se izbeglo curenje, veličina filtera je uvećana na 5 mm, dok je oblast filtracije realizovana sa radijusom od 2 mm. Filter je integrisan u dva sloja u sendvič strukturi. Kater je korišćen za sečenje ulaza, izlaza i ivica u PVC folije za laminiranje, koje su korišćene za gornji i donji sloj. Gornji i donji slojevi sastavljeni su u završnoj fazi pomoću tople laminacije. Izgled proizvedenog 3D mikrofluidnog čipa prikazan je na slici 21(b).

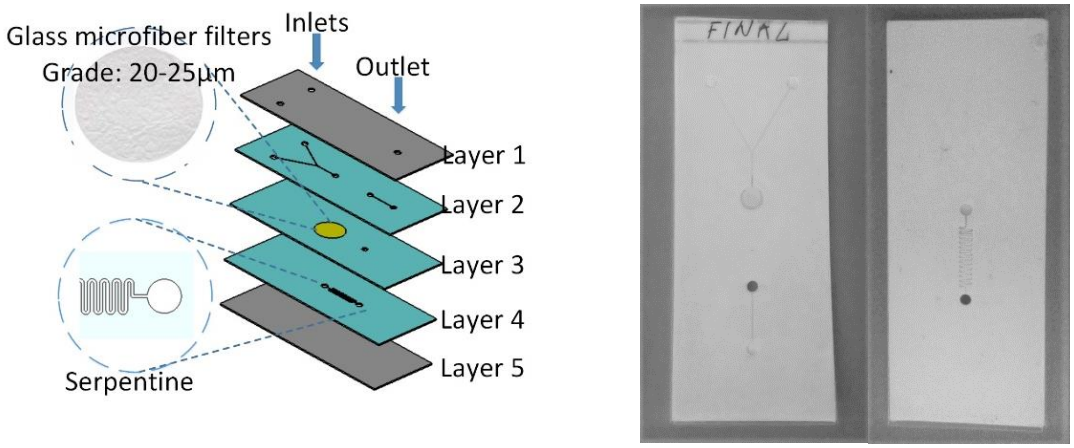

Slika 21 (a) višeslojni čip u SAVA tehnologiji, (b) pogled na mikrofluidni čip od gore i od dole

Za testiranje funkcionalnosti čipa sa filterom napravljen je mešavina dejonizovane vode i čestica polena (čestice polena trske). Eksperimentalna postavka je ista kao i kod eksperimenta za određivanje maksimalnog protoka. Na dva ulaza mešavina

voda/polen je dovođena je na ulaz čipa protokom od 100 µl/min, a izlaz je držan u kiveti od 2,5 ml. Slika 22 prikazuje tri kivete: sa leve strane je rastvor vode/polena, u srednjoj je čista dejonizovana voda (za poređenje), a desno je filtrirana tečnost. Vidi se da je količina čestica polena značajno smanjena. Kako su čestice polena trske veličine 22,7 ± 2,6 µm, a filter dimenzija pora 20 - 25 µm, sve srednje i velike čestice su filtrirane, dok su neke manje prošle kroz filter.

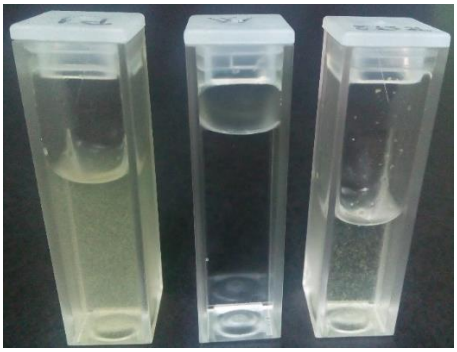

Slika 22 Rezultati filtracije

Zaključak

Mikrofluidika kao oblast naučnog istraživanja razvija se eksponencijalno u proteklih 20 godina. Iako su do sada načinjena brojna otkrića i unapređenja još veći deo njih čeka da bude pronađen i poboljšan. Glavno dostignuće ove teze ogleda se u inovativnom dizajnu mikromešača za mikrofluidne čipove i sasvim novoj tehnologiji fabrikacije mikrofluidnih uređaja, nazvanoj SAVA tehnologija. Pored gorenavedenog u okviru teze napravljeni su i drugi dizajni mikrofluidnih čipova u svrhu testiranja nove fabrikacione tehnologije. Zarad verifikacije parametara i performansi novog dizajna, urađene su simulacije tri mikrofluidna mikromešača. Ove simulacije pomogle i su optimizaciju predloženih dizajna za potrebe fabrikacije. Sama fabrikacija mikrofluidnih čipova sprovedena je u tri različite tehnologije. Nova, predložena SAVA tehnologija fabrikacije podrobno je testirana. Zatim je testirana mikforluidna funkcionalnost čipova proizvedenih za potrebe ove doktorske teze. Upoređene su: performanse novog mikromešača sa najčešće korišćenim mikrofluidnim strukturama, različite eksperimentaline postavke i konkurentnost nove SAVA tehnologije. Na kraju, prikazana su tri primera biomedicinske primene.

Za potrebe testiranja SAVA tehnologije razvijeno je 6 mikrofluidnih struktura: 1. čip sa jednostavnik kanalima različite širine – za određivanje minimalne širine kanala, 2. čip sa kružnim i pravougaonim komorama – za determinisanje maksimalne veličine komore, 3. čip sa standardnim Y kanalom – za poređenje sa drugim tehnologijama i

testiranje primena, 4. mikromešača sa paralelogramskim barijerama – za poređenje različitih tehnologija fabrikacije, 5. čip sa serpentinom – za testiranje agilnosti dizajna koje je moguće fabrikovati u SAVA tehnologiji i 6. mikromešač inovativnog dizajna – da precizno podešavanje malih koncentracija mešanja u mikrofluidnom čipu kod eksperimenata za isporuku leka.

Simulirano je tri mikrofluidna miksera: prvi - mikromešač sa paralelogramskim barijerama čiji dizajn odgovara dimnezijama potrebnim za fabrikaciju u PVC tehnologiji; drugi - mikromešač sa paralelogramskim barijerama čiji dizajn odgovara dimnezijama potrebnim za fabrikaciju u SAVA tehnologiji i treći - inovativni mikromešač sa polukružnim barijerama čiji dizajn odgovara dimnezijama potrebnim za fabrikaciju u PDMS tehnologiji.

S obzirom na to da je mešanje jedna od najčešće korišćenih funkcija u mikrofluidnom čipu testirane su sve tri tehnologije fabrikacije. Zaključak koji se može izvući iz eksperimenata koji su testirali mikrofluidne miksere je da je: PDMS mikromešač – najprecizniji za male koncentracije ali nemoguće de distići putpunu efikasnost pri mešanju, PVC mikromešač – ima najmanje precizno i najnestabilnije mešanje koje je posledica ograničene preciznosti i minimalnih dimenzija tehnologije dok SAVA mikromešač – ima zadovoljvajuća podešavanja performansi mešanja dok može da postigne punu efikasnost pri mešanju (potpuno mešanje tečnosti u kanalu).

Mikrofluidni čipovi su fabrikovani u tri tehnologije od kojih su dve opšte poznate naučnoj javnosti: izlivanje PDMSa u kalupima i ksurografija, dok je treća tehnologija nastala tokom same izrade ove teze – SAVA tehnologija. Svi parametri fabrikacije čipova za potrebe teze opsežno i detaljno su dokumentovani, posebno za SAVA tehnologiju. Ovo je učinjeno zarad otvaranja ove tehnologije za buduće primene. Za procenu kvaliteta SAVA tehnologije testirane su:

1) Transparentnost – koja se pokazala da je u klasi PDMS i FlexDym čipova, dakle da se u njoj može koristiti optička detekcija, što znači da se u tom pogledu ova tehnologija može upotrebiti kao ekonomičnija zamena,
2) Dielektrične osobine – kao važan parametar pri primeni mikrostrip tehnologije kao glavnog predstavnika neoptičkih očitavanja,
3) SEM i optička mikroskopija – daju uvid u preciznost i kvalitet laserskog reza, očuvanost komora posle tople laminacije,
4) Mehaničke osobine – zarad provere mehaničke kompatibilnosti materijala, tj. koliko hibridna tehnologija zadržava od svojstava različitih materijala koje koristi i
5) Termička stabilnost – koja ispituje granice temperature na kojoj je hibridna tehnologja još uvek upotrebljiva.

Sprovedeni mikrofluidični eksperimenti odredili su maksimalan protok kroz mikrofluidni čip iz SAVA tehnologije. Testovi su ukazali na to da su konekcije sa ulazima i izlazima najslabije take ove tehnologije. Odnosno, da čipovi mogu da izdrže i veće protoke ali konekcije ne mogu. Unapređenje ovih kontakata jedan je od daljih pravaca istraživanja. Osim maksimalnog protoka, testirana je i efikasnost mešanja kod novog predstavljenog dizajna, gde se vidi da je njegova glavna prednost precizno podešavanje efikasnosti za male koncentracije. Zatim su testirana mešanja u čipovima urađenim u ksurografiji i SAVA tehnologiji. U ovim eksperimentima akcenat je bio na optimizaciji eksperimentalnih postavki.

Kroz poslednja tri eksperimenta otškrinuta su vrata u svet primena nove SAVA tehnologije u biomedicini. U privom eksperimetnu korišćeni su već provereni čipovi iz ksurografije ali su kao tečnosti korišćeni rastvori za ispiranje usta na bazi hlorheksidina. U drugom su korišćeni SAVA čipovi a kroz njih je mešana veštačka pljuvačka sa hlorheksidinom ali i još tri tečnosti koje su značajne za stomatologiju – fluoridima, hidroksiapatitima i CPP-ACP-om.

Table of Content

List of Figures

List of Tables

List of Abbreviations

Abbreviation	
2D	Two-Dimensional
3D	Three-Dimensional
ABS	acrylonitrile butadiene styrene
ASSURED	Affordability Sensitivity Specificity User friendliness Rapid and robust Equipment-free Deliverable to end-users.
BSE	backscattered electrons
C	chlorhexidine
CAD	computer-aided design
CE	capillary electrophoresis
CHX	chlorhexidine
CPP-ACP	casein-phosphopeptide amorphous calcium phosphate
CW	continuous wave
DLP	digital light processing
DNA	deoxyribonucleic acid
ECAD	electronic computer-aided design
F	fluoride solution
FDM	fused deposition modelling
FE-SEM	field emission scanning electron microscopes
GPC	gas-phase chromatography
GUI	graphic user interface
HPLC	high-pressure liquid chromatography
LTCC	low temperature co-fired ceramics
MEMS	MicroElectroMechanical Systems
N/A	not aplicable
Nd:YAG	neodymium-doped yttrium aluminum garnet
NIR	near-infrared
PC	personal computer
PCO	polycyclo-olefin
PCR	polymerized chain reaction
PDMS	polydimethylsiloxane
PLA	polylactic acid
POC	point-of-care
PTFE	polytetrafluoroethylene
PVC	polyvinyl chloride

REM	reflection electron microscope
S	artificial saliva
SAVA	hybrid fabrication technology with PVC/CeramTape/PVC layer structure
SE	secondary electrons
SEM	Scanning electron microscope
SLA	stereolithography
SMA	*SubMiniature version A*
STEM	scanning transmission electron microscope
STM	scanning tunnelling microscopy
SU-8	epoxy-based negative photoresist
TEM	transmission electron microscope
TTL	time-to-live
USB	universal serial bus
UV	ultraviolet
VIS	visible spectrophotometer
VP-SEM	variable pressure scanning electron microscope
WHO	World Health Organisation
ZM	zinc-hydroxyapatite

Chapter I
Introduction

"Il vaut mieux savoir un peu de tout que tout sur très peu."

- Blaise Pascal

1.1 About microfluidics

Microfluidic as a term has two meanings: 1) it is a **science** and 2) it is a **technology**. Scientific aspect determines the behaviour of fluids in channels of the micrometre size order. The volume of the fluid, by which the microfluidic devices are manipulated, goes to the femtolitre. The behaviour of the fluid on the microscale is radically different in relation to the macroscale. The technological aspect is devoted to the production and miniaturization of devices, consisting of microchannels or even nanochannels. In contrast to miniaturization of integrated circuits and MEMS (MicroElectroMechanical Systems) devices, in which the entire device is scaled, for the microfluidic devices, the only important thing is to scale the space through which the fluid moves. The sensitivity of the device is determined by the smallest amount of microfluid that can be used. In order to gain an impression about the sizes and volumes that the microfluidics deal

with, the scale (Figure 1.1) shows a scale with devices used in the microfluidic, and it is compared with the size of known objects.

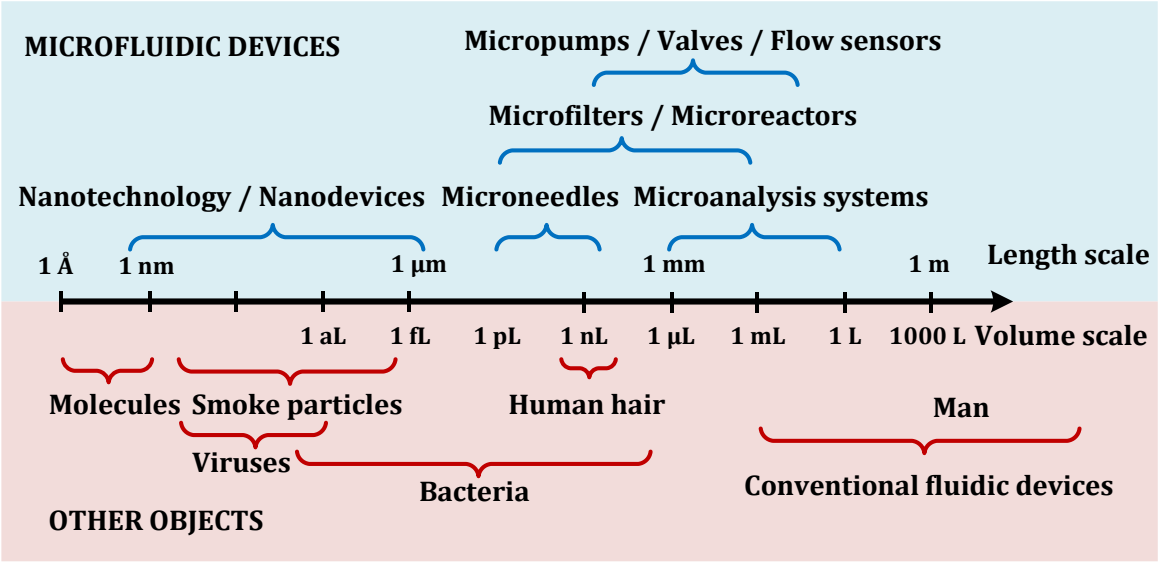

Figure 1.1 Characteristic dimensions of microfluidic devices compared with dimensions in nature

1.2 About microfluidic chips

Chip in microfluidic implies a set of microchannels which are etched, imprinted or curved in the material, such as glass, silica or polymer, most often polydimethylsiloxane (PDMS). Microchannels are connected inside the chip and they perform an explicit function such as mixing, filtration, sorting, separation, control of the biochemical environment, etc. Connection with macro surroundings is established by making holes in the chip which represent inlets and outlets. The liquid in the chip can be inserted actively or passively. In the case of active liquid injection, external devices for pressure control pumps are used. The passive injection is conducted by hydrostatic pressure, more precisely - capillary forces. Mass diversity of microfluidic chips is shown in Figure 1.2.

The microfluidic chip can also be a simulation of specific and controlled environment. This is an extremely important and a very smooth step between *in vitro* and *in vivo* experiments [1].

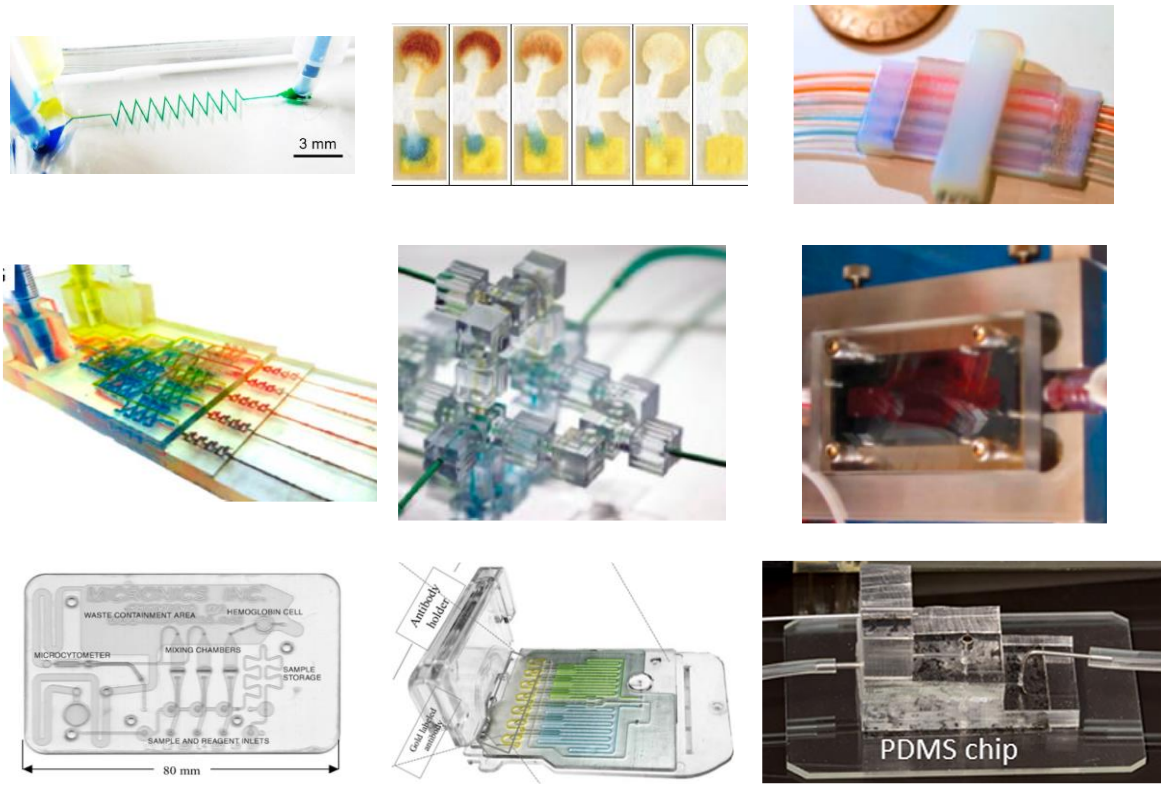

Figure 1.2 Examples of different types of microfluidic chips [2-7]

Main components of microfluidic chip are micro: microchannel, micromixer, microchamber, micropump and macrovalve.

1.3 About materials

Main division of microfluidic materials is on: **inorganic, organic and hybrid** (or composite) materials. Inorganic materials are silicon, glass and ceramics, organic materials are different polymers such as PTFE (polytetrafluoroethylene), PDMS (polydimethylsiloxane), PCO (polycyclo-olefin), PC (polycarbonate) while main hybrid material representatives are ceramic materials used in LTCC (low temperature co-fired ceramics) [8]. Inorganic materials are primarily used as substrates for microfluidic fabrication cause of their well-known mechanical and chemical properties as well as fabrication techniques available. They had tuneable thermal conductivity, surface stability and solvent compatibility [9-11]. First materials used for microfluidic fabrication are silica and glass. Silicon has become the material at its time primarily because of the link with electronic engineering fabrication technologies such as photolithography [12]. Biomedicine imposed polymers as primary material for microfluidic chip fabrication due to its transparency and low chemical/cell interaction.

Now, more than50 years after first mention of microfluidics, when we well explored both fabrication worlds it is time for hybrids.

Old-style proof-of-concept works are developed at the academic research institutions there is a certain level of concern that exists regarding real applications and medical research. There are two issues that need to be taken in to consideration. First, the re-evaluation and overall stability and biocompatibility of the core microfluidic performance during management of real samples. Second, scaling-up of each fabrication process section (microfabrication, bonding, preparing and other requirements), their interdependencies and expenses. Excising gap in these aspects harshly limits the most of microfluidic application [8]. The historical timeline of developments in materials and microfluidics are depicted in Figure 1.3.

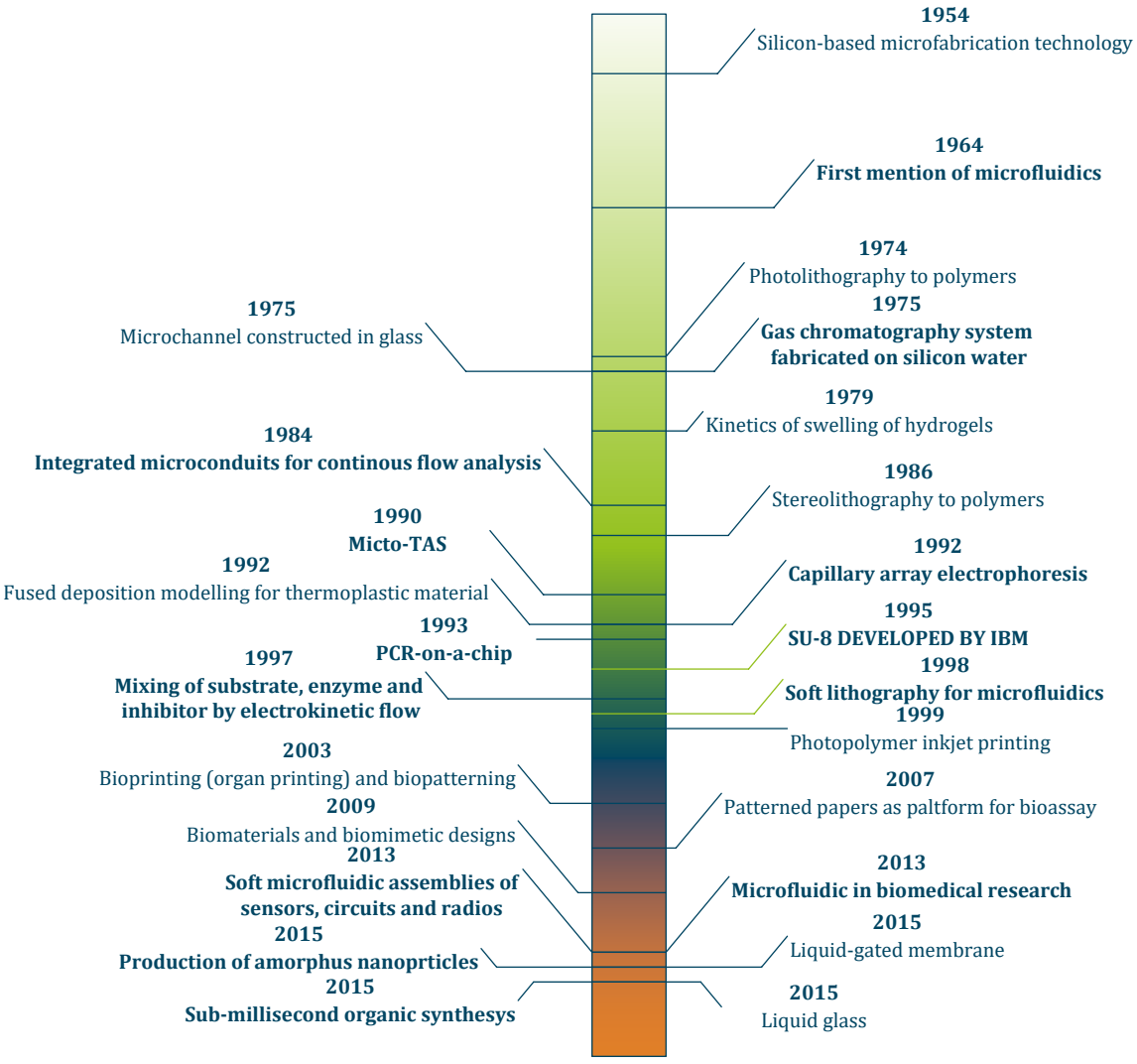

Figure 1.3 Historical timeline of developments in materials and microfluidics [11]

Materials, devices and tools used for microfluidic chip fabrication and characterisation are listed below, together with the producer information as well as semantic links to the thesis functional parts.

Chapter II
Subject, Problem and Aim of This Research

Microfluidics, one of the most attractive and fastest developed areas of modern science and technology, has found many applications in medicine, biology and chemistry. To address advanced designing challenges of the microfluidic devices, the research is mainly focused on the development of efficient, low-cost and rapid fabrication technology with a wide range of applications [13]. Microfluidic application in biomedicine and pharmacy as personalisation of drug delivery and precise droplet generation are one of the burning topics today. Existing microfluidic fabrication technologies can only encourage more microfluidic research not nearly to satisfy them. Nowadays, selection of an adequate microfluidic fabrication technology is a narrow choice. That need and must be changed. Development of new fabrication technologies

is an excessive necessity for further microfluidic development during broader research areas. Making of a quality, precise and low-cost microfluidic chip is yet to come.

The development of microfluidics seeks to revolutionize medicine and molecular and chemical biology. In the last few years, a large amount of research in medicine has turned to personalizing patient treatment. Microfluidics play a significant role in this research. DNA analysis, protein and enzyme analysis, and single cell analysis are powerful diagnostic tools [14-23]. Precise control of the movement and mixing of microfluid enables easier and more precise personalized delivery of the medicine.

A device that integrates several analyses on a single chip, which are performed in laboratories, is called a Lab-on-chip. The analyses performed by a Lab-on-chip are focused on diagnostics in medicine and DNA analysis. It is less often used for reactions and synthesis of elements in chemistry. A huge advantage is miniaturization and parallelization. Performing the above analyses requires equipped laboratories, which take up several rooms. In contrast, a Lab-on-chip can fit in the palm of your hand. This chip consists of millions of microchannels, integrated pumps, valves and electrodes. The direction in which the research and development of this device is going is to enable thousands of biochemical analyses from just one drop of blood. DNA analyses are based on polymerized chain reaction (PCR) which requires rapid temperature changes. The development of PCR based microfluidic chips is in its peak. The current capabilities of the device are analysing DNA a thousand times faster than classical methods. In addition to DNA analysis, there are chips that analyse viruses and bacteria. The interaction of a small number of cells can be analysed under a microscope, after they have been stained in a microchannel. In this case, the fluid is mixed with the dye, which is transmitted through the cells in a laminar flow. Individual cells can be isolated and manipulated in a microfluidic system. Specific microfluidic systems that can generate droplets, which encapsulate cells, are needed in this case. They usually work on the principle of T-connection or focused flow. In the case of a T-joint, water flows continuously through the wider channel, while oil is periodically released into the channel through the narrower channel at a right angle to the channel. The size and shape of the droplets depends on the period of oil release into the channel and the width of the channel. In the case of focused flow generation, we have two continuous fluid flows that are at right angles to the central channel through which another fluid is periodically fed. A fluid that has a continuous flow must not mix with a fluid with a periodic flow, most often it is oil and water.

Microfluid mixing is one of the most important processes in microfluidics. Rapid and uniform mixing is required in many biochemical analyses, drug delivery, enzyme analysis, DNA analysis, etc. [2, 19, 24, 25]. Mixing fluid on the microscale is drastically

different from mixing on the macroscale because the fluid flow in the microchannel is laminar.

The main aim of this doctoral dissertation was to develop new and applied microfluidic chip fabrication technology from electronic engineer point of view.

The specific objectives of the research within the doctoral dissertation can be classified as follows:

- Problem definition and translation in the field of microfluidics
- Determination of experimental conditions and required microfluidic chip structure for classes of precision dosing
- Microfluidic chip structure design
- Simulation of design and selection of the most adequate chips for application in biomedicine
- Fabrication of chips in different manufacturing technologies (PDMS, LTCC and PVC - polyvinyl chloride)
- Develop a new microfluidic chip fabrication technology
- Fabrication of the chip in new microfluidic chip fabrication technology
- Testing (conducting and recording experiments) and chips characterization
- Image processing, comparison with simulations and analysis of results
- Fabrication technology optimization and external control
- Checking chips for similar problems from the same class of biomedical problems

Chapter III

Field Overview

Micro and nano-fluidics represent the most progressive areas of modern science and technology, due to a wide range of applicability in many fields of our life such as medicine, biology, chemistry, engineering or environmental protection [6, 21, 26-29].

The microfluidics has four roots [12]:

1. **Molecular analysis** – chronologically first –There are 3 microanalytical methods - gas-phase chromatography (GPC), high-pressure liquid chromatography (HPLC) and capillary electrophoresis (CE) which are made possible to, together with laser optical detection, simultaneously reach high sensitivity and high resolution using very small amounts of sample.
2. **Biodefence** - Chemical and biological weapons posed major military and terrorist threats. There was the incentive for the expansion of microfluidic systems
3. **Molecular biology** - With blast of genomics (especially high-throughput DNA sequencing) microfluidics open tactics to overcome existing problems.
4. **Microelectronics** - The original idea of microfluidics was that electronic microfabrication technologies such as photolithography and associated technologies would be straight usable in microfluidics. These techniques were related for glass or silicon as substrates, but microfluidic preferred polymers especially in biomedical applications.

There are several rapidly emerging disciplines in medicine that in the first place require improved consideration of basic medical physiology, and from the other side necessitate critical, more rational approach to diagnostic procedures, drug delivery, administration and development. It has been recognized that individualized diagnostics and treatment together with the point-of-care analytical systems need to fulfil rigid criteria in order to be applicable in everyday medical practice; firstly, all point-of-care (POC) devices should offer more economical substitute when compared with expensive and long-lasting medical tests, in addition to that they must increase the number of available techniques for the medical applications, and finally, they have to improve with each new design in terms of increased sensitivity and selectivity while remaining more resource aware [30]. In the field of basic sciences, such as biology, microfluidic devices offer the chance to substantially improve the methods used in contemporary biological research, since microfluidic devices are capable of working with smaller specimen dimensions, shorter reaction times are needed, and there is the opportunity for simultaneous and multiple operations, holding a promise to implement new methods, techniques and experimentations that are not achievable on the macro scale [31]. Similarly, from the standpoints of both synthetic chemistry and industrial chemical applications during the past two decades far-reaching evolvement in the fabrication of microfluidic systems has been achieved, and microfluidic reactor technology became a golden standard as an instrument in chemical synthesis for both scientific purposes and commercial products, and as a result a catalogue of chemistries executed in a microfluidic reactor already exists [32]. In the contemporary engineering, in the various disciplines microfluidic devices designed for manipulation of fluids are widely used in different contexts, but frequently their fabrication requires atypical geometries and the interaction of different physical phenomena, for instance, pressure gradients, electro kinetics, and capillarity and all these requirements resulted in remarkable variants of well-known and thoroughly described fluid dynamical challenges together with some newly observed fluid responses [33]. Environment protection gained increased attention during the past several decades since enormous development in the various industrial fields, such as pharmaceutical, medical and biochemical industries, has been registered and consequently led to an increasing number of emerging pollutants followed by stricter and demanding ecological policies. Simultaneously with the increasing amount of the registered contaminant agents, greater tasks and requirements are placed in front of environmental protection, analysis and monitoring. There are numerous effective analytical techniques that are widely used in environmental analysis, but some of them currently face significant drawbacks such as complex and expensive instrumentations, analyses are frequently long-lasting and costly resulting in inadequate estimation of pollutant presence, distribution and concentrations. As a result some researchers and environmental

protection professionals started with the use, design and fabrication of different microfluidic devices in order to achieve significant innovations in environment monitoring analysis, since they recognized the fact that microfluidic devices offer some substantial improvements in comparison with traditional techniques, comprising the possibility of rapid pollutant detection and immediate identification of all compounds, together with lower amounts of both specimen and reagent consumption with the promising potential for continuous field monitoring with highly sensitive, specific and selective detection abilities while functioning without supervision in the field for prolonged periods of time, for days to months and years [34].

The microchannel is essential part of a microfluidic chip. It is used to connect inlets and outlets with the functional part of the chip. Furthermore, microchannel itself can be functionalised for example, control droplet volume, chemical concentration, and perform sorting [35] or particle separation [36]. Dimensions of the microchannels can vary, as long as they contain microliter volume of the liquid and at least one of dimensions is in micro scale a channel can be considered as microchannel. More precisely, while channel hydraulic diameter (hydraulic diameter is equal 4 times cross-sectional area divided with wetter perimeter of cross-section) is below 1 mm [37]. While the microchambers are spaces in the microfluidic chip most frequently used for storing of the reagents or cell culturing [38, 39]. The microchambers are frequently called microreactors since, chemical reaction or other active process can be conducted in them [39]. One of the most frequent functional components of the microfluidic chip is micromixer with the role of mixing two or more liquids inside of the microfluidic chip [25, 40]. Although, this may look trivial at the first glance, mixing of liquids in the channel or chamber is extremely hard due to type of the flow present in the chip or space/volume restrictions. Moreover, the micromixers ability to mix microscopic amounts of various fluids has been recognized as being essential in a wide span of nowadays and emerging systems in medicine, biochemical engineering, biology, chemistry and other sciences, with diverse pallet of potential applications such as inkjet printing, pharmaceutical drug development and manufacturing, specialty and dangerous chemical manufacturing, genetic material analysis and early diagnosis of various diseases [41].

Micropumps comprise important group of the different devices that have been used in microfluidics where their ability to provide sufficient energy necessary to fluid flow within various microfluidic systems has been extensively employed [28]. Initial version of micropumps went through major changes and nowadays they are offering many important and beneficial possibilities extremely valuable in many fields of microfluidics applications, such as lower energy consumption, creation of portable devices, ability to use microscopic samples with very small specimens dimension,

weight and volume, opportunity to work with different microfluid flow rate spans and finally, cost effectiveness. Micropumps have been designed and used in various fields and nowadays play important role as integral part of various applications comprising biochemical and biomedical assays, analyses based on microfluidic technology, controlled drug delivery, cells cultures and many others. There are two main types of micropumps, mechanical and non-mechanical with completely different operating mechanisms and operations. The group of mechanical micropumps consists of both electrostatic and electroactive polymer composite devices, piezoelectric micropumps, electromagnetic micropumps and thermal/electromagnetic actuation micropumps. All mechanical micropumps have moving mechanical elements, such as for example pumping diaphragms and various forms of checking valves. Piezoelectric, electrostatic and electroactive, thermo pneumatic, electroactive polymer composites, shape memory alloys and thermally expandable polymers are most frequently used and investigated micropumps. In contrast to that non mechanical group consists of following micropumps types: magnetohydrodynamic devices, electrohydrodynamic micropumps, electroosmotic micropumps, bubble-type, evaporation-type micropumps, and electrowetting and electromechanical micropumps. They have no moving mechanical parts and actuate fluids via electroosmotic, electrowetting and hydrodynamic effects, transforming non mechanical energy to some extent into kinetic momentum so as to drive the fluid contained inside an organization of designed microchannels. Traditionally, micropumps have been used for a long period of time in ink jet printers together within the microelectronic cooling applications, and finally in the field of the fuel cell industry, but recently they gained increased attention for the use in various biomedical purposes such as transportation of the medical specimens, samples and reagents flows in so called micro total analysis systems which are originally developed in order to obtain precise delivery, mixing, reaction and analysis processes on a single platform. The final goal with using micropumps is that they should obtain the ability to accurately control the fluid flow level together with absolute regulation of the infusion volume whereas at the same time accomplishing low resources consumption with a minimal backflow pressure accompanied by physiologically safe actuation. According to all these requirements it is understandable that many of the currently described and designed micropumps still need to go through substantial modifications before integration into commercial and practical applications, and consequently**,** getting a hold of a specific micropump that is safe, suitable and acceptable for in vivo application, for specific medical procedure still presents a major challenge for researchers and health care providers. It has been clearly pointed out that accurate and efficient control of droplet generation is of outmost importance when it comes to droplets microfluidics applications that span from basic material production to complex lab-on-a-chip systems.

The techniques for droplet generation are passive or active. In passive methods, droplets are generated without additional external actuation, while in active methods the use of additional energy input in promoting interfacial instabilities for droplet generation is necessary. For both of the above mentioned methods in depth understanding and clarification of underlying mechanisms could be useful for efficiently emerging recent techniques meeting different requirements that are continuously ascending from possible applications. There are several configurations used in droplet generation systems including microfluidic cross-flow, co-flow, flow-focusing, and step emulsification configurations, and, also there are many contemporary methods that employ either external forces from electrical, magnetic and centrifugal fields or techniques of modifying intrinsic properties of flows or fluids, for example velocity, viscosity, interfacial tension, channel wettability, and fluid density, with a primarily goal focused on their implementations and actuation devices [42].

Biosensors are defined as a sensing device that incorporates a biological sensing element and a transducer to produce electrochemical, optical, mass, or other signals in proportion to quantitative information about the analytes in the given samples. On the other hand, the microfluidic chip represents the scale down platform with some beneficial properties such as economic analysis that requires low component consumption, reduced specimen volumes and reduced handling time. As a result, the proper and carefully chosen arrangement of biosensors and microfluidic chips improves analytical capability and contributes to increased number of possible applications [43]. From a historical perspective, a biosensor is created by linking a biological component with a physiochemical detector and the general structure of biosensors consists of analyte recognition, signal transduction, and readout.

Optical detection systems are the group of complex arrangements recently introduced in the field of microfluidics, where the integration of micro-optical functions into microfluidic devices has been performed. In all optical detection devices, sensor dimensions and geometry still strongly affect the detection limits, primarily because of the analyte transport limitation and not because of the signal transduction limitation. When it comes to the level of analysis, the micro or nanoscale sensors are limited to picomolar order detection for practical time scales[44].

A lab-on-a-chip integrates and implements multilaboratory functions in a miniaturized microfluidic device that deals with extremely small volumes of fluid, enables rapid sample screening, analyses targeted agents, and manipulates fluid or analytes.

More precisely, enabling control of fluids on micro-scale, microfluidics chips or lab-on-chips can be used in numerous practical applications such as: micromixers, micro-pumps, droplet generation, biosensors, optical detection systems, and many others.

During previous years, various technologies were used for fabrication of microfluidic devices, to mention some of them, most frequently applied: PDMS, LTCC, 3D printing, xurographic technique, dry film lamination (ORDYL), etc. All of them resulted in expanding microfluidic area to many different fields of application. PDMS polymer has many advantages for microfluidic chip such as biocompatibility, optical transparency (in the range 240 - 1100 nm) and mechanical flexibility and stretchability [45]. These properties open new fields of application for PDMS-based microfluidic chips for creation of organs-on-chips [46] or point-of-care diagnostics [47]. However, for microfluidic devices PDMS process requires non-trivial lithography method, for design optimization it is necessary to repeat the complete fabrication flow [48] and manufacturing of circular channels is really challenging task [49]. To solve mentioned drawbacks, other authors suggested some unconventional techniques, for instance, using lubricant-infused mould [50], combining PDMS membrane with SU-8 and quartz [51], developing materials with better performances than PDMS [52]. Microfluidic devices can be fabricated also in ceramic-based LTCC technology, thanks to possibility to create complex multilayer structures [53]. For manufacturing of a microfluidic chip in LTCC process, usually LTCC tapes are used from various producers (CeramTec, DuPont, Heraeus, ESL, etc.) [54], laser for formation of microchannels in desired geometry, and after that lamination and sintering (in a furnace, using carefully selected thermal profile). Before firing, non-baked LTCC tapes are mechanically flexible and numerous geometrical shapes can be cut [55]. Different shapes of laser-micromachined channels were reported such as serpentine, meander, etc. [40], [56]. An important advantage of the LTCC process is opportunity to test every layer of multilayered structure, separately [57]. LTCC-based microfluidic chips have chemical and temperature stability, very good mechanical properties and possibility to be combined with structures and components from other technologies [23]. For some applications, drawback of LTCC technology can be non-transparency, thus it is necessary to perform bonding of LTCC structure with other transparent materials, such as PDMS [58], [59] or glass [60]. Disadvantage of this technology is also changing shape and dimensions of microchannels (and sometimes occlusion) during lamination or firing process [61].

The next interesting procedure for microfluidic devices manufacturing is 3D printing process, through applying additive manufacturing. This process attracted significant attention in previous period due to possibility to create very complex shapes, very quickly and cost-effectively, usually supported by thermoplastic materials, for example, acrylonitrile butadiene styrene (ABS) and polylactic acid (PLA) [62]. The

printing principle is uninterrupted layer-by-layer, and final structure is distortion and delamination-free [63]. There are several low cost printers on the market. The fused deposition modelling (FDM), Polyjet, and digital light processing stereolithography (DLP-SLA) printing techniques for microfluidic chips were compared in the article Comparing Microfluidic Performance of Three-Dimensional (3D) Printing Platforms [64]. However, limitation of this process are low resolution of fabricated channels and materials which are usually used are not optically transparent (which is very important for some microfluidic applications). The channel widths which can be achieved are approximately of 150 μm [65], but in most cases the leak-proof channels are wider than 800 μm [66]. To improve performances of 3D printed microfluidic devices, different solutions were proposed such as: using multilaterals 3D printing [67], combination of 3D printing (3D moulds) and PDMS [68], [69], [70].

Moreover, xurography can be used as rapid prototyping technique for manufacturing cheap microfluidic chips [71, 72]. This technique is cost-effective and based on cutting the PVC foils which are laminated in order to create 3D microfluidic chip [73]. The disadvantage of xurography is in uneven edges of the microchannels. Research groups in the field of microfluidics usually used one fabrication process for creation of the chips, thus there is a lack of studies which report mixing combining different methods.

Chapter IV

Materials and Methods

4.1 Materials and Instruments

Microfluidic researches have prompted technological revolutions in many scientific disciplines: electronics, microfabrication, nanofabrication, chemical synthesis, single cell analysis, pharmaceutics, medical treatment, biology, and diagnosis. The huge range of materials devoted to microfluidics is a crucial element for efficient microfluidic applications. Increased synergy between microfluidic aptitudes and material development caused rapid progress – evolution of microfluidic research in these areas. This chapter describes importance of materials in microfluidic research. Also, it refers to how advances in materials fabrication have extended the limits of microfluidic platforms and how the upgraded microfluidic capabilities are, in turn, fostering materials design. The positive feedback between material innovation and microfluidic systems is getting tighter by every discovery. The optimal selection of a suitable material selection for a targeted application is of great importance and signifies a technical challenge. [8, 11]. It is a never-ending loop.

4.1.1 Materials

The materials used for fabrication of microfluidic chips is listed below and depicted in Figure 4.1.

- PVC foil - A4 hot lamination foil (MBL® 80MIC and MBL® 125MIC, Minoan Binding Laminating d.o.o, Serbia) with the thickness of 80 μm and 125 μm - for fabrication of presented microfluidic chips or cover layers of the hybrid chips;
- Ceramtape (Ceramtape GC, CERAMTEC GmbH®, Germany) with the thickness of 300 μm - for fabrication of presented middle layer of microfluidic chips;
- Filter papers (Whatman® 1441-150, USA) with grade of 20-25 μm - for filtration pads;
- Deionised water (Grade 2 by ISO 3696 (1987)) - as liquid in microfluidic experiments
- Blue, yellow, red, green and purple water based food colorants (Aroma 1990®, Serbia) - as colorants for liquid in microfluidic experiments
- Pollen particles (isolated *typha* pollen particles) - for microfluidic particle experiments*
- Glass substrate (75 mm × 50 mm size, 0.96 mm thickness, Corning, USA)
- PDMS base and curing agent (Sylgard 184, Dow Corning, USA)
- Artificial saliva (registered under the Republic of Serbia master preparations)
- Chlorhexidine solution (Eludril Classic, Pierre Fabre Medicament, Bologna, France)
- Fluoride solution (Fluorogal Mite, Galenika, Belgrade, Serbia)
- Zinc-hydroxyapatite (Zahn-Milch, Dr. Kurt Wolff, Bielefeld, Germany)
- Casein-phosphopeptide amorphous calcium phosphate – CPP-ACP (Tooth Mousse, GC America, Alsip, IL, USA

* Curtesy of PhD Branko Šikoparja, BioSense Institute, University of Novi Sad, Novi Sad, Serbia (ORCHID ID 0000-0002-6766-4149)

PVC foils

Ceramtape

Filter papers

Deionised water

Water colours

Pollen particles

Glass slides

PDMS

Artificial saliva

Figure 4.1 Materials used for chip fabrication and experiments

4.1.2 Fabrication Instruments

The instruments – machines and small tools used for chip fabrication and experiments is listed below and depicted in Figure 4.2.

- Plotter Cutter (CE6000-60 PLUS®, Graphtec America, Inc., USA) with the 45° cutting blade (CB09U, Graphtec America, Inc., USA) and Cutting Mat (12" Silhouette Cameo Cutting Mat, USA) - for carving inlets, outlets and edges of PVC layers for microfluidic chips
- Laser (Rofin-Sinar Power Line D-100, Germany) –for cut out the Ceramtapes and filter papers
- Laminator - A4 card laminator (FG320, Minoan Binding Laminating, Serbia) – for bondage between PVC layers and PVC and Ceramtape
- Uniaxial press (Carver® 3895CEB, USA) – for bondage between Ceramtape layers
- UV exposer (UV-KUB2, Kloé, France)

- Desiccator (LLG, Germany)
- RheolabQC rotary viscometer (Anton Paar, Graz, Austria)

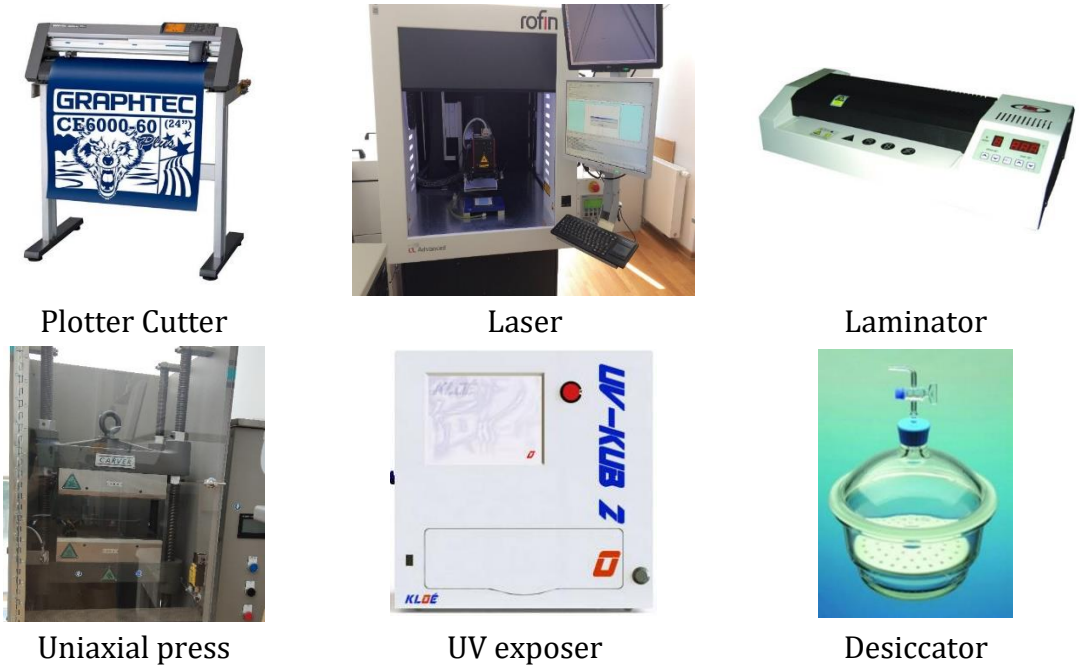

Plotter Cutter | Laser | Laminator

Uniaxial press | UV exposer | Desiccator

Figure 4.2 Machine and small tools for chip fabrication

4.1.3 Characterisation instruments

All machine and devices used in this thesis are listed below and depicted in Figure 4.3.

- Syringe pump model NE 4000 Multi Pulser, KF Technology, Italy, and camera (Digital USB Microscope, S02 (1000x), China) - for control of microfluidic flow in the chip
- Camera (Digital USB Microscope, S02 (1000x), China) for recording microfluidic flow in the chip
- Memmert oven UN20, Germany - for temperature exposure oven
- SEM for micrographs of fabricated channels (TM3030 Hitachi, Japan)
- Profiler Huwitz Panasis with bioimaging software for 3D profile of curved channels
- UV-visible spectrophotometer INESA L6S in the wavelength range between 300 nm and 1000 nm - for optical characterization
- Vector network analyser - Agilent VNA E5071C in the frequency range between 500 MHz and 8.5 GHz - For dielectric characterization

- Nanoindenter Agilent G200 - for mechanical characterization using nanoindentation method
- Pressure controller – for flow control (Elweflow, France).


Syringe pump


Camera


Memmert oven


SEM


Profiler


UV-VIS


Vector network analyser


Nanoindenter


Pressure controller

Figure 4.3 Machine and devices for chip characterisation

4.1.4 Software

Software used for preparation of the thesis, simulations and experimental data processing are listed below and depicted in Figure 4.4.

- Microsoft Office - Word - for thesis writing
- Microsoft Office - Power point – for diagram construction and presentations
- Microsoft Office - Excel – for data calculations
- Microsoft Visio - for design and diagram drawing
- GraphPad Prism - for diagram drawings
- LibreCAD - for chip design drawings
- COMSOL - for chip simulation.

Figure 4.4 Used software

4.2 Methods and Instruments

In general, algorithm of realisation an idea to product consists of five steps: 1. an Idea (Design), 2. Verification of that idea (Simulation), 3. Fabrication, 4. Testing (Characterisation) and 5. Product launching (Figure 4.5).

Figure 4.5 Path from idea to prototype[*]

[*] https://curatti.com/convert-product-idea/ accessed on 30.06.2019

Methods used in this thesis covering first for steps of the above mentioned algorithm:

1. Methods for Design,
2. Methods for Simulation,
3. Methods for Fabrication and
4. Methods for Characterisation.

4.2.1 Model Design

Design of a microfluidic chip is a one or a series 2D or 3D vector drawings, depending of a simulation programme and fabrication technique. For vector drawings Microsoft Visio® and LibreCAD® programmes are used. These software were selected for drawing microfluidic designs based on previous experience and availability to author.

Model design is an initial step in every idea realisation process. Some of the designs used in this thesis are common designs, designs widely known and used while, others are entirely new and innovative. Common model designs are chosen to demonstrate a certain characteristic or set of characteristics, achieved with novel fabrication techniques, when comparison with other technologies was needed or requested. New model designs, concepts in this thesis, demonstrated novel ideas and their success or failure in terms of feasibility, usability and quality. The designs used and made for this thesis are described in detail in section 5.1 of this work.

4.2.2 Model Simulation – COMSOL Multiphysics®

COMSOL Multiphysics® is a general-purpose platform software for modelling science and engineering applications. Among numerous features (electromagnetics, structural mechanics, acoustics, heat transfer, and chemical engineering behaviour) this software is suitable for simulation of microfluidic behaviour (fluid flow) in the channels and chambers. This platform is powerful surrounding for processing and presentation of acquired results. It is a common tool for simulation of microfluidic experiments and it is widely used.

The Microfluidics Module are easily-operated tools for studying microfluidic devices. Important applications include simulations of lab-on-a-chip devices, digital microfluidics, electrokinetic and magnetokinetic devices, and inkjets. The Microfluidics Module includes ready-to-use user interfaces and simulation tools, so called physics interfaces, for single-phase flow, porous media flow, two-phase flow, and transport phenomena (Figure 4.6).

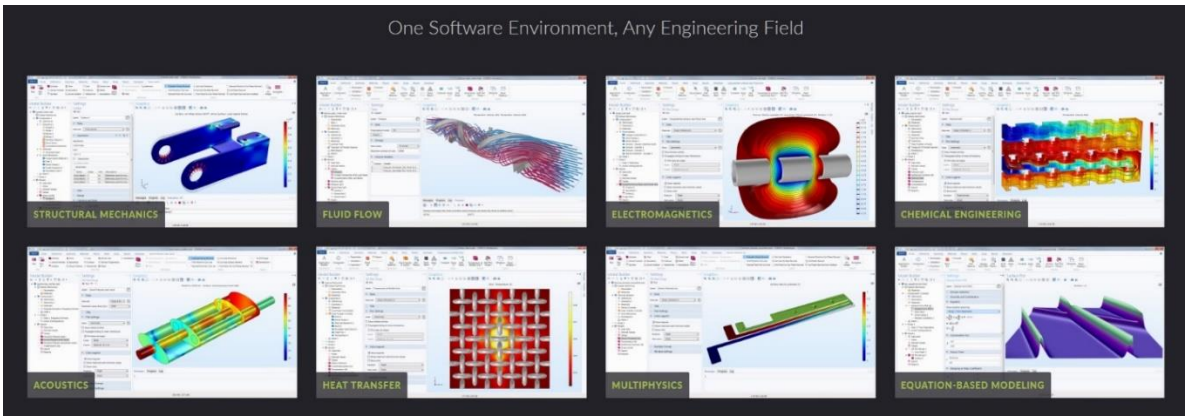

Figure 4.6 Powers of COMSOL simulation platform through different fields[*]

Microfluidic flows occur on length scales that are orders of magnitude smaller than macroscopic flows. Manipulation of fluids at the microscale has a number of advantages – typically microfluidic systems are smaller, operate faster, and require less fluid than their macroscopic equivalents.

This is apparent in the fluid flow itself as the viscous forces, which are generated by shear over the isovelocity surfaces, dominate over the inertial forces. The Reynolds number (Re) that characterizes the ratio of these two forces is typically low, so the flow is usually laminar.

COMSOL's general-purpose multiphysics features are uniquely suited for handling the many microscale effects that are utilized in microfluidic devices. It is easy to set up coupled electrokinetic and magnetodynamic simulations – including electrophoresis, magnetophoresis, dielectrophoresis, electroosmosis, and electrowetting. In addition, chemical diffusion and reactions for dilute species functionality included in the module enable you to simulate processes occurring in lab-on-a-chip devices. For simulating rarefied gas flows, you can use the specialized boundary conditions that activate flow simulation in the slip flow regime. The Microfluidics Module also provides dedicated methods for simulation of two-phase flow with the level set, phase field, and moving mesh methods. For each of these, the capabilities of the Microfluidics Module include surface tension forces, capillary forces, and Marangoni effects.

To model a microfluidic device, you begin by defining the geometry in the software by importing a CAD (computer-aided design) file or via the geometry modelling tools that are built into COMSOL Multiphysics. For importing geometry models, several choices are available to you: the CAD Import Module, for import of mechanical CAD models; the ECAD (electronic computer-aided design) Import Module for import of electronic layouts; and the LiveLink™ products for CAD for a direct link to models created in a

[*] https://www.comsol.com/ accessed on 30.06.2019

dedicated CAD software package. In the next step, you select appropriate fluid properties and choose a suitable physics interface. Initial conditions and boundary conditions are set up within the interface. Next, you define the mesh. In many cases, COMSOL's automatically created default mesh, which is produced from physics-dependent defaults, will be appropriate for the problem. A solver is selected, again with defaults appropriate for the relevant physics, and the problem is solved. Finally, you can visualize the results.

The Fluid Flow interfaces use physical quantities, such as pressure and flow rate, and physical properties, like viscosity and density, to define a fluid-flow problem. The physics interface for laminar flow covers incompressible and weakly compressible flows.

Simulations in this thesis are done in Microfluidic module and described in detail in section 5.2.

4.2.3 Fabrication - Plotter Cutting

Xurography is a technique which structures thin foils with a plotter knife. This is a low-cost rapid prototyping technique. Plotter cutter used in this technique is the same that the sign industry conventionally uses for cutting graphics in glue vinyl films. Considering plotter cutter resolution there are two different parameters that can be detected, one is the mechanical resolution – meaning resolution of a step motor, while other is the addressable resolution – resolution of the programmable step size. Three types of cutting methods can be detected [72] and application requirements approve which one should be used.

1. **Drag knife** - Drag knife cutting uses a swivel blade that follows the cutting path of the feature as it moves relative to the material. This introduces lateral force from the blade at sharp feature corners, which can break the tip when cutting harder or thicker substrates.
2. **True tangential** - Controls blade position with an addressable motor. When cutting corners, the blade lifts completely out of the material and rotates to the new direction. Line segments can be over-cut to ensure the material is completely cut from top to bottom at feature corners. This is useful when cutting thick materials.
3. **Emulated tangential** - Uses a swivel blade but lifts the blade just to the surface of the material before pivoting on the tip at a feature corner. This reduces lateral force on the blade. Over-cuts in emulated tangential plotters bring the

blade into position before initiating a cut and ensure feature corners are completely severed from the rest of the material [72].

The cutting plotter used in this thesis is CE6000-60 PLUS, Graphtec America, Inc., USA with the 45° cutting blade (CB09U). Type of this plotter cutter is drag knife. Engraved microchannels in the PVC laminating films were cut on this device with the support of the cutting mat.

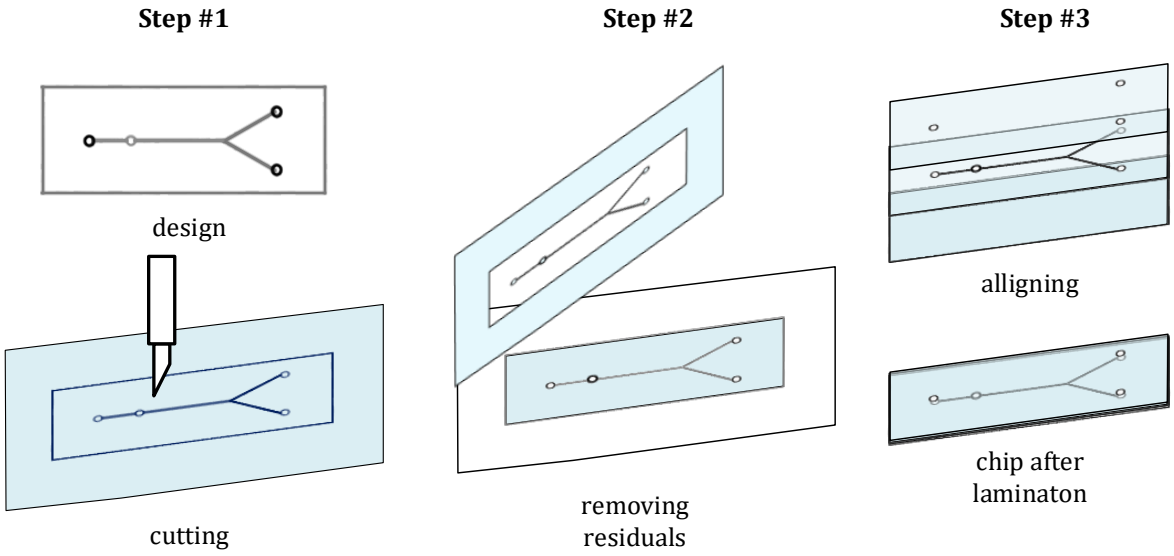

Figure 4.7 Plotter cutter fabrication steps

Simple 3 step cutting process has been used. Step #1 - preparation and cutting, Step #2 removing the residuals and Step #3 aligning and hot lamination finishing (Figure 4.7). First step involves preparing the PVC sheet and cutting mat -clean it from the particles, such as dust, put it under the grit roller (Figure 4.8), adjust cutting design and parameters in the cutting software and run the cut. Second step includes removing the residuals and detaching the PVC layers from the mat. Final step of this technique is hot lamination process. This step repeats one time fewer than the number of layers. Namely, first two layers, with the most details in their design are laminated and then one by one other layers are connected.

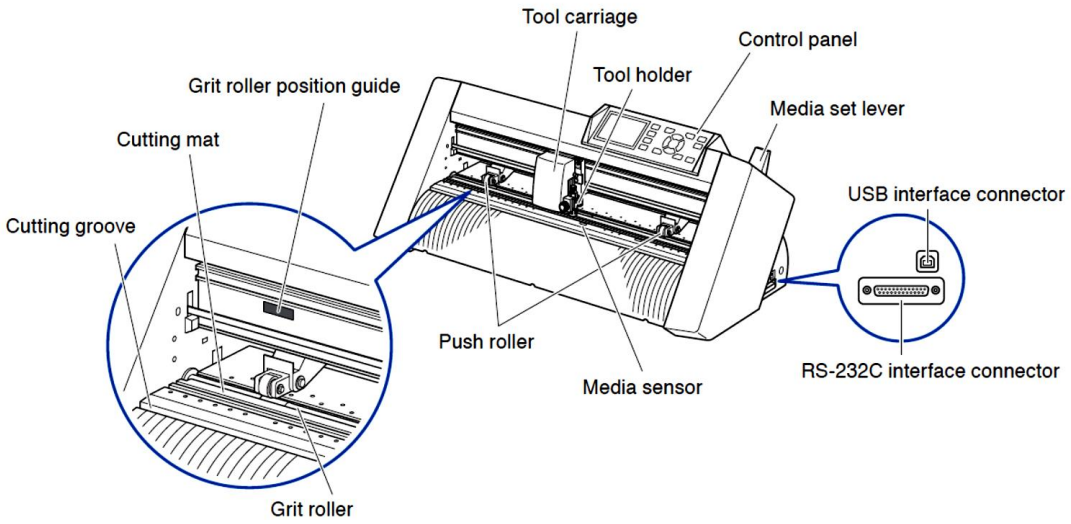

Figure 4.8 Graphtec® CE6000-60 PLUS Parts and Nomenclature

4.2.4 Fabrication - Laser Cutting

Laser manufacturing process enables fast and precise cutting of the different structure designs. A Nd:YAG (Neodymium-doped Yttrium Aluminum Garnet) laser with the operating wavelength of 1064 nm (Rofin-Sinar Power Line D-100, Germany) can be used for cutting, engraving, etching, or marking of metals and plastics. This type of laser has found a lot of applications in different fields of engineering and medicine. The precise cutting and engraving possibilities found the application for channel fabrication in different manufacturing technologies of microfluidic chips.

The main components of the laser system are presented in Figure 4.9. The laser system contains a laser head, marking head and the system for cooling, and supplying the laser. Components of the laser system are placed in the supply cabinet that is closed with a shutter during the cutting process because of the danger of the direct and scattered laser beam. The PC is connected to the laser by software Visual Laser Marker and the cutting process control and visualization are enabled with the camera on the marking head.

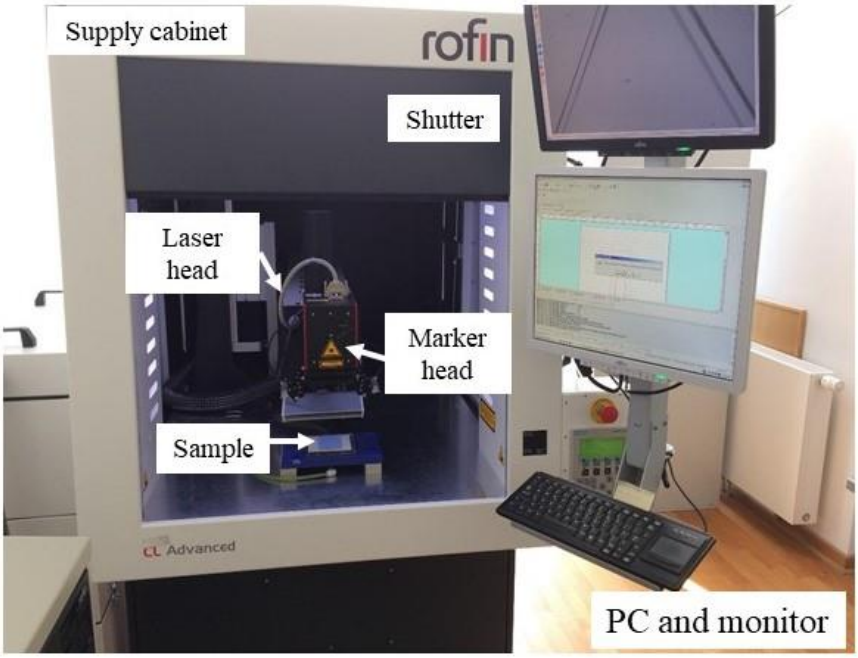

Figure 4.9 The laser system contains supply cabinet with laser and marker head, and cooling and supplying system. During the cutting process, the system is closed and the camera inside the cabinet is showing the cutting process on the monitor

The laser beam is produced in the laser head and the beam manipulation is done inside the marking head of the laser system. Figure 4.10 presents the scheme of the system that is connected to the PC and uses PC signals, according to the cutting structure design, for manipulation of two mirrors along x and y direction. In that way, the laser beam is focused on the sample and the projected design of the structure is transferred to the laser marking field.

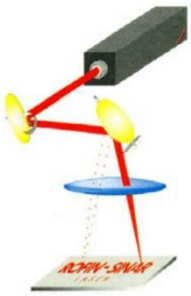

Figure 4.10 Manipulation of the laser beam according to the PC signal inside the marker head

In order to manufacture precise structure designs, the set of cutting parameters have to be optimized for a specific material. A laser parameter set contains many parameters that can be adapted for different material cutting. The most relevant parameters for cutting are diode current. frequency, speed of the marking beam and a number of

repeating marking processes. The laser power depends on the current and frequency values, and the cutting process is the most sensitive to these two parameters. If the current intensity is very big, the material can be melted or damaged. On the other hand, a low value of the current will not cut the material. The frequency parameter determines the operational mode of the laser. In the pulse mode, frequency determines the number of pulses of the laser beam and the laser is emitting the short pulses with high peak powers. When the frequency is set to zero, the laser is working in the continuous wave (CW) regime and a laser beam is continuously emitted. The choice for using pulse and continuous mode is made depending on the cutting material. The cutting speed parameter determines the speed of the moving marker beam along the material and a number of the repeating marking processes can be set for repeating the same design cutting.

The optimal set of parameters depends on the type of material and material thickness. If the parameter set is not optimized, the material can be damaged, melted or burned during the cutting process or the structure would not be cut well. The parameters of laser cutting and their range of manipulation are presented in Table 4.1.

Table 4.1 Laser parameters and their ranges that can be used in the cutting process.

Parameter*	Range
Current	up to 40 A
Frequency	up to 65 kHz
Speed	up to 500 mm/s

4.2.5 Fabrication - Photolithography and PDMS fabrication

There are two main steps to manufacture a microfluidic chip in PDMS technology: (1) fabrication of a mould and (2) replica moulding. Mould can be created in many different ways. In the literature most used method for mould fabrication is SU-8 photolithography [52, 74-77] and in the last years, beside SU-8 photolithography, dry film photolithography [78, 79]. Fabricated mould examples for both techniques are shown in Figure 4.11.

* In addition to these parameters there are 3 more but irelevant for this research type.

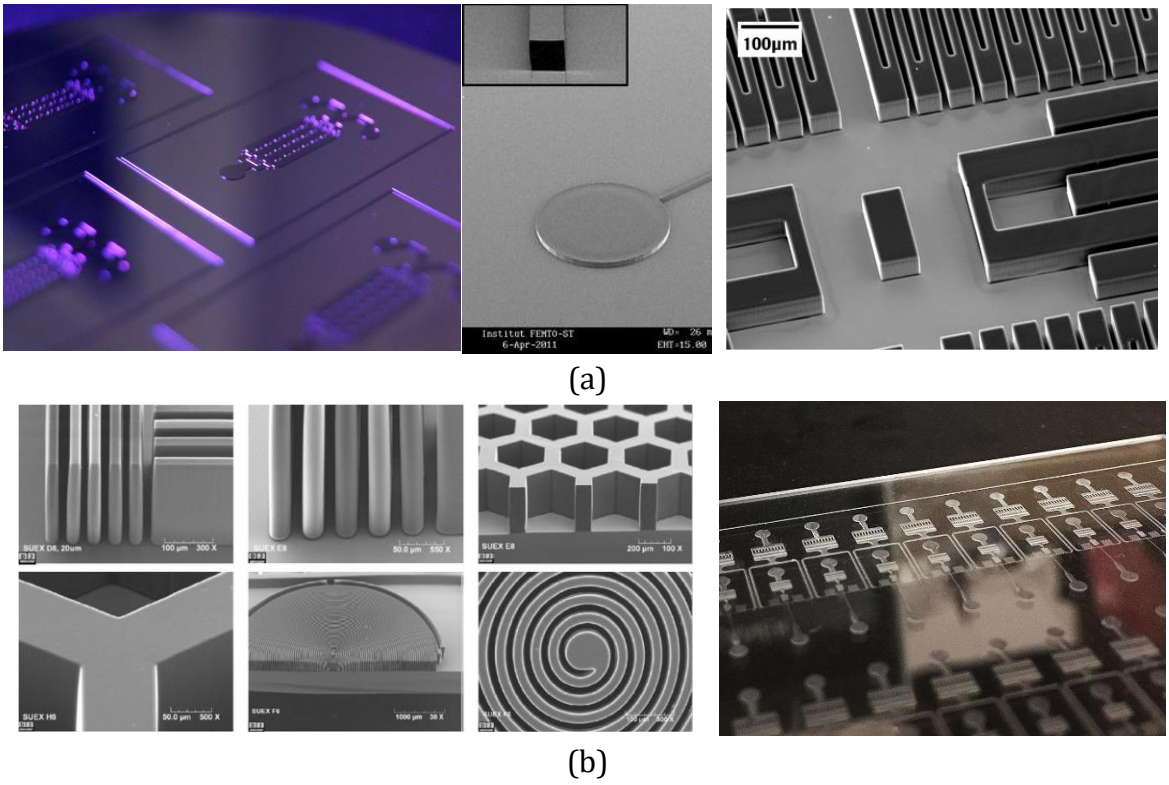

Figure 4.11 Moulds examples (a) SU-8 Photolithography s [75, 80, 81]; (b) Dry film lithography [80, 82]

4.2.5.1 Photolithography with SU-8 on Si wafer

Photolithography can be used on flat surfaces to pattern a wide variety of features. The main process is shown in Figure 4.12. For advanced applications, a single layer structure is not enough - a multiple layer structure should be generated. This complex layered structures can be produced by repeating the main process using multiple masks and aligning each newly deposited or etched layer to previously created features. To avoid contamination and unintentional exposure of the photoresist, most of the procedures in this process are performed in a yellow-lit cleanroom.

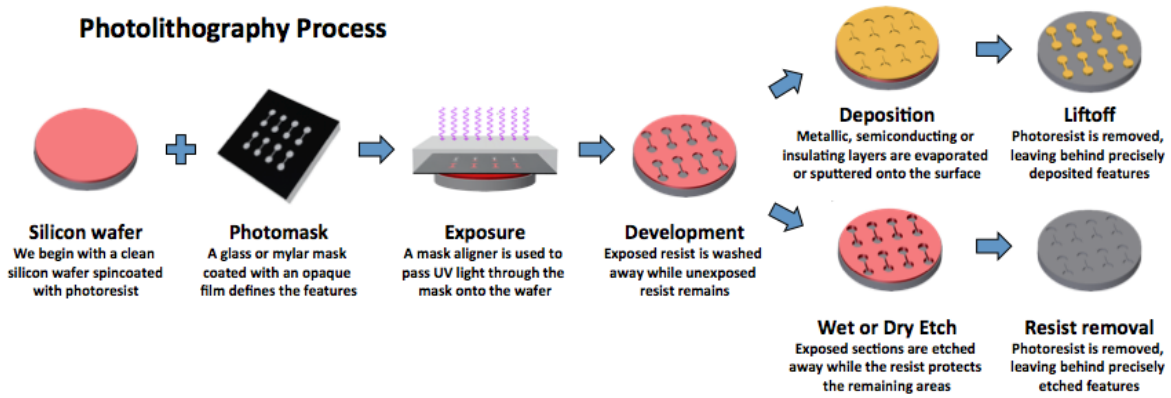

Figure 4.12 Photolithography process steps [83]

4.2.6 Characterisation – Syringe pump

Experiments, in this thesis, which required steady and precise flow were conducted with syringe pump. Syringe pump (Figure 4.13) is a device which performs infusion (some include infuse and withdraw capability) of fluid. This infusion is gradually administrated small amounts of fluid. This device is usually used for controlled drug delivery to the patient, but it showed very handy for chemical and biomedical research experiments.

Figure 4.13 Syringe pump used for experiments in the thesis

Characteristics of the pump:

- Infuses and withdraws.
  - Accepts 2 different sized small syringes or large syringes, up to 60 cc and partially filled.

  - Dispense continuously at a fixed pumping rate as low as 1.459 µl/hr with a 1 mL syringe or as high as 127.2 ml/min with a 60 mL syringe.
  - Change pumping rate and direction while pumping.
  - Selectable rate units: µl/hr, µl/mn, ml/hr, ml/mn.
- Dispense a specified volume.
- Total volume pumped separately accumulated for infusion and withdrawal.
- Dispense according to a pumping program to:
  - Pre-program dispense volumes.
  - Each volume can be different.
  - Automatically change pumping rates or pumping direction.
  - Ramp up or down the pumping rate.
  - Timed delays between dispenses.
  - Automatically pause the program and wait for the user to continue the dispense.
  - Synchronize dispenses with other equipment or pumps to change pumping rates in reaction to a sensor or signals from other pumps.
  - Send signals to other equipment.
  - Change pumping rates in reaction to a sensor.
  - Program the audible alarm to beep at any time to alert the operator.
- Operates stand-alone, from an RS-232 computer network or from the TTL logic interface.

4.2.7 Characterisation – Pressure Controller

Pressure controller was used when more agile control of the flow was needed comparing to syringe pump. Pressure controller (Figure 4.14) is a device that uses air pressure to push the fluid.

Figure 4.14 Pressure controller used for experiments in the thesis

Pressure controller characteristics:

- Pressure stability: 0.005 %
- Sensor resolution: 0.006 %
- Settling time: 40 ms
- Response time: 9 ms
- Minimum pressure increment: 0.006 % (12.2 μbar)
- Input pressure: 1.5 bar – 10 bar
    - Non corrosive
    - Non explosive
    - Dry and oil-free gasses
- Liquide compatibility: no liquid should enter the pressure controller (any aqueous or organic solvent, oil or biological sample solution can be propelled)
- Range:
    - 3 channels up to 200 mbar
- Pulsation free - No pulsation with high and low flow rates
- In-house piezoelectric optimization & calibration and a challenging bench testing of technical features enabling such performances
- Internal & external trigger connectors

4.2.8 Characterisation – SEM

An electron microscope is a microscope that uses a beam of accelerated electrons as a source of illumination. There are 4 different types of electron microscopes:

1. Transmission electron microscope (TEM)
2. Scanning electron microscope (SEM)
3. Reflection electron microscope (REM)
4. Scanning transmission electron microscope (STEM)
5. Scanning tunnelling microscopy (STM)

SEM uses a focused beam of electrons for scanning the sample surface and forming an image. Since the electrons interact with the atoms from the sample surface, this type of electron microscopy can determine surface topography and composition. An image is produced as a raster scan pattern, which is combination of the beam position beam and detected signal intensity.

Hitachi High-Tech launched the world's first tabletop/benchtop electron microscope. Model TM-3030, shown in Figure 4.15, was developed to provide a more user-friendly and easily accessible scanning electron microscope equipped with cutting-edge technologies.

Basic performance:

- The TM3030/TM3030Plus are equipped with premium signal detectors which have been incorporated in FE-SEM (Field Emission Scanning Electron Microscopes) and VP-SEM (Variable Pressure Scanning Electron Microscope) and provide unparalleled image quality.
- The detectors can be effectively operated under low-vacuum conditions and can support SE (secondary electrons) and BSE (backscattered electrons) image observation without metal coating.
- The TM3030 can be used to observe BSE images. The TM3030Plus can be used to view BSE images, SE images, and mixed images. Image modes can be switched simply with a click of a button on the GUI (graphic user interface).
- Magnification range: 15 to 60,000x (Up to 240,000x with digital zoom)

Figure 4.15 TM 3030 Hitachi Scanning Electron Microscope

This microscope is exceptionally user friendly, operation and sample preparation are easy and the results were excellent for research conducted in this thesis. TH 3030 consists of a main unit and supporting computer. Main unit (Figure 4.16) has control for vacuum/air chamber and manual sample position control in two planar axes.

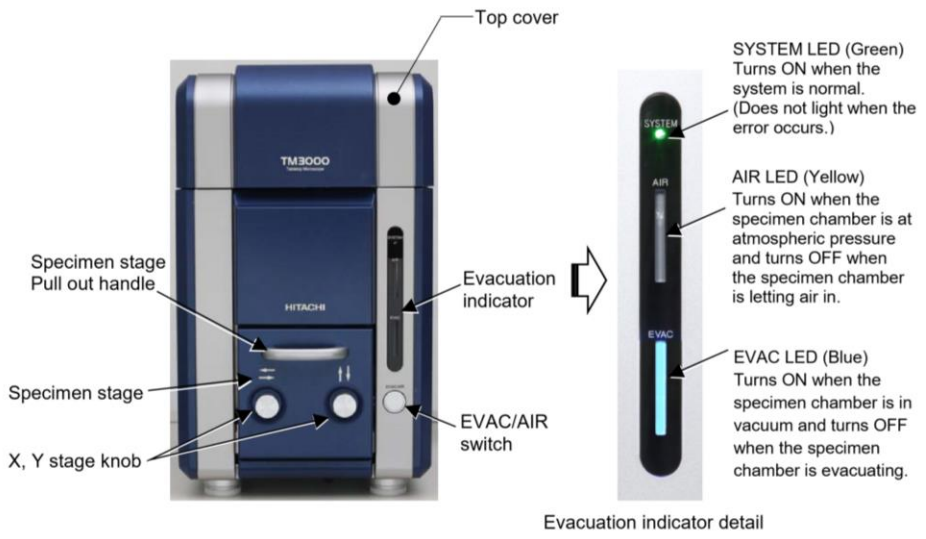

Figure 4.16 TM3030 main unit

TM 3030 software (Figure 4.17) has simple and efficient basic controls for acquiring SEM micrographs. Image can be acquired in one of 4 modes (Compo, Shadow 1, Shadow2 and Topo) depending on sample nature and wanted characteristics. Auto focus as well as auto brightness and contrast works in most of the cases, especially for flat samples.

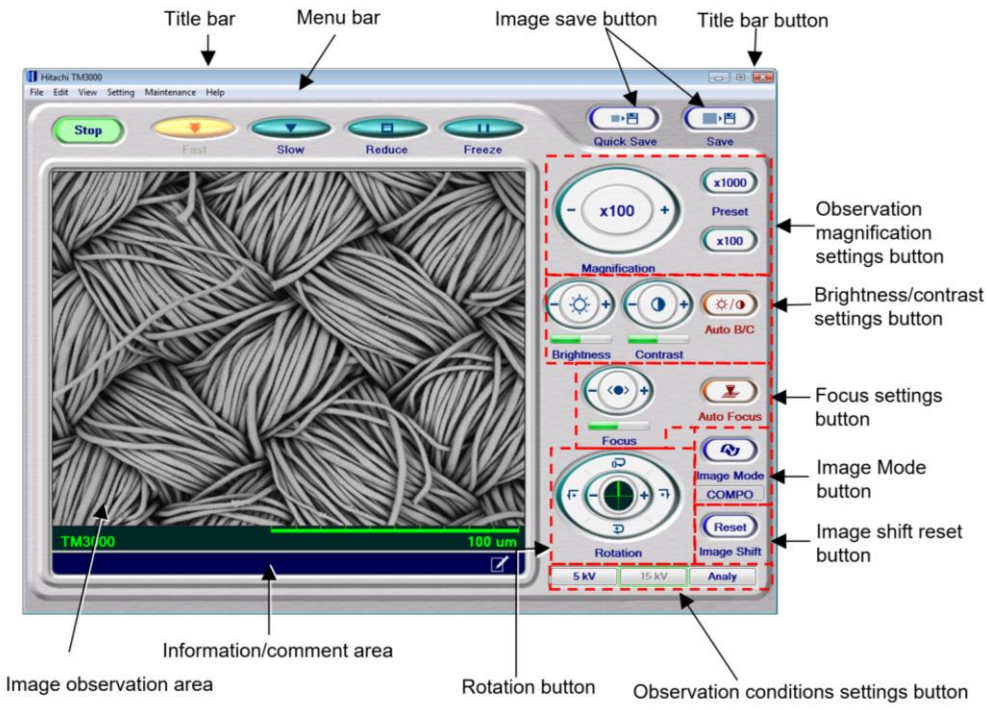

Figure 4.17 TM 3030 software operation window

4.2.9 Characterisation – Optical Profilometry

For characterisation of fabricated microfluidic chip components: 2D measuring of dimensions and 3D profile extraction Huvitz BioImager® HRM-300 with Panasis software (Figure 4.18) was used. Profilometer is an instrument mainly used for surface characterisation measurement and 3D representation of structures. In this thesis Profilometer is used for observing fabricated microfluidic designs, their parts, quality of fabricated cuts and carvings as well as layer thickness and roughness of the sample.

Figure 4.18 Profiler - Huvitz BioImager HRM-300 with Panasis software

4.2.10 Characterisation – Optical transmission

Spectrophotometry is a commonly used technique for the estimation of material optical properties in different wavelength ranges of the electromagnetic specter. By UV-Vis spectrophotometry reflection, transmission and absorption of the light passing through the sample can be quantified in visible, UV, and near-infrared (NIR) ranges.

Figure 4.19 presents the UV-VIS spectrophotometer that was used for measurements performed in this thesis. The device contains movable cell holders adapted for cuvettes, but it can also be adapted for thin material sheets. Multiple cell holders enable simultaneous measurements of different samples. During measurements, the lid closes the system in order to avoid the influence of the environmental light on the measured results. The device uses a deuterium lamp for UV light emission and a Tungsten filament for visible and NIR light emission. During measurements, the incident ray passes through the sample and the results are detected as a transmitted ray. The relative value of the light intensity between the two beams enables quantification of transmitted and absorbed light by the sample. The wavelength range covered with the UV-VIS spectrophotometer is 190 – 1100 nm.

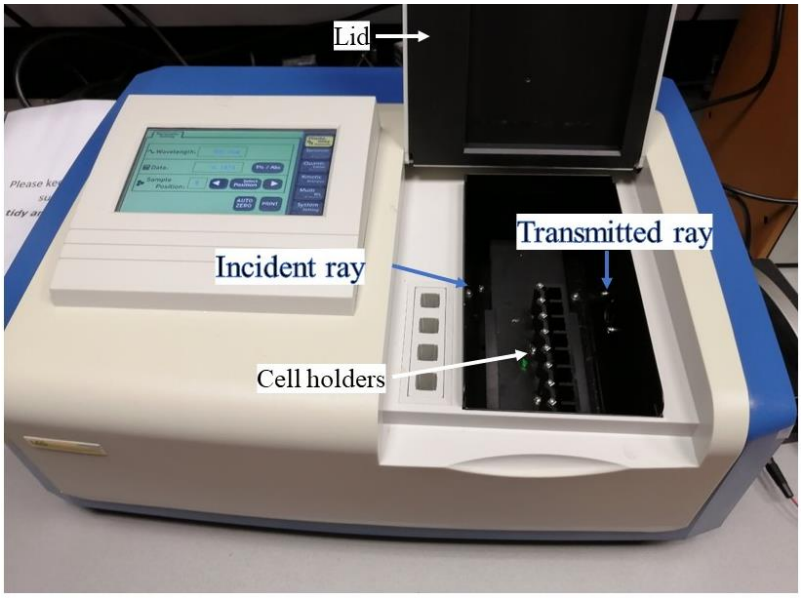

Figure 4.19 UV-Vis spectrophotometer - DSH-L6-L6S

4.2.11 Characterisation – Nanoindentations

All the nanoindentation analysis were performed using a Nanoindenter G200 (Agilent Technologies®, Figure 4.20(a), under dry conditions, using a Berkovich tip (Micro Star

Technologies®). Tests accuracy was verified by performing indentation tests in a standard reference material (in conformance with ISO 14577-3) – Corning 7980 (high purity synthetic amorphous silicon dioxide manufactured by flame hydrolysis). The obtained values were found to be in agreement with those reported in the Certification of Calibration of this material measured sonically at room temperature: elastic modulus around 74 GPa using Poisson ratio of 0.18. Also, the repeatability was verified by comparison of the values of the physical properties of the reference material before and after performed measurements on microfluidic chips. The system has force and displacement resolutions of 50 nN and 0.1 nm, respectively. The apparatus is enclosed in an insulated cabinet to provide thermal stability and sound noise reduction. A Berkovich diamond indenter tip was used for all the measurements. The indented samples were located in the microscope, and then positioned beneath the indenter using the x-y table with piezo motors. The distance between the indenter and the microscope was constant during the test. Microscope to Indenter calibration is preformed, meaning that the desired location under the microscope was the location of performed measurement with accuracy of 1.5 μm. For each sample, same indentations protocols were used.

(a) Nanoindenter G200

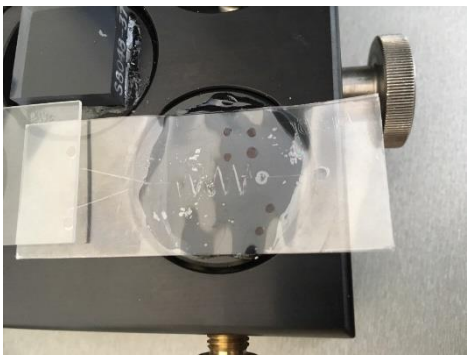

(b) Sample tray with PVC chip

Figure 4.20(a) Nanoindenter, (b) PVC chip ready for indentation

Chapter V
Design, Simulation and Fabrication

5.1 Design

Various microfluidic chip designs are made for this thesis for different experimental purposes. Moreover, one design has been made for the characterisation purpose of SAVA technology. As mentioned earlier, some designs are commonly in use while others have been novel.

5.1.1 Channel width characterisation design

The main element of every microfluidic chip design is a channel. To be able to characterise the channel width of chips fabricated in SAVA technology a design with channel width variations has been made. The design has been shown in Figure 5.1 and the channel width variations have been as following 50 µm, 100 µm, 200 µm, 300 µm, 500 µm and 1000 µm, starting from left to right.

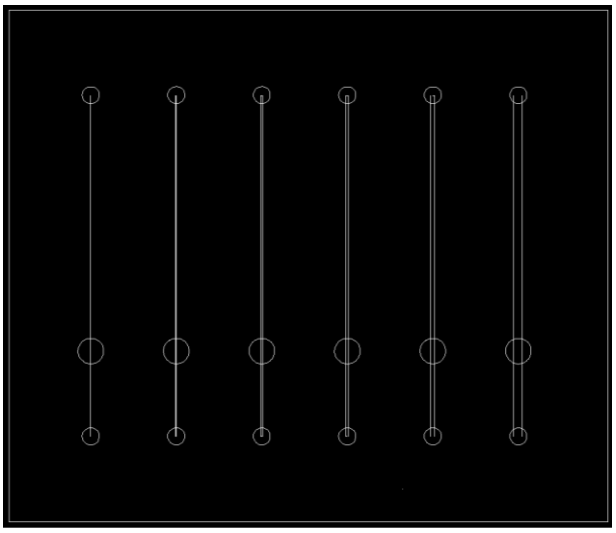

Figure 5.1 Different channel widths

5.1.2 Chamber width characterisation design

Next to the channel, vital element of microfluidic chips are chambers. To be able to characterise the maximum chamber size which is possible to fabricate in SAVA technology a design with chambers with different sizes has been made. The design has been shown in Figure 5.2 and the rectangular chamber width variations have been as following 2 mm, 3 mm, 4 mm, 5 mm and 6 mm, with length of 15 mm, starting from bottom to top while circle diameter correspond to rectangular width respectively.

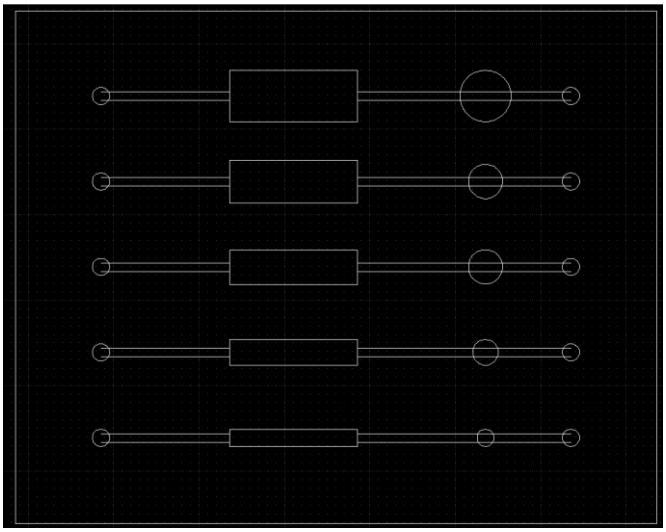

Figure 5.2 Different chamber areas

5.1.3 Simple channel standard design

This is an elementary, common design. This design is used for application examples with saliva as well as pulse mixing measurements.

Y-channel chips without any obstacles inside of the channel, with the input channels set at an angle of 60°, and the width of 800 µm - 1000 µm for PVC chips and 200 µm for SAVA chips. Figure 5.3 reveals designs of the chips (a) in xurographic technique and (b) in SAVA technique.

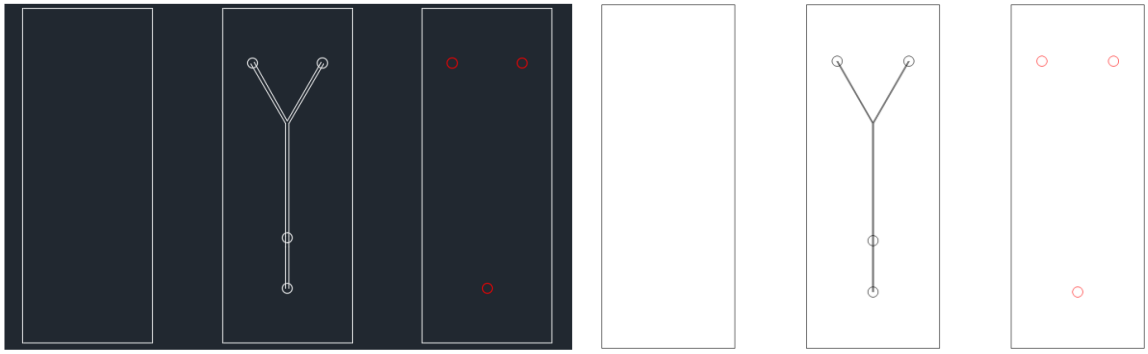

(a) (b)

Figure 5.3 The scheme of the chip design in: (a) PVC technology [84] and (b) SAVA technique

5.1.4 Micromixer standard design with parallelogram barriers

This is a common design. Optimisation for xurographic technique was necessary.

Design of the micromixer chip with parallelogram barriers implies definition of dimensions and drawing of chip size in total (Figure 5.5 blue lines), size and position of inlets and outlet (Figure 5.5 red lines) and actual functional design (length, width and position) of channel with parallelogram barriers (Figure 5.5 black lines). More precisely the design contains one Y junction, channel with 18 parallelogram barriers, 2 inlets and 1 outlet.

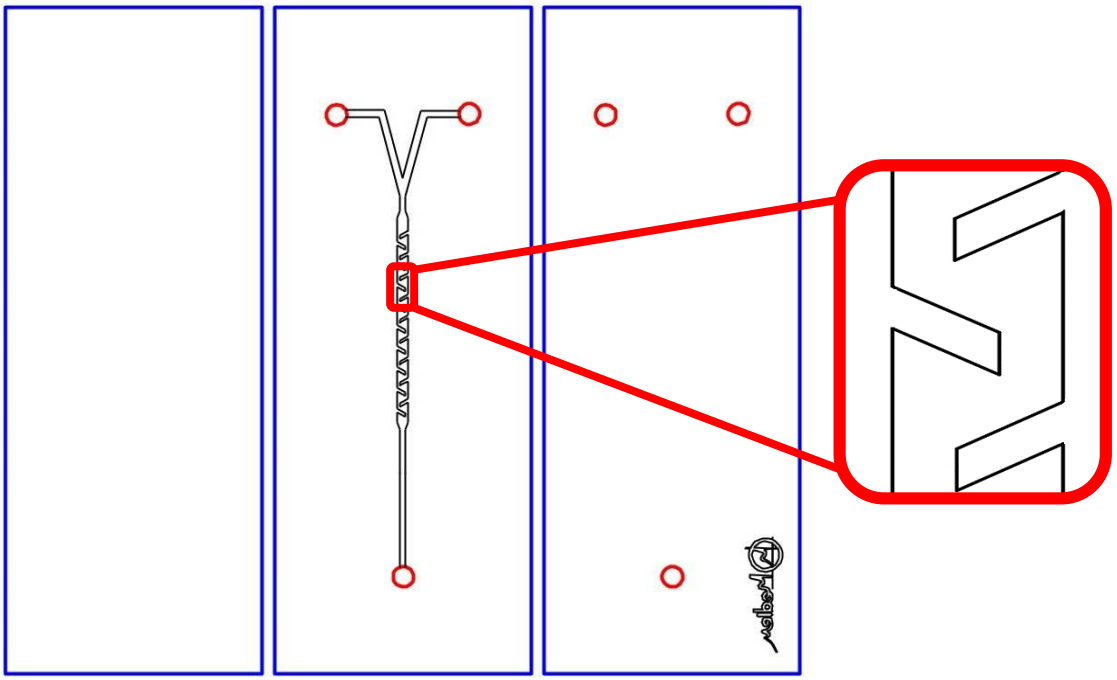

Figure 5.4 Micro-mixer chip design used mainly with PVC technology

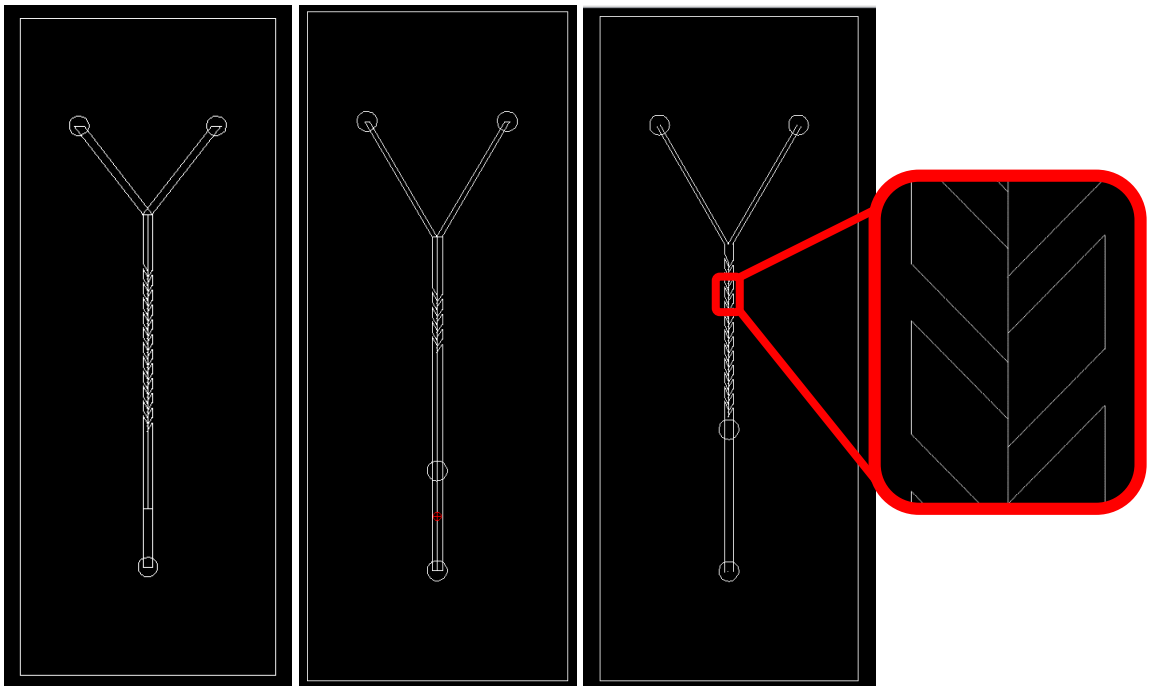

Figure 5.5 Micro-mixer chip designs used for SAVA technology

Two different designs are fabricated in xurographic technique. Parallelogram barrier length is variated to be 75 % and 60 % of channel width, calculating 768 μm and 526 μm correspondingly. Other dimensions of the chip design are the same: barrier width, channel width, channel width in Y junction (input channel width) and inlet/outlet

diameter and they are 326 μm, 1024 μm, 667 μm, 2000 μm respectively. Total number of parallelogram barrier pairs, in both design, is 9. It is lower than simulated 10 because of the limitation in the space of the used chip holder.

5.1.5 Micromixer novel design

This is a novel design.

For microfluidic mixing performance testing beside well known microfluidic design with parallelogram barriers and innovative semi-circular design was created. This novel design, due to its complexity, was fabricated in PDMS technology. Fabrication of this design in xurographic and SAVA hybrid technology was not possible, at least in current state of these technologies, due to islands that exists in the channel. Design consist of consecutive array of 10 blocks in inlet to outlet direction. Each block have five semi circles positioned as in Figure 5.6.

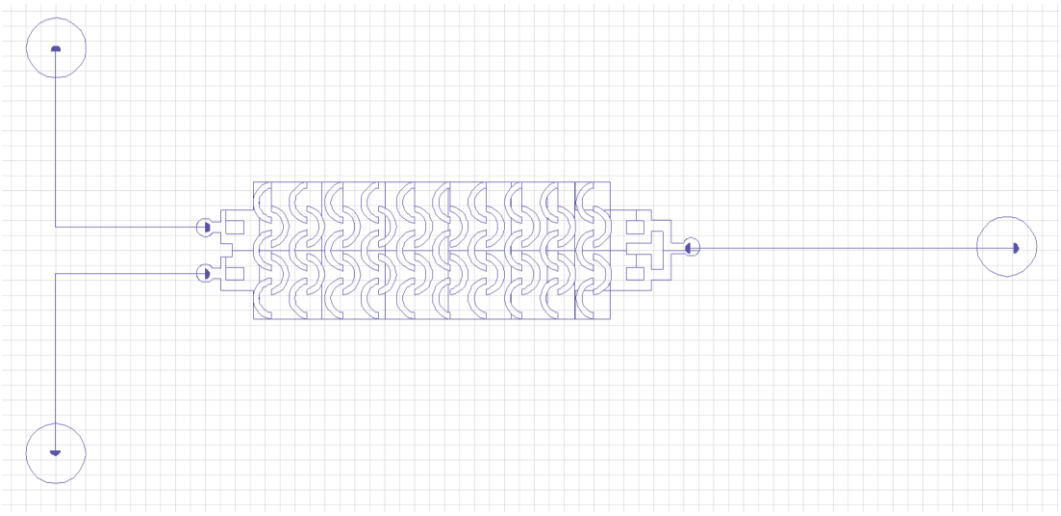

Figure 5.6 Novel design of microfluidic mixer [85]

Fabricated structure had following dimensions: total length of channel – 6000 μm, total width of the channel – 2000 μm, semi-circle width 50 μm (Figure 5.7). Structure had array of 10 blocks, where each block had 5 semi-circles, which was in accordance with the design.

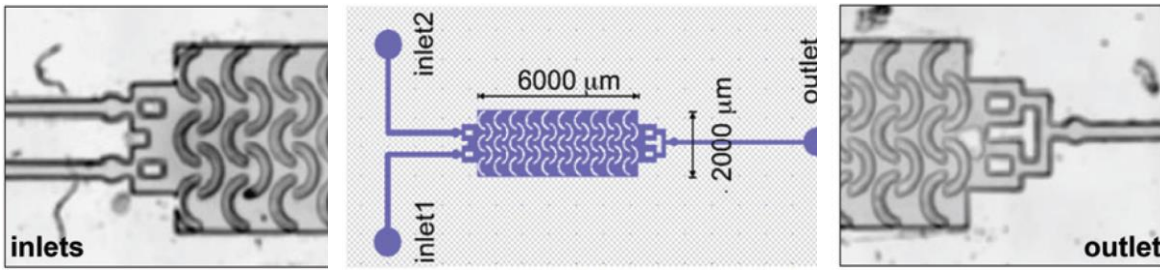

(a) (b) (c)

Figure 5.7 (a) and (c) microscopic image of inlets and outlet section of the PDMS fabricated chip, (b) mask layout [85]

5.1.6 Micromixer serpentine design

In order to test SAVA technology abilities, two serpentine designs has been made, Figure 5.8. These designs are well known and widely used design which has been used for technology comparison.

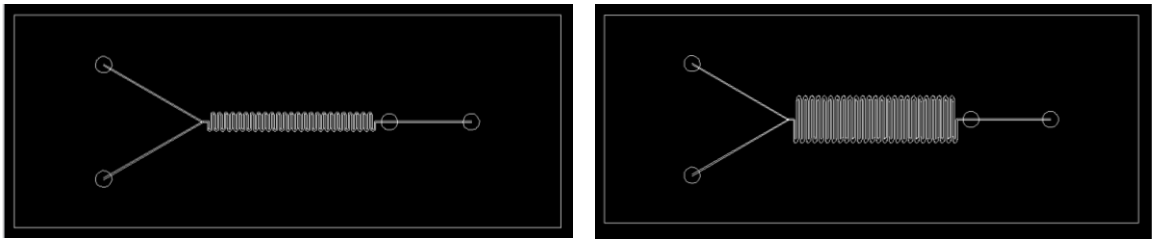

(a) (b)

Figure 5.8 The serpentine micro-mixer design: (a) serpentine-short and (b) serpentine-long

5.2 Simulation

5.2.1 Micromixer for Xurographic Technique

Micromixer chip microfluidic simulations have been done in Comsol Multiphysics® program package. This simulator is selected for its possibility to combine several physical models into one model and because of ability to define physical model and do the simulations without entering deep in mathematical models used for its calculations.

First, for this thesis, mixing performance of water like fluids in the mixer design with parallelogram barriers has been simulated. Micromixer designs with 5, 7 and 10 pairs of parallelogram barriers are simulated.

As it can be seen in Figure 5.9 mixers with 5 and 7 pairs of barriers did not achieved the full mixing performance, meaning reached mixing in the full channel width, as are mixers with 10 pairs of barriers.

Therefore, for accomplishment of the full width mixing 10 or more pairs of parallelogram barriers are recommended.

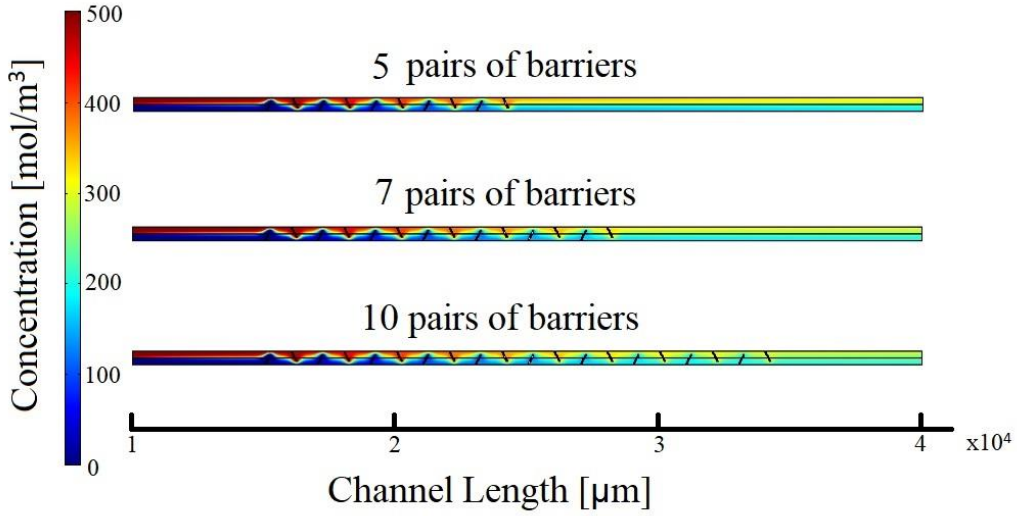

Figure 5.9 Comsol® simulation of number of parallelogram barriers

For the microflixer with the novel design we can see that the mixing ratio can be controlled by changing the obstacles dimensions. Figure 5.10 and Figure 5.11 represents simulation of fine tuning under same condition. Advance of this design is that fine tuning can be achieved. But, for the full mixing some other type of micromixer is recomended.

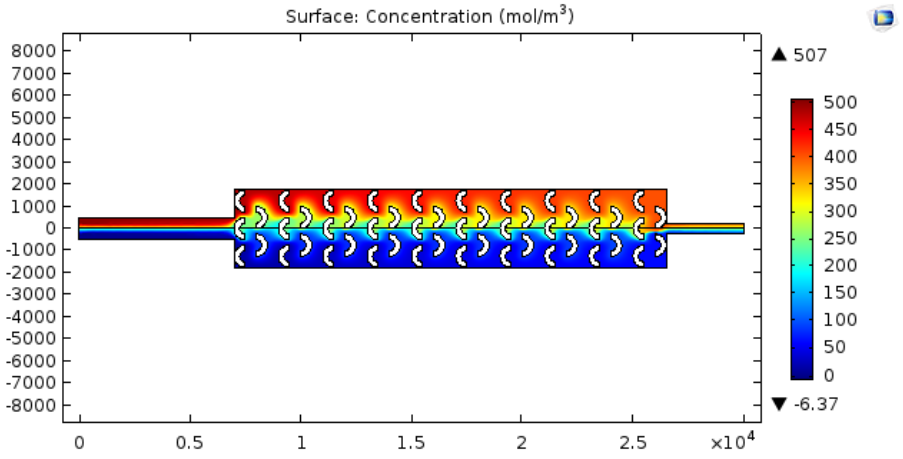

Figure 5.10 Novel design simulation result with shorter semi-circular barriers

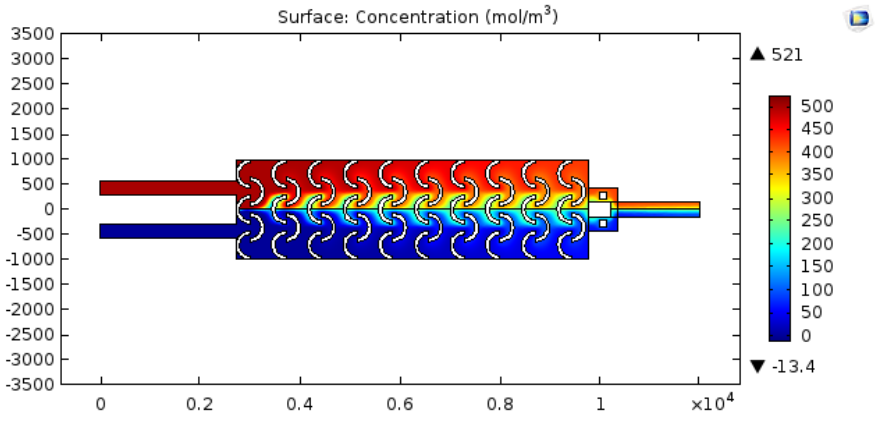

Figure 5.11 Novel design simulation result with longer semi-circular barriers

5.2.2 Micromixer for SAVA Technique

Microfluidic chip simulations for SAVA micromixer have also been performed using Comsol Multiphysics® software tool. COMSOL Multiphysics® software uses finite element method for numerical solving of different equations dictated by physical laws. In microfluidic simulations, fundamental equation used for the description of fluid motion in micro channels is Navier-Stokes equation [86].

5.2.2.1 Micromixer with parallelogram barriers simulations

In order to determine optimal mixing of two fluids at outlet of the channel with the smallest variation of the concentration, the influence of different geometrical parameters of micromixer were analysed.

Firstly, we investigated the influence of the length of the barriers to the quality of the mixing. The length of the barriers varies from 300 μm to 500 μm with the step of 100 μm, while other parameters were kept constant. The simulation results of the variation of the fluid concentration at the outlet of the structure is shown in Figure 5.12, where y-axes represent vertical cross section of the channel. In that manner, we observed the variation of the mixed fluid concentration at the outlet of the mixer. It can be seen that if length of barriers increases, the efficiently of the mixing increases too. It is also visible at Figure 5.13 that visually shows the simulation results of mixing of two fluids along the microfluidic mixer obtained using Comsol Multiphysics® software tool for three analysed sets of parameters.

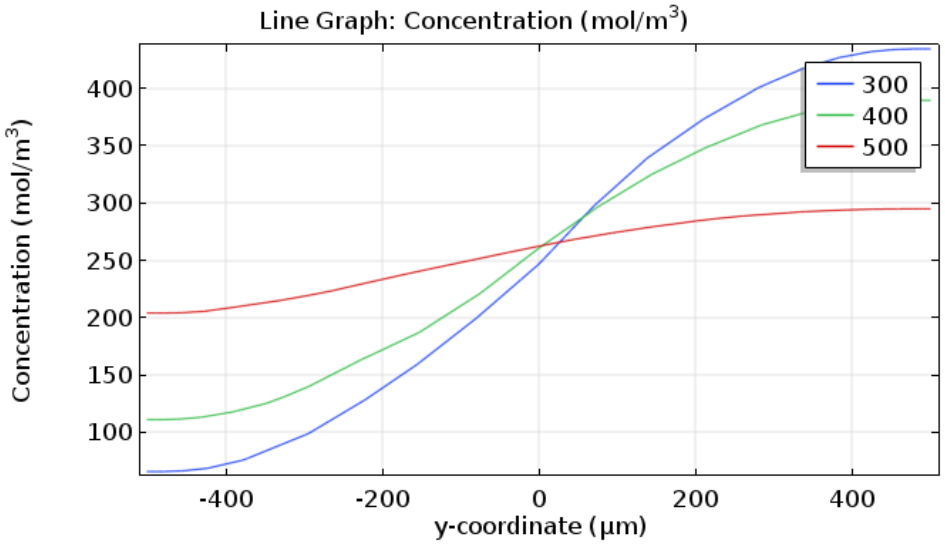

Figure 5.12 The influence of the length of the barriers (l) to the quality of the mixing [87]

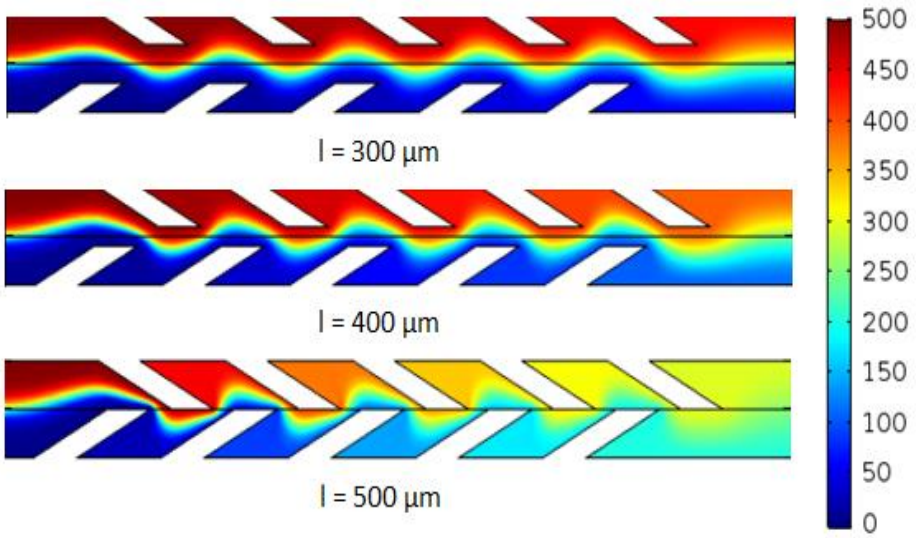

Figure 5.13 Influence of the barriers length (l) on the variation of fluid mixing along the mixer length [87]

Varying the width of barriers is shown in Figure 5.14. With changing the width of the barriers from 300 µm to 500 µm the efficiency of mixing of the fluid at output increases for more than 43%.

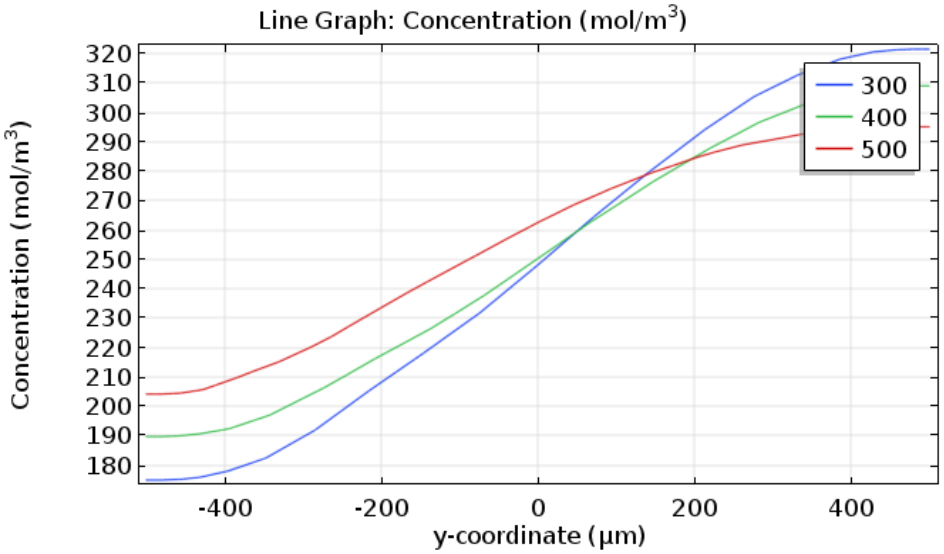

Figure 5.14 Influence of the width of the barriers (p) on the variation of fluid mixing at outlet of the mixer [87]

Figure 5.15 illustrates simulation results for different distances between barriers i.e. the periodicity of the parallelogram barriers. The distance between barriers varied from 1000 µm to 1400 µm with 200 µm step. From the difference in the concentration at the outlet of the channel it is evident that mixing quality is the highest for the smallest periodicity, i.e. in our case d = 1000 µm.

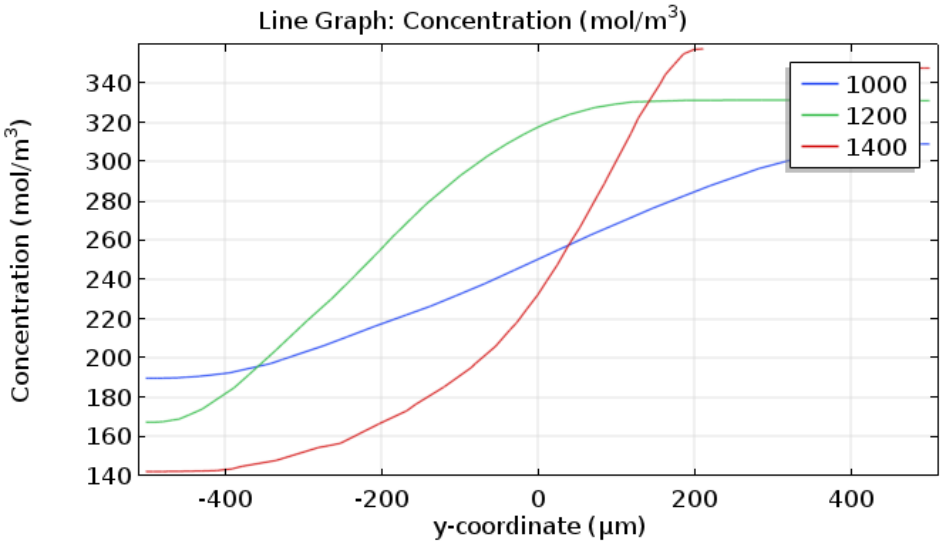

Figure 5.15 The influence of the distance between barriers (d) on the variation of fluid mixing at outlet of the mixer [87]

The influence of the different angle between barriers and the microfluidic channel to the concentration of the mixed fluid is shown in Figure 5.16. Mixing quality is highest

for the barrier angle of 30°. With increment of the barrier angle mixing performance decreases.

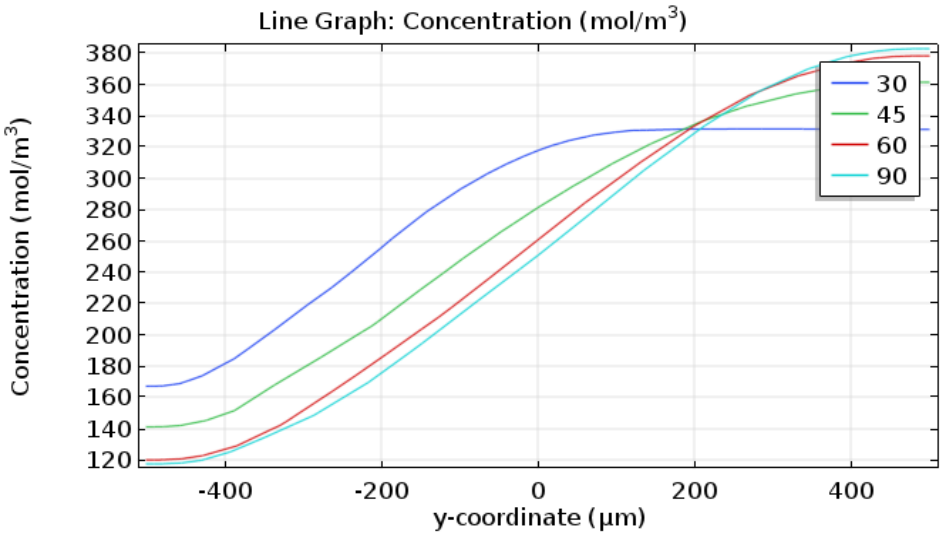

Figure 5.16 The influence of the barrier`s angle (α) the variation of fluid mixing at outlet of the mixer [87]

Based on the previous analysis the optimal set of the parameters was set as: l = 500 µm, p = 500 µm, α = 30° and d = 1000 µm. With this set of the parameters, the variation of the concentration of the mixed fluid at the mixer output is smaller than 5% for a constant input flow rates.

The previous simulations have been performed for constant flow rates at both inlets equal to 10 µL/min. Since the quality of the mixing is determined by the flow rates and the total length of the structure, to determine the optimal length of the mixer, i.e. the number of the barriers pairs N, the flow rates were varied. The 5, 10, 20, 50 and 100 µL/min was used for the simulation at both inlets, simultaneously. In order to determine required number of pairs N, as a condition for good mixing quality we use that the variation of the concentration at the outlet is smaller than 5%. Figure 5.17 shows the influence of the flow rate to the length of the structure, i.e. the number of the rhomboidal pairs.

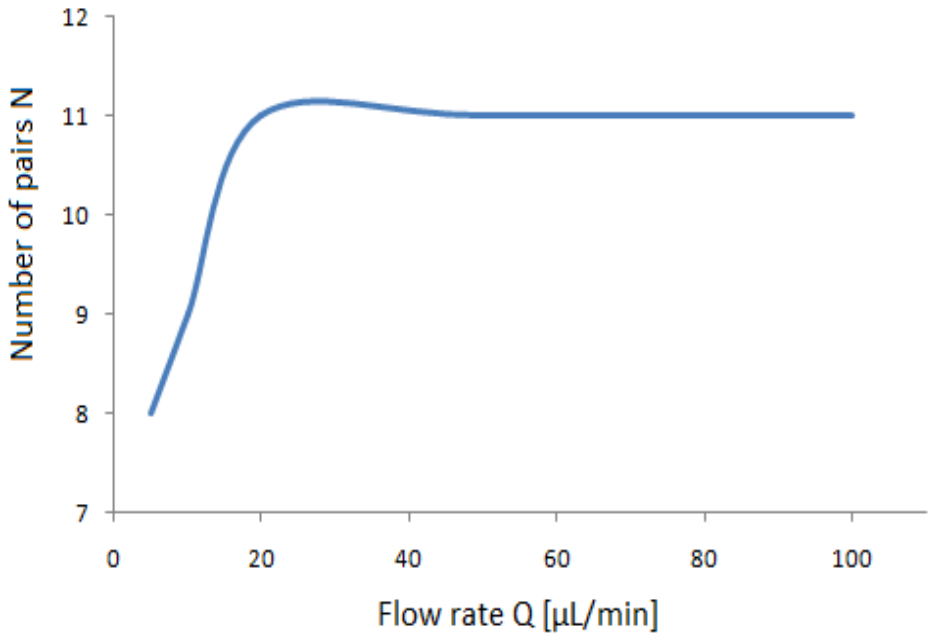

Figure 5.17 Influence of the flow rate on the number of barrier pairs to obtain good mixing quality with the variation of the concentration at the outlet smaller than 5% [87]

Up to flow rate of 20 µL/min the number of barrier pairs increasing with the flow rate, and hence the length of the microfluidic mixer increases too. For the flow rate higher than 20 µL/min, the length of the structure can stay constant. Consequentially, the 11 pairs of barriers are enough to obtain good mixing quality.

If a flow rate is high enough, the length of the structure does not affect the mixing quality, and therefore the proposed mixer topology can be used for the design of compact microfluidic mixer. On the other hand, proposed mixer presents a universal planar solution and it is compatible with different fabrication technologies such as 3D printing, xurographic technique, PDMS or SAVA technology.

5.2.2.2 Pulse flow simulations

Multiphysics simulation software was used to investigate the flow characteristics within Y shaped channel for different input pressure signals (sin, ramp, step), their periods (1 s and 1.5 s) and amplitudes (10 mbar, 50 mbar and 100 mbar). Three different signal shapes were used for inlet pressure in simulations: sine, step and ramp. In Figure 5.18 used signal shapes with period of 1 s are shown. For visualization of the mixing process, different colours of fluids were used, representing the concentration of fluids. The concentration of one liquid was set to 500 mol/m^3 and concentration of the other one was set to zero.

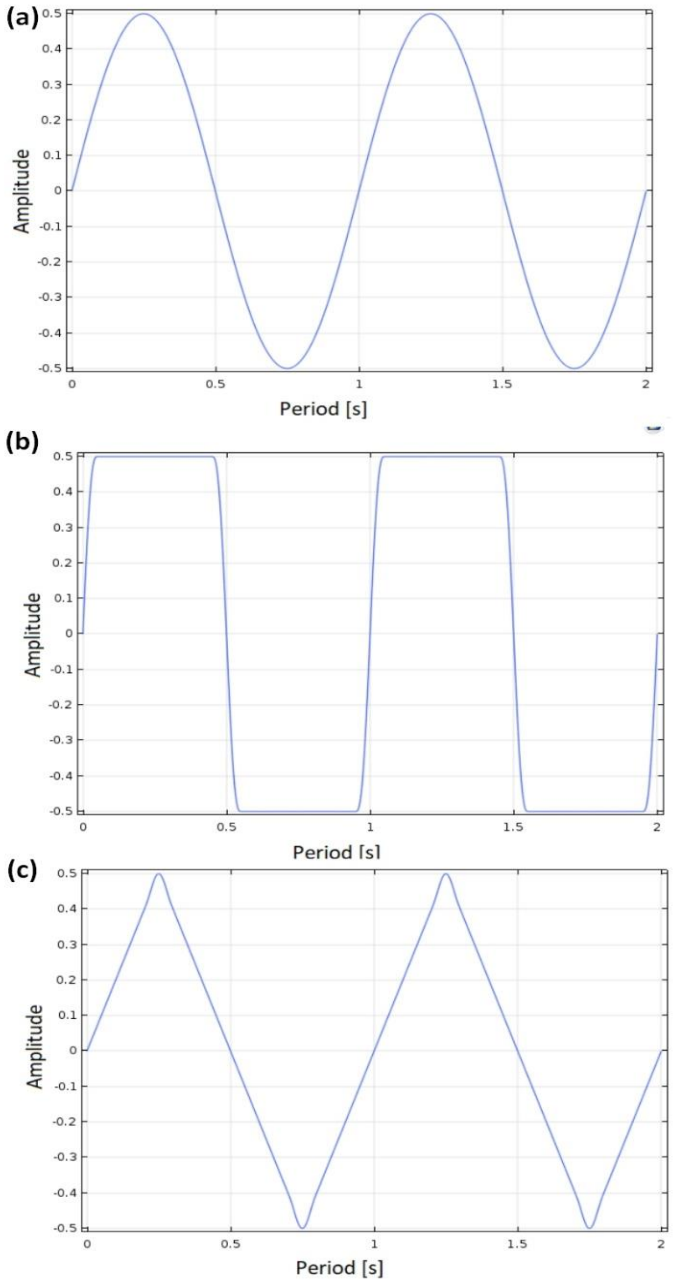

Figure 5.18 Pressure signal at inlet of the chip: (a) Sine, (b) step, and (c) ramp

Figure 5.19 represents the part of the micro channel in two specific cases. Figure 5.19(a) shows simulation results for constant pressure flows of 50 mbar at both inlets, while Figure 5.19(b) shows simulation results for sine shaped pressure signals at both inlets. It can be seen that liquids mix only in their contact region, which is the property of laminar flow. Figure 5.19(b) represents mixing of liquids with sine shaped pressure signal on both inlets with amplitude of 50 mbar. Mixing in this case covers almost the whole channel and it can be seen that mixing of liquids is significantly better.

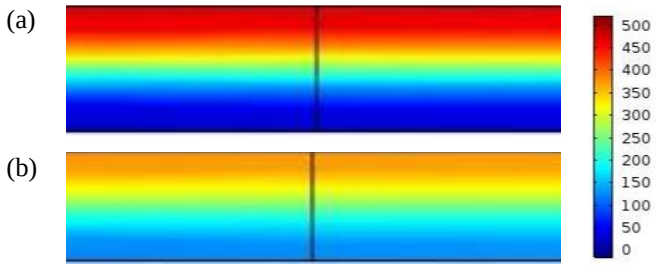

Figure 5.19 Mixing of liquid for: (a) Constant pressure flows at inlets of mixer, and (b) Sine shaped pressure signal at inlets

Figure 5.20 shows the average value of concentration along the observation zone for the different signal shapes and pressures during 10 s. Results presented in Figure 5.20 are simulation results with 1 s signal period. As it was expected, the better mixing of two fluids can be achieved for higher pressure values. Therefore, for 100 mbar pressure, mixing is achieved after 2 s, for 50 mbar after 4 s and for 10 mbar 10 s is not enough to achieve proper mixing of two fluids. Figure 5.20 also shows that step signal gives the best mixing results in term of response time and mixing concentration.

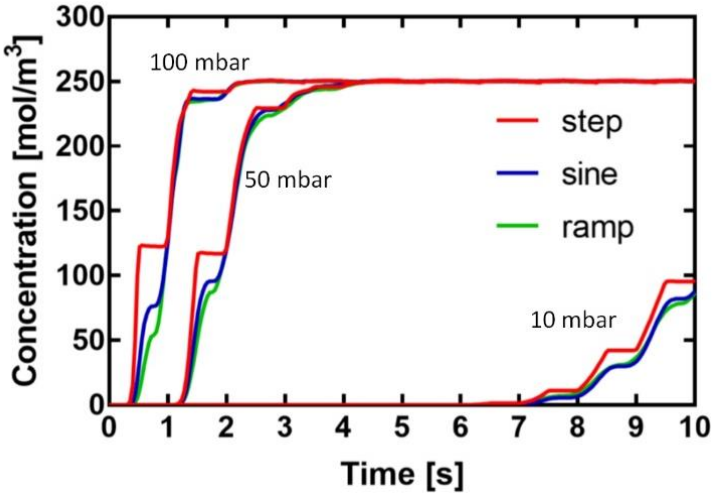

Figure 5.20 Average value of concentration along the observation zone. Simulation results for step, sine and ramp signal shapes at pressures of 10 mbar, 50 mbar and 100 mbar

5.3 Fabrication

Three different fabrication procedures are used for manufacturing microfluidic chips for this thesis:

1. Fabrication of PDMS chips – PDMS moulding,
2. Fabrication of PVC chips – Xurography and
3. Fabrication of Hybrid – (PVC/CeramTape/PVC - SAVA) chips.

Fabrication of polymer chips (PDMS chips) demands expensive chemicals and more or less costly infrastructure while PVC fabrication is low-coast technology without significant cost for used materials nor fabrication facility. Consequences of these facts are high precision of PDMS chips in comparison with PVC chips and good fabrication successful rate (more than 95 %*) of PDMS based chips while PVC chips has successful fabrication rate less than 10 %†.

5.3.1 Fabrication of PDMS chips

The microfluidic channels in a microfluidic device are moulded into a layer of polydimethylsiloxane (PDMS), a transparent biocompatible polymer. Moulding is accomplished by pouring uncured PDMS onto a pre-patterned master. For the purpose of this thesis master moulds were ordered for the novel design from commercial source. A well-mixed PDMS base and curing agent (with 10:1 ratio respectively) were poured over master mould in the process of soft lithography. Previously, in order to eliminate air bubbles, the mixture was put in desiccator for 30 minutes. The master with the PDMS was cured at 80 °C for 2 hours in the oven. After peeling off from the master, the replica was cut on the desired dimensions and holed for inlets and outlets were made with biopsy puncher (1 mm in diameter). Further, the PDMS surface with the design and clean glass slide were exposed to oxygen plasma for 2 minutes and piece together as soon as possible. The surface of the punched PDMS chip was exposed to oxygen plasma for 2 minutes, and was placed as soon as possible against a clean glass slide to form a permanent bond. Fabricated chip from mould made by design on Figure 5.6 can be seen in Figure 5.21(a) and its microscopic view in Figure 5.21(b).

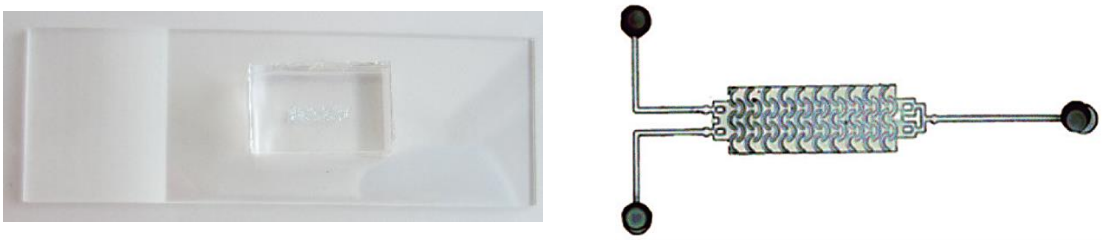

(a) (b)

Figure 5.21 PDMS fabricated chip

* Calculation based on PDMS chips made during this thesis
† Calculation based on PVC chips made during this thesis

5.3.2 Fabrication of PVC chips – Xurography technique

Fabrication of the chip went through following two steps:

Step#1 Plotter cutting of PVC layers;
Step#2 Lamination of the cut PVC layers (first Layer 1 and 2 are laminated and then Layer 3 with the bond of first two layers).

The different designs fabricated in this technology are illustrated in Figure 5.22. The optimised fabrication parameters used for chip manufacturing, presented in this thesis, are listed in Table 5.1.

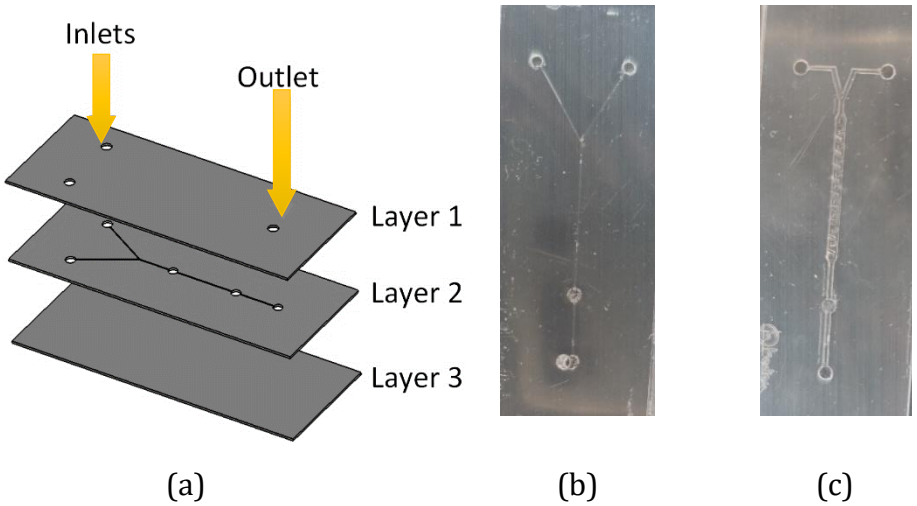

Figure 5.22(a) Simple microfluidic chip in Xurography technique (L1-PVC/L2-PVC/L3-PVC); Photographs of chips with different designs: (b) simple channel, (c) micro-mixer with parallelogram barriers

In order to acquire the best possible performance with existing equipment following fabrication parameters of the Plotter Cutter and Laminator were optimised: cutting speed (for inlet/outlet, border and channel), cutting force, lamination temperature and lamination speed were optimised. Cutting speed depended on desired design. If design had small parts (in order of magnitude about 100 μm – 200 μm), like parallelogram barriers or frequent curves, like serpentine design cutting speed must be reduced to the slowest speed (to 1 cm/s). Even then, uncut or overcut sections were frequent. Inlet/outlet, or similar, more robust designs were feasible with 30 cm/s while, borders could be cut at maximum speed (60 cm/s). Preparation for cutting process, fixation of PVC foil on flexible polyimide carrier with double sided duct tape was also challenging. If bondage of PVC foil and polyimide carrier was strong cutting process had more success (cuts were more precise, number of defects was smaller) than detaching was poorer (there were more elongations and tear up were more frequent) and vice versa,

if the bondage was week cutting process had more defect, but detaching was easier. To optimise strength of the bond between PVC and polyimide film baby powder was used.

Lamination temperature and speed were easy to optimise. If temperature was below 150 °C chips were cracking (PVC layers detached one from each other) and if temperature was higher than 170 °C PVC foil was too soft and channel, as well as other structures were clogged during lamination process. The same was for lamination speed, if the speed was high above 5, lamination was not coherent enough while speed lower than 3 caused collapse of the channel upper wall of clogging of the design.

Taking in consideration all of these problems success rate of PVC chips fabricated in xurography technique was about 10 %. This was the main motivation for invention of the new fabrication technique which has been named as SAVA technique.

Table 5.1 Xurography fabrication parameters

STEP#1: Plotter cutting		
Parameter	**Value**	**Note**
Cutting speed – inlet/outlet	30 [cm/s]	from range 1 – 60 [cm/s]
Cutting speed – border	60 [cm/s]	from range 1 – 60 [cm/s]
Cutting speed – channel	1 – 10 [cm/s]	from range 1 – 60 [cm/s]
Cutting force – 80 µm PVC	19	from range 1 – 38*
Cutting force – 125 µm PVC	26	from range 1 – 38*
STEP#2: Lamination		
Parameter	**Value**	**Note**
Temperature	120 °C – 180 °C	150 °C if not indicated otherwise
Speed	10 cm/min	from range 10 cm/min – 90 cm/min

5.3.2.1 Micro-mixer with parallelogram barriers

Two different designs are fabricated. Parallelogram barrier length is variated to be 75 % and 60 % of channel width, calculating 768 µm and 526 µm correspondingly. Other dimensions of the chip design are the same: barrier width, channel width, channel width in Y junction (input channel width) and inlet/outlet diameter and they are 326 µm, 1024 µm, 667 µm, 2000 µm respectively. Total number of parallelogram barriers in both design is 9. It is lower than simulated 10 because of the limitation in the space of the chip holder we used.

* Cutting Pressure is in range from 0.2 N to 4.41 N (20 to 450 gf) in 38 steps

Fabricated dimensions are measured on SEM and one example of micrograph with inserted labels is shown in Figure 5.23. Since the cutter blade has an angle of 45° all cuts have certain slope. During measurement, the narrowest part of the parameter was used as measured dimension.

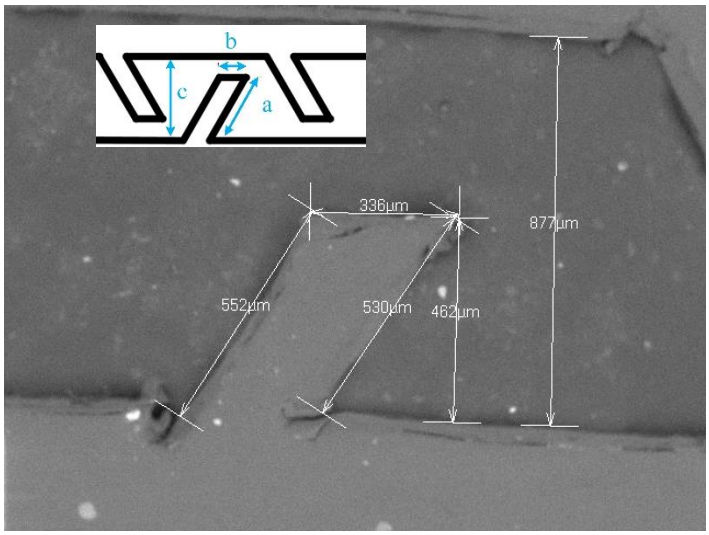

Figure 5.23 SEM micrograph of fabricated parallelogram barrier. Insert: labels of the parallelogram barriers (a – barrier length, b – barrier width, c – channel width)

Relations between designed and fabricated dimensions are shown in Figure 5.24. Standard deviation of measured results is also considered and shown for fabricated samples.

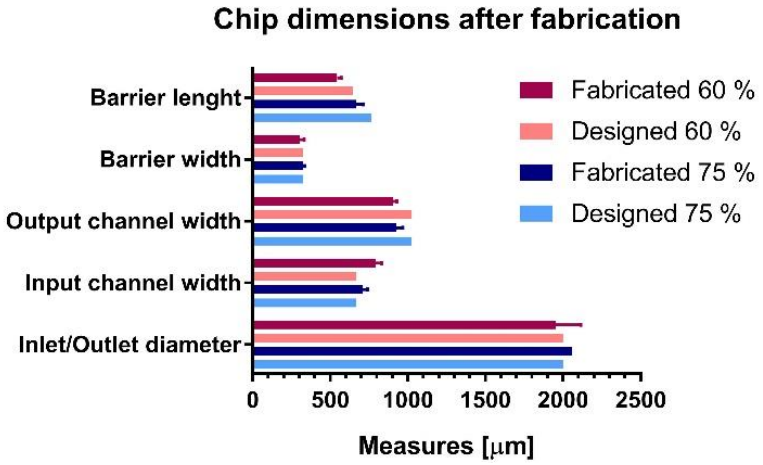

Figure 5.24 Fabricated micromixer chip dimension discussion

From the Figure 5.24 it is clearly visible that horizontal dimensions endured much smaller changes in dimensions than vertical ones. Moreover, the barrier length as a critical parameter of the chip, was shorter in case of 75 % design for 12.9 % and in the case of 60 % design for 15.5 %.

5.3.3 Fabrication of Hybrid chips – SAVA technology (PVC/Ceramtape/PVC) fabricated chips

Fabrication of the chip went through three following steps:

Step#1 Laser cutting of the middle layer in the Ceramtape as for standard preparation of Ceramtape for LTCC technology;

Step#2 Plotter cutting of PVC layers as for standard xurographic technique;

Step#3 Lamination of the cut layers organised as in Figure 5.25 (a) as for standard xurographic technique (laminated first Layer 1 and 2 and then Layer 3). Figure 5.25 (b), (c), (d), (e) and (f) show photographs of different designs (simple channel, serpentine-short, serpentine-long, micromixer with parallelogram barriers - $N = 4$ and micromixer with parallelogram barriers $N = 11$) cut in Ceramtape using laser. In all chips, microfluidic channels have width of 200 μm, while inlet and outlet holes have diameter of 2 mm. The exact fabrication parameters used for manufacturing chips, are listed in Table 5.2.

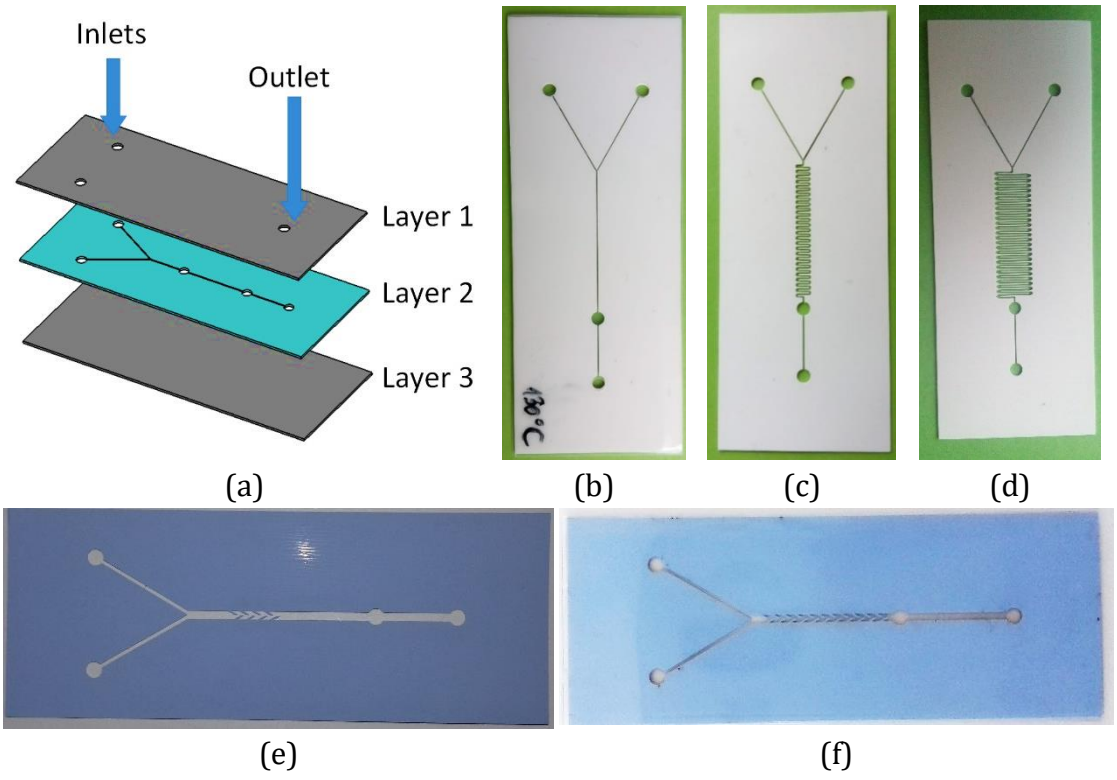

Figure 5.25(a) Simple microfluidic chip in SAVA technology (L1-PVC/L2-Ceramtape/L3-PVC); Photographs of chips with different designs: (b) simple channel, (c) serpentine -short, (d) serpentine-long, (e) and (f) micromixer with parallelogram barriers

Table 5.2 Hybrid fabrication technology parameters

STEP#1a: Laser cutting – White Ceramtape (thickness - 200 µm)		
Parameter	**Value**	**Unit**
Current	28	A
Frequency	10	kHz
Speed	15	mm/s
No. of sweeps	1	N/A
STEP#1a: Laser cutting – Blue Ceramtape (thickness - 300 µm)		
Parameter	**Value**	**Unit**
Current	28.6	A
Frequency	10	kHz
Speed	30	mm/s
No. of sweeps	2	N/A
STEP#2: Plotter cutting		
Parameter	**Value**	**Note**
Cutting speed – inlet/outlet	30 cm/s	from range 1 cm/s – 60 cm/s
Cutting speed – border	60 cm/s	from range 1 cm/s – 60 cm/s
Cutting force – 80 µm PVC	19	from range 1 - 38*
Cutting force – 125 µm PVC	26	from range 1 - 38*
STEP#3: Lamination		
Parameter	**Value**	**Note**
Temperature	120 °C – 180 °C	150 °C in not indicated otherwise
Speed	10 cm/min	from range 10 cm/min – 90 cm/min

Advantages and disadvantages of SAVA technology are summarised in Table 5.3.

Table 5.3 Advantages and disadvantages

Advantages	***Disadvantages***
• fabricate and test every layer separately • 3000 times higher flow rates than xurography chips • the screen or inkjet printing process can be used to print electrodes or sensitive layer directly on foil or Ceramtape • low cost chips • rapid fabrication	• limited time usage of the chip • small soaking of the middle layer

* Cutting Pressure is in range from 0.2 N to 4.41 N (20 to 450 gf) in 38 steps

Chapter VI
Characterisation – Results and discussion

6.1 Optical transmission

Light transmittance of the microfluidic chip was measured in the wavelength range from 300 nm to 1000 nm. Four different configurations have been analysed in which the foil was placed on one or both sides on Ceramtape for two different foil thicknesses: 80 μm and 125 μm. Figure 6.1 shows the optical transmission as a function of the wavelength for 4 different configurations. The proposed microfluidic topology shows good optical properties with transmittance better than 80 %, while the wavelength dependence showing only a small variation above wavelength of 340 nm.

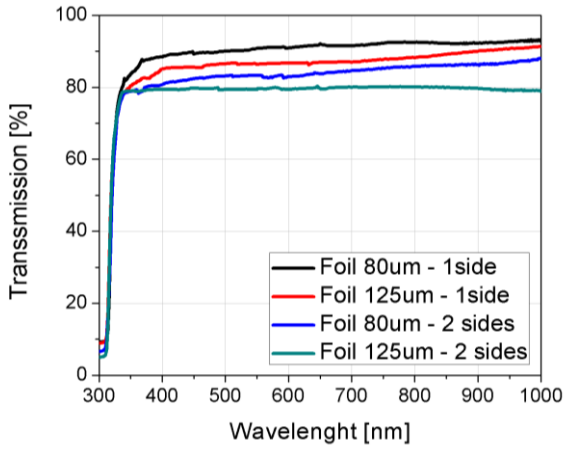

Figure 6.1 Optical transmission as a function of the wavelength for four different configurations [13]

6.2 Dielectric properties

The effective permittivity of the proposed multi-layered configuration has been determined using phase shift method, i.e. measurement of the phase delay of the sinusoidal signal that propagating along the transmission line [88], [89]. For this purpose, the microstrip line was manufactured on the multi-layered substrate made of the combination of Ceramtape and plastic laminating films, as depicted in Figure 6.2. The conductive layers, namely microstrip line and ground layer, have been realized using sticky aluminium tape. Based on the four set of measurements of two lines with different lengths and two thicknesses of the foil, the effective permittivity of the combination of the inhomogeneous dielectric substrate has been calculated using an equation for effective dielectric permittivity of the multi-layered substrate [66]. The phase and amplitude characteristics of the microstrip line has been determined using Agilent VNA E5071C in the frequency range between 500 MHz and 8.5 GHz. The Figure 6.3 displays layouts of the microstrip line with SMA connectors used in the measurement setup, whereas Figure 6.4(a) depicts the extracted values of the effective permittivity of the multi-layered configuration and effective permittivity of each layer. The dielectric losses were calculated based on amplitude of the propagation signal [89], and the extracted values are shown in Figure 6.4(b).

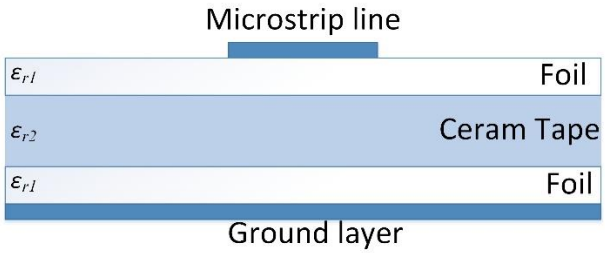

Figure 6.2 The configuration of the microstrip line on multi-layered substrate used for permittivity characterization [13]

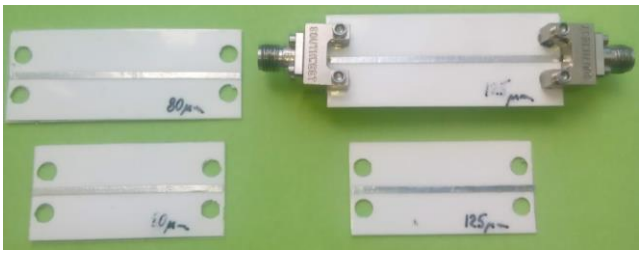

Figure 6.3 The layouts of the microstrip line with SMA connectors used for permittivity characterization [13]

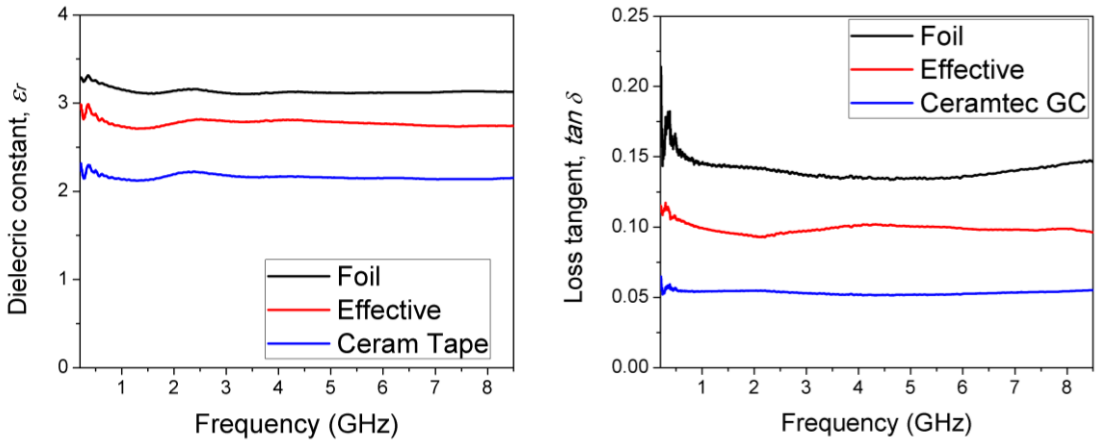

(a) (b)

Figure 6.4 Extracted value of the: (a) effective permittivity, (b) tan δ [13]

6.3 SEM and optical microscopy analysis

For determinate the minimal functional channel width, we made a simple chip structure with 6 different channel widths of 50 μm, 100 μm, 200 μm, 300 μm, 500 μm and 1000 μm and one inlet, outlet and observation field per channel. Figure 6.5 shows two of these chips after lamination between two 125 μm PVC foils.

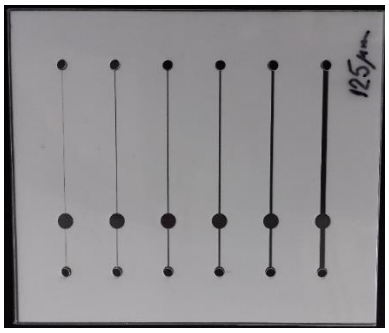

Figure 6.5 Photographs of chips with different micro-channel widths [13]

Verification and quality of cuts was observed on magnification rate from 80 to 1200 times, by means of SEM. Figure 6.6 presents laser cut channels with different widths. It can be detected that for narrower channels measured width is larger than predefined value. For channels of 100 μm and wider laser beam can be adjusted so the exact width is possible to achieve, while for channel with the width of 50 μm laser has only 2 passes and no improvement can be done. Nevertheless, from 4 chips that were made (2 laminated with 80 μm and 2 with 125 μm foil) all channels were passable.

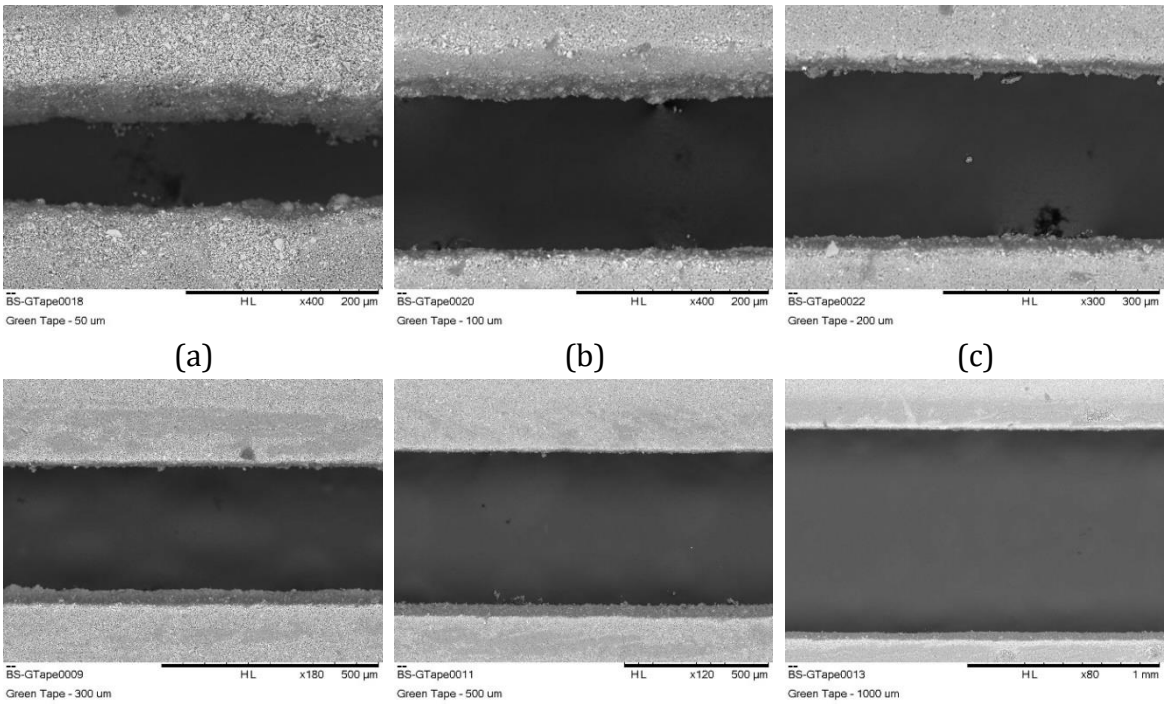

Figure 6.6 SEM micrographs of laser cut channels with different widths at optimal magnifications: (a) 50 μm, x400, (b) 100 μm, x400, (c) 200 μm, x300, (d) 300 μm, x180, (e) 500 μm, x120, (f) 1000 μm, x80 [13]

Figure 6.7 shows SEM micrograph of edges of the laser cut Ceramtape at high magnification. As it can be perceived, edges are quite flat even on magnification of 1200 times, with the irregularities smaller than 10 μm.

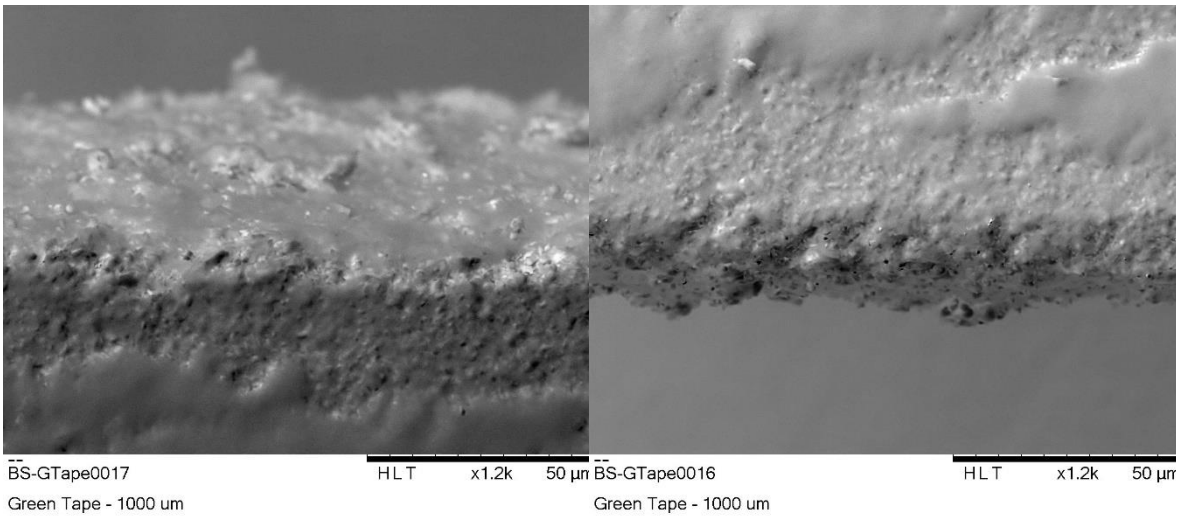

(a) (b)

Figure 6.7 SEM micrographs of laser cut channels edges on x1k2 magnification: (a) left edge, (b) right edge [13]

On the profiler we checked the thickness of the Ceramtape layer. As it can be seen in Figure 6.8, the thickness of the layer is around 280 μm (in fabrication data sheet it is about 300 μm). Roughness of the laser cut is not greater than roughness of the surface of the material.

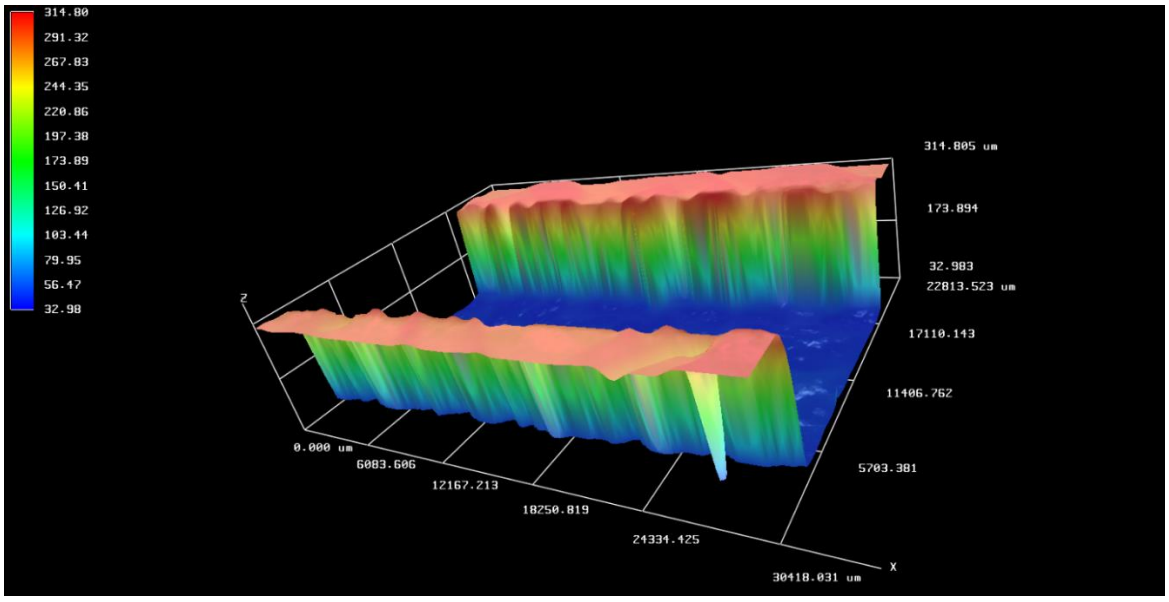

Figure 6.8 Profile thickness and roughness of the middle layer (Ceramtape layer) cut channel [13]

Beside channels, chambers with rectangle and circle shapes were made. Width of the rectangle and diameter of the circle were I – 1 mm, II – 2 mm, III – 3 mm, IV – 4 mm, V – 5 mm and length of the rectangle chambers was 10 mm, as it can be seen in Figure 10 for rectangle chambers maximum width for lamination with 80 μm foil was 3 mm and for 125 μm foil was 2 mm. Connection of 1st and 3rd layer occurs on larger chamber widths as a consequence of large area lamination and deformation of PVC foil caused by temperature. Maximal diameter of circle chambers was 4 mm, while on 5 mm diameter midpoint of the chamber was impaired. All chips for chambers testing are laminated at 150 °C.

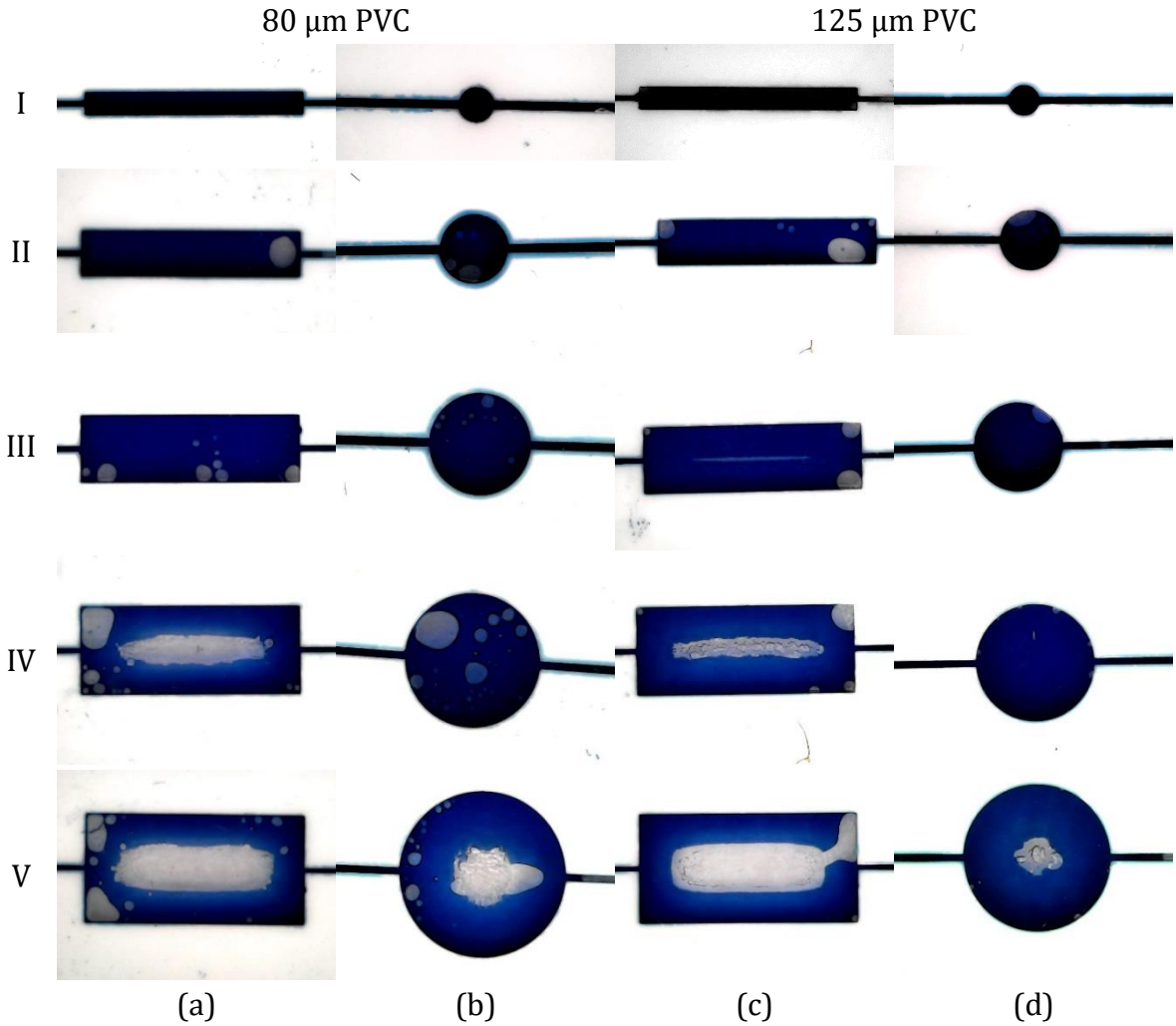

Figure 6.9 Tests of limitations for the chambers widths/diameters: (a) rectangles laminated with 80 μm PVC; (b) circles laminated with 80 μm PVC; (c) rectangles laminated with 125 μm PVC; and (d) circles laminated with 80 μm PVC [13]

6.4 Mechanical characterization

Main point of mechanical characterisation of selected materials was to determine basic mechanical properties of materials which are used for chip fabrication (like uncured Ceramtape), and to compare these properties to already known properties of other materials. Conclusion of these tests was to perceive is flexibility of selected materials belongs to the same range as well as to determine are some of these materials suitable for membranes, as one possible class of functionalisation of a microfluidic chip.

Examination of samples was performed at room temperature and Poisson's ratio of the samples was set on the value from the Table 6.1- literature value.

Table 6.1 Poisson ratio values

Material	Poisson Ratio	Reference
PDMS	0.5	Polymer Data Handbook
PVC	0.4	http://polymerdatabase.com
Ceramtape	0.32	Material Data Sheet

For the purpose of this thesis, six different nanoindentation protocols have been used. They are summarised in the Table 6.2 and depicted Figure 6.10. Protocols vary in 4 parameters: type, depth, load and hold time. The type of the protocol defines which parameter is main and needs to be achieved to finish first step of the protocol. Thus, if the type is displacement - load is incremented until set displacement is not achieved. Accordingly, if the type is load - load is incrementing until its maximum value. To summarise, load is always the parameter nanoindenter measures and displacement is the calculated parameter, the difference is that in the displacement type, measurement finishes first step when displacement is achieved and in the load type, when load is achieved. Consequently, the load type measurements are always more accurate than displacement type.

Table 6.2 Nanoindentation protocols

No.	Type	Depth [µm]	Load [mN]	Hold time [s]
1.	Displacement	2	NA	10
2.	Displacement	3	NA	10
3.	Load	NA	1	1
4.	Load	NA	1	2
5.	Load	NA	10	10
6.	Load	NA	100	10

Further, the parameters depth and load correspond to maximum set values for the selected type of protocol. The last parameter – peak hold time has been varied slightly but not considered into discussion, since it is very complex and at the same time not in the focus of this thesis.

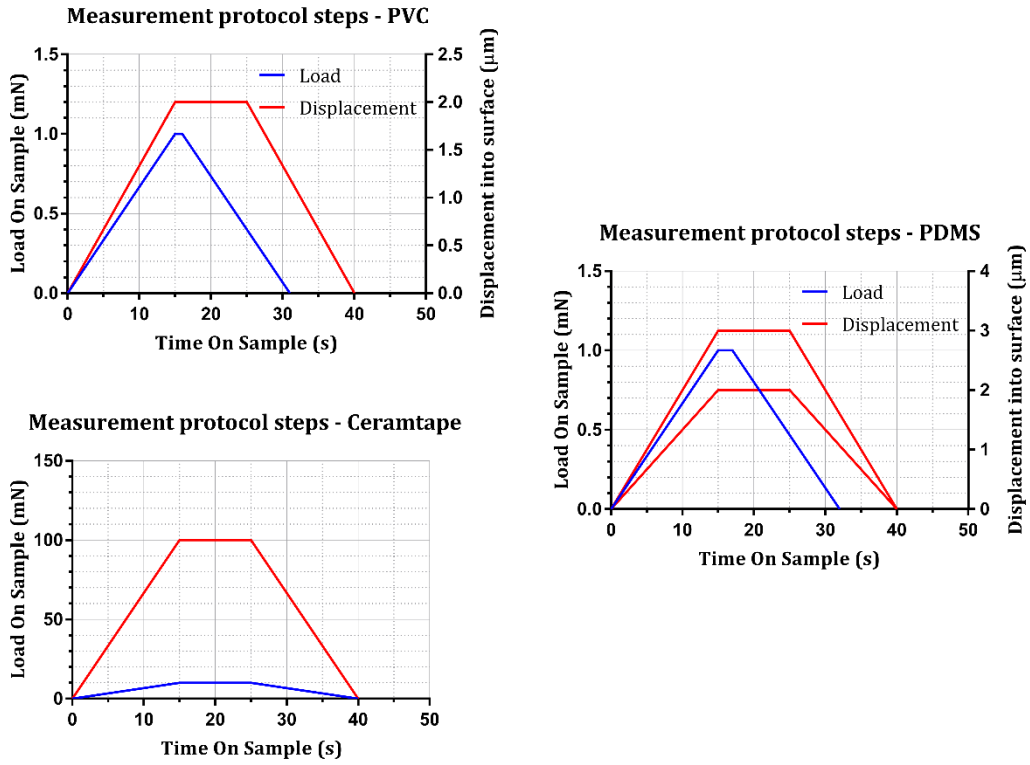

Figure 6.10 Nanoindentation protocol steps for all tests

Detailed step description of the protocol No. 5 from the Table 6.2 is depicted on Figure 6.11. Consequently, the first step is the loading stage at constant loading time of 15 s and maximum load of 10 mN. This phase is executed after proving that the thermal drift is lower to a value of 0.2 nm/s. The second step involves upholding a hold load plateau following loading. The holding period (1 s, 2 s or 10 s) has been selected long enough since there is no substantial so called "nose" phenomenon of the unloading phase and at the same time short enough in order to minimize the influence of the thermal drift. The third step is the unloading stage until 90 % (or 100 % in some cases of Ceramtape testing) of the maximum load at constant unloading time of 15 s. Percent to unload was set to be 90 % for PDMS specimen because it allows a compromise between the creation of an assessable viscoelastic return and to keep a quasi-constant connection zone while unloading. For Ceramtape specimen percent to unload was set to be 100 %, since nanoindentation on raw (unbaked) Ceramtape was not reported in the literature.

In general, the literature data suggest that unloading ratio beyond 25 % causes incorrect fitting of the experimental curves.

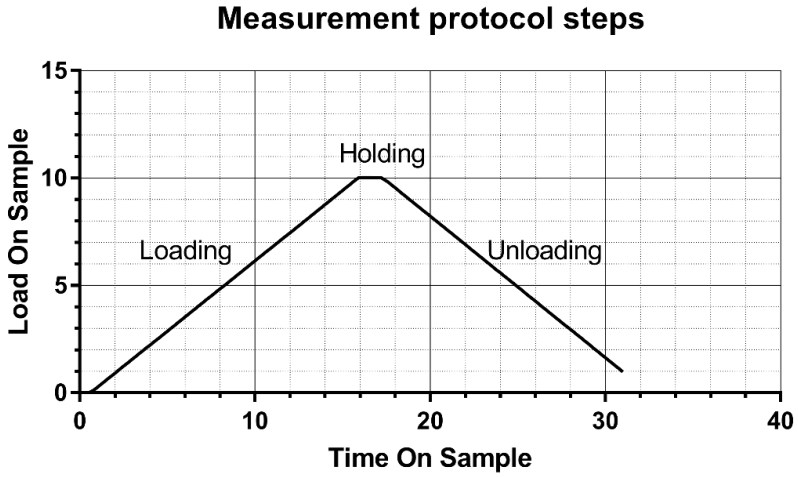

Figure 6.11 Nanoindentation protocol steps

The protocols #1 and #2 (Figure 6.12) had a purpose to determine optimal load for nanoindentation of PDMS and PVC, while for Ceramtape the maximal load was set on 10 mN and 100 mN since it is always used as middle layer and never a membrane layer. Regarding PDMS testing, considering the protocol #1 is easily visible that the measurement noise is very high and that loads of 0.1 mN and lower cannot be used with the current instrument. Moreover, the protocol #2 depict that the loads above 0.1 mN can be set up as maximum load. Concerning PVC testing (0), only protocol #1 is used and results show that for displacement into surface of 2 μm the maximum load needed to be about 10 mN.

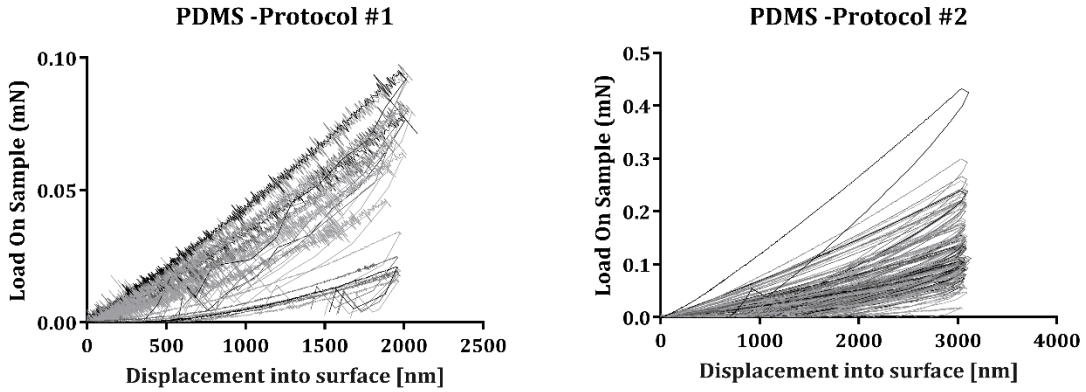

Figure 6.12 PDMS measurements – Displacement type

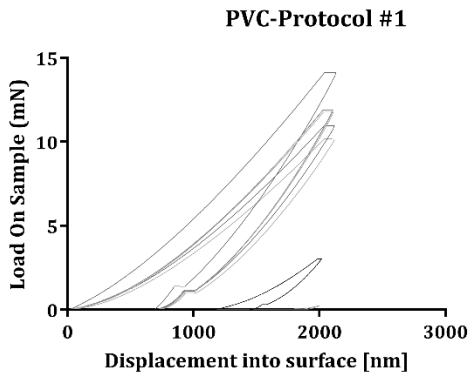

Figure 6.13 PVC measurements – Displacement type

Measurement protocols #3, #4, #5 and #6 of Load vs. displacement curves on Figure 6.14 and Figure 6.16 were set up on 100 measurement points fairly distributed on the sample in the form of 10 x 10 matrix, with 150 μm distance between measurement points. Not all measurement points were obtained, nevertheless the smallest sample had 58 points while all others had more than 90 well performed measurements.

The PDMS Load vs. displacement curves shows that this material is uniform and almost perfectly elastic, which was expected result and here is demonstrated for comparison to other less known materials, like uncured Ceramtape. This was done with the protocol #4. While, the PVC Load vs. displacement curves displays that this material is not so homogenous and not so elastic like PDMS but more plastic (the distribution of the curves is broader and the hysteresis between load and unload part of the curves is wider) Figure 6.14. The thickness of the PVC material, was it 80 μm or 125 μm did not show any significant differences. In both cases for the load of 10 mN the displacement into surface was around 400 nm. Moreover, the PVC layer which was laminated on 150 °C displacement is a bit smaller, as expected, since it gets harder and it is about 365 nm (Figure 6.15). All PVC measurement used protocol #3.

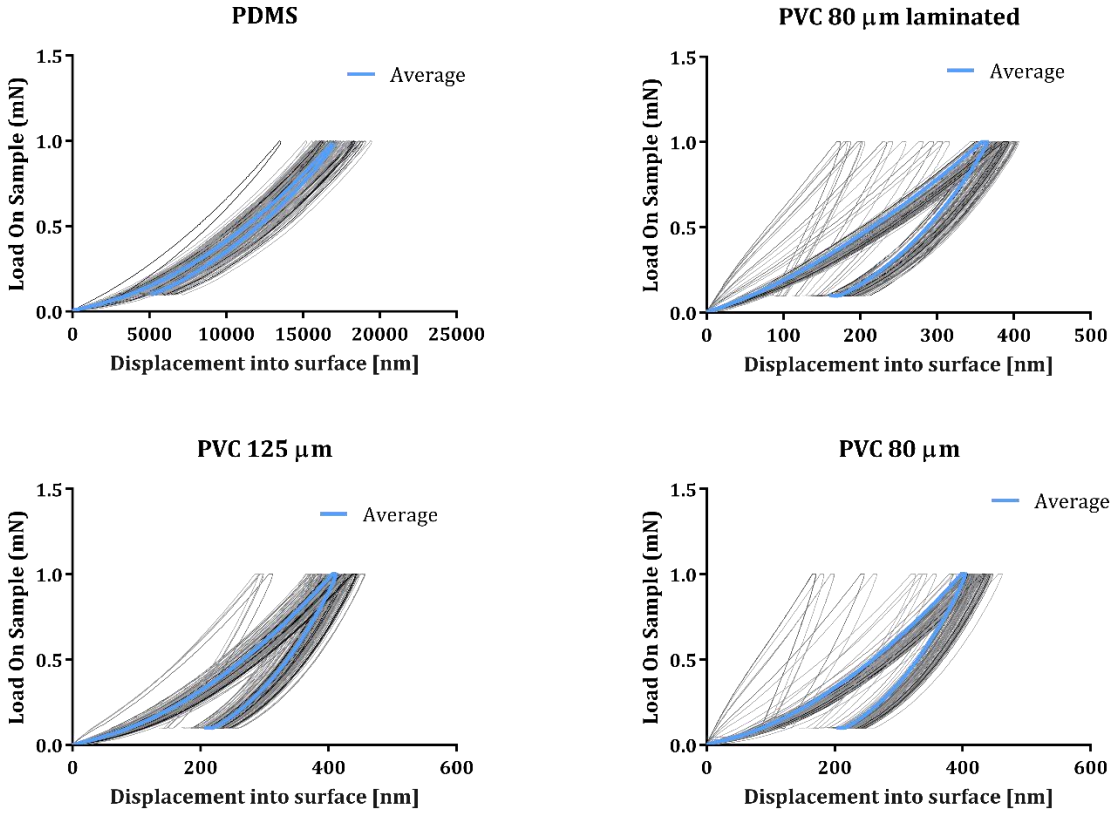

Figure 6.14 Load vs. Displacement curved of PDMS and PVC

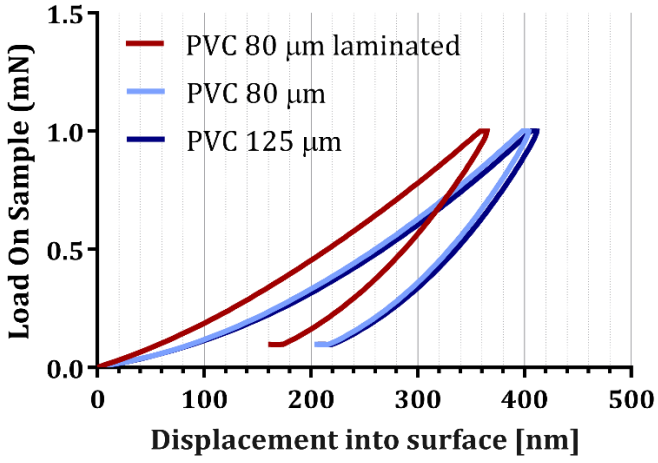

Figure 6.15 Average curves for PVC

Furthermore, the Ceramtape protocols #5 and #6 were performed on uncured and cured Ceramtape. The Ceramtape material composition is not available for scientific public but, it is known that it is a glass ceramic base material composed of an anorthite

glass (calcium aluminosilicate) with ceramic filler [90]. Uncured, Ceramtape is elastic material while, after curing at 900 °C it becomes firm and fragile like we expect ceramic to be. Elasticity in uncured phase is probably consequence of different epoxy resins. This material is also porous, which can be seen on microscopy images in Figure 6.7.

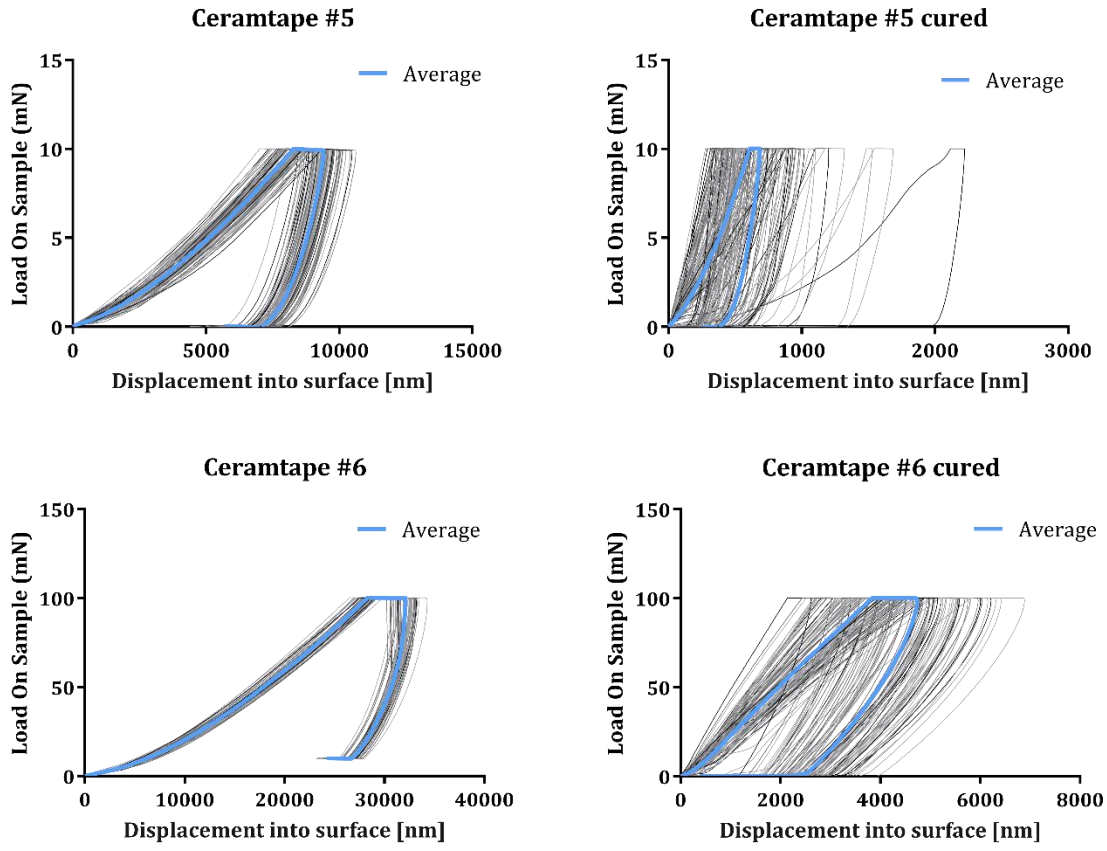

Figure 6.16 Load vs. Displacement curves of Ceramtape

The Load vs. Displacement curves for Ceramtape shows significant plastic performance but uniform behaviour of the uncured Ceramtape, Figure 6.16. Besides, uncured Ceramtape has uniform structure even on higher load. The significant difference in uncured and cured curves is consequence of porosity, as well as material composition change, since some fillers evaporate during curing. Using different loads changes depts. Nonetheless, behaviour of the curing process consequences is very similar. A cleaner picture is obtained when all average curves are put in the same graph depicted in Figure 6.17, and even more intuitive if x-axis is logarithmic.

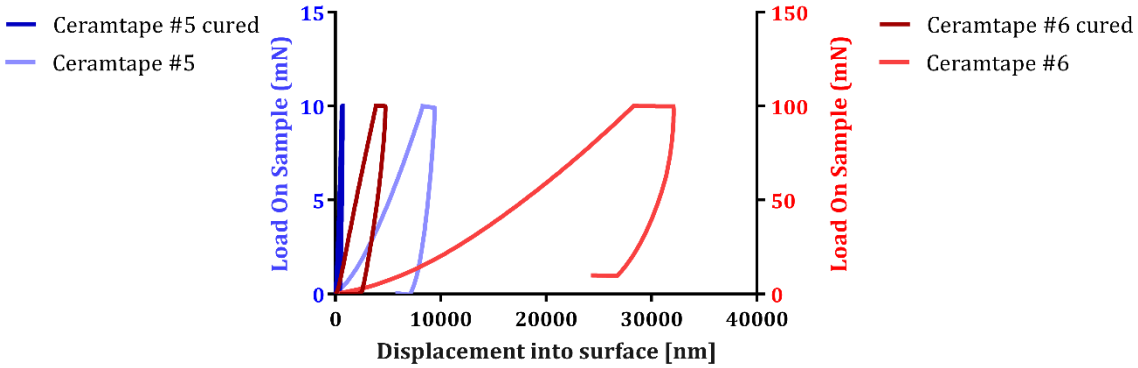

Figure 6.17 Average curves for Ceramtape

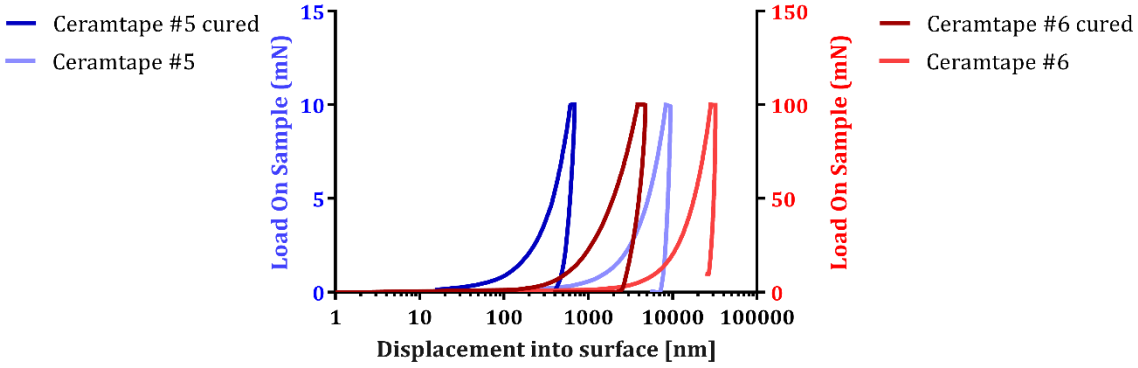

Figure 6.18 Average curves for Ceramtape – logarithmic scale

Additionally, observing Young's modulus and Hardness of these tree materials we can see that Ceramtape is somewhere between PDMS and PVC (Figure 6.19) which makes this material suitable for hybrid microfluidic chip fabrication.

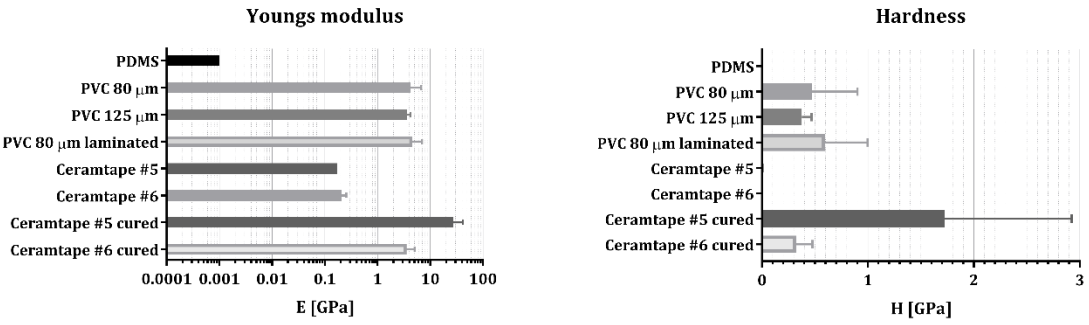

Figure 6.19 Young's modulus and Hardness of used materials

For the purpose of microfluidic chips this aptitude was enough to make good counterpart for the PVC. For the microfluidic chips fabricated for this thesis only uncured Ceramtape was used.

6.5 Temperature exposure

To test temperature stability six identical chips were fabricated. These chips have 3-layer structure (PVC/Ceramtape/PVC) where PVC layers have thickness of 80 μm and lamination process was held at 150 °C. Chips were exposed for 5 min (in the preheated oven) to the temperatures from 80 °C to 180 °C, with the step of 20 °C. Figure 6.20 (a) shows six chips before, whereas Figure 6.20 (b), (c) and (d) shows chips after the temperature exposure. On the temperature of 100 °C PVC foil is heated but there is no deformation of the channel after medium pressure to the foil. Moreover, on 120 °C chip still looks intact but there is mild deformation of the channel while applying medium pressure. While, on 140 °C there is visible deformation of chip, air bubbles are scattered through the surface and channel suffers significant deformation under medium pressure. Further, on 160 °C and higher PVC foil is melting and channel closing can be seen.

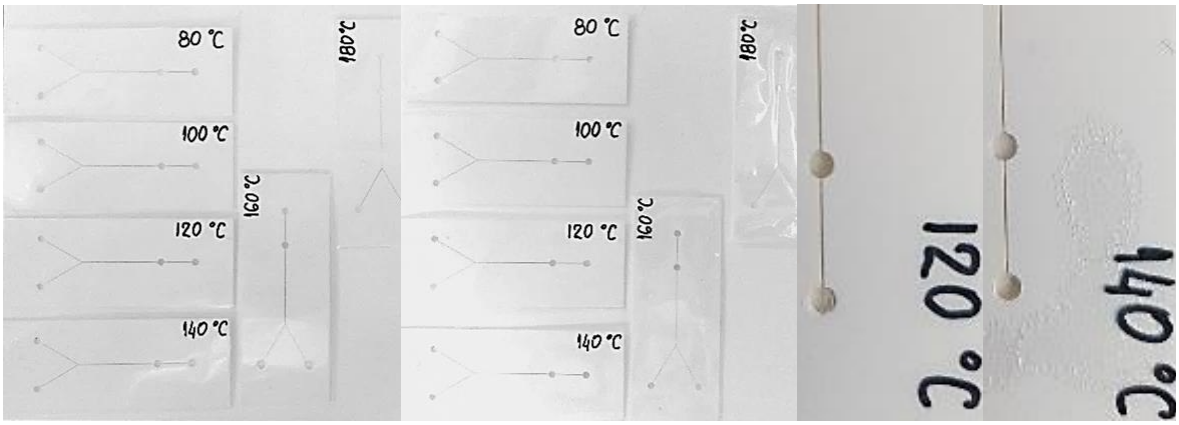

(a) (b) (c) (d)

Figure 6.20 Thermally treated chips: (a) before temperature exposure, (b) after temperature exposure, (c) chip on 120 °C after exposure, without significant change in the structure, (d) chip on 140 °C with deformation and air bubbles in the structure [13]

6.6 Microfluidic testing

6.6.1 Determination of maximal flow

To test adhesion and leaks of the chip with fluid inside, a simple microfluidic experimental set-up was created. This set-up consisted of a syringe pump, syringes, tubes and connectors as well as chip holder with patches and the PVC and hybrid (PVC/Ceramtape/PVC) chips (Figure 6.21).

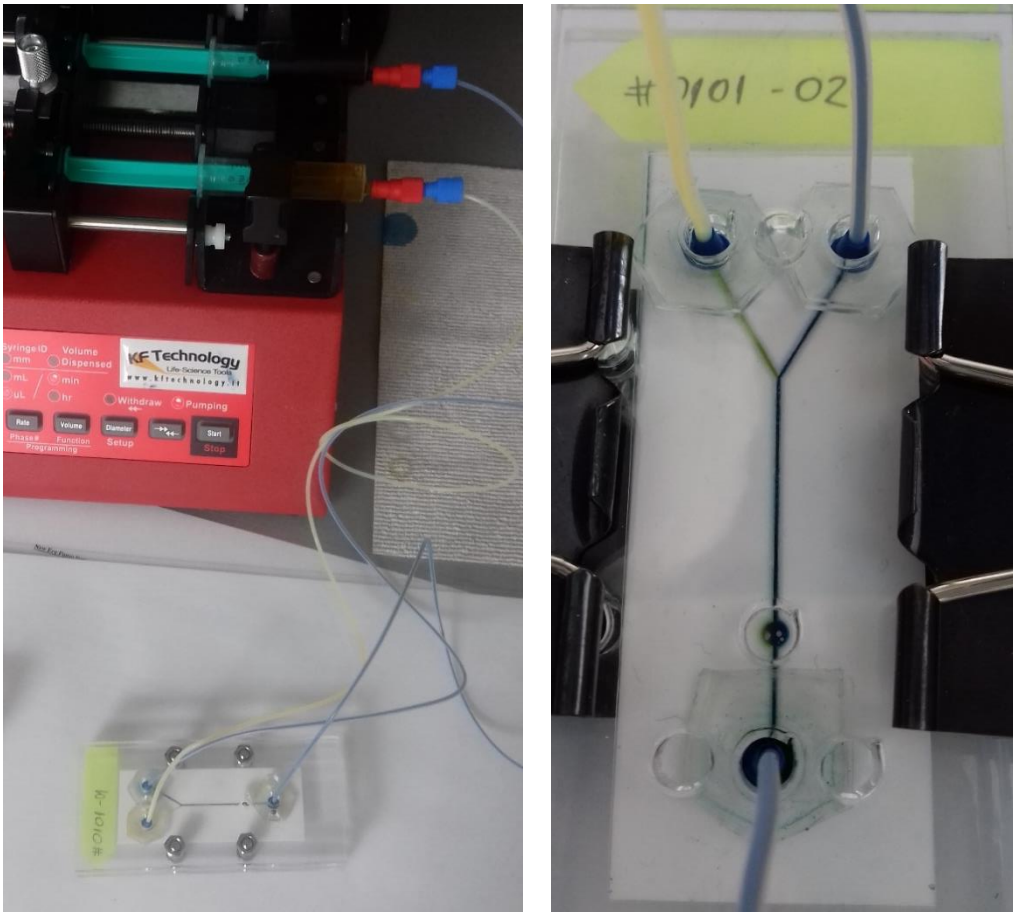

a) b)

Figure 6.21 Microfluidic experimental set-up: (a) Syringe pump, tubes connectors and chip holder, (b) chip holder details

For determination of maximal flow rate through the PVC chips, 2 sets of 3 chips were made. First set was made from 80 µm PVC foil while second set was made from 125 µm PVC foil. Moreover, for the both set lamination temperatures of 120 °C, 150 °C and 180 °C were used. Flow rate was varied from 0.1 µl/min until the leakage of the chip with the step of 0.1 µl/min (Table 6.3).

Table 6.3 Flow rate ranges and steps for PVC chips

Range	From	To	Step
I	0.1 µl/min	max	0.1 µl/min

For determination of maximal flow rate through the hybrid chips, 2 sets of 6 chips were made. For the first set chips with simple channel design cut in Ceramtape were laminated with 80 µm PVC foil on both sides on temperature from 130 °C to 180 °C with the step of 10 °C. While, for the second test, 125 µm PVC foils were used on the same temperatures. Flow rate was tested in 5 ranges described in detail in Table 6.4, for 20 s each. All chips resisted all flow rates in all ranges without any leakages. At flow rate of 15 ml/min silicon patches that holds the tubing started to leak so conducting tests on higher flow rates were not possible.

For comparison, 2 another sets of chips were made with only one change – instead of Ceramtape layer we used 80 µm PVC foil for the first set and 125 µm PVC foil for the second test as middle layer cut on the plotter cutter as in standard xurography technique with the same design used for Ceramtape. Only 2 of the chips have been successfully fabricated and resisted flow rate lower than 5 µl/min without leakages, others were clogged on inlets or outlets. These tests demonstrated that presented technology for fabrication microfluidic chips can resist 3000 times higher flow rates than chips manufactured using standard xurography technique.

Table 6.4 Flow rate ranges and steps for SAVA chips

Range	From	To	Step
I	0.1 µl/min	1.0 µl/min	0.1 µl/min
II	1 µl/min	10 µl/min	1 µl/min
III	10 µl/min	100 µl/min	10 µl/min
IV	100 µl/min	1 ml/min	100 µl/min
V	1 ml/min	15 ml/min	1 ml/min

6.6.2 Flow mixing in PDMS chips with novel design

The novel microfluidic design has semi-circular barriers in order to create the chaotic advection with diffusion. For this purpose, we used pressure controller for flow control. Experimental set-up consist of pressure controller, two normally closed valves (for faster, easier and more precise flow control) and microscope, depicted in Figure 6.22.

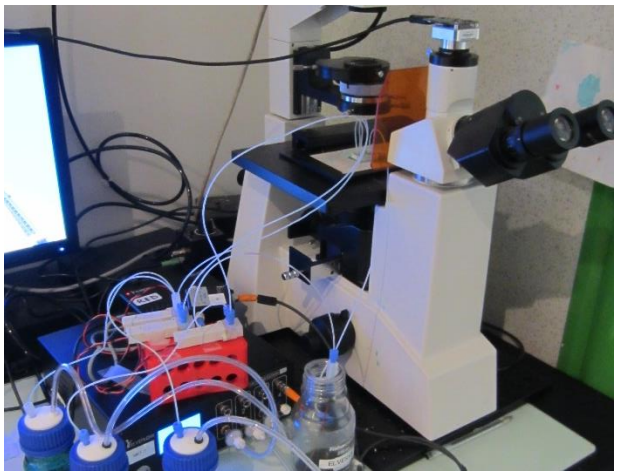

Figure 6.22 Experimental set-up for PDMS chip flow mixing

To check the microfluidic mixing efficiency pressure was varied to change flow rate. Figure 6.23 illustrate how mixing efficiency can be influenced by applying different pressures. The lowest pressure of 40 mbar is the one that achieves the highest mixing. By increasing the pressure and thus the flow rate mixing decreases. Although, this design gives good mixing only for the low pressure the tuning of the mixing is very precise. This implies that this design can be modified in a way that instead one outlet, two outlets exists. In this way small concentrations can be achieved if in one input an active component is delivered and on the other input a buffer solution. Further, by controlling the pressure on one input only small concentration of active substance will be delivered. This feature makes this improved novel design a good candidate for drug delivery systems.

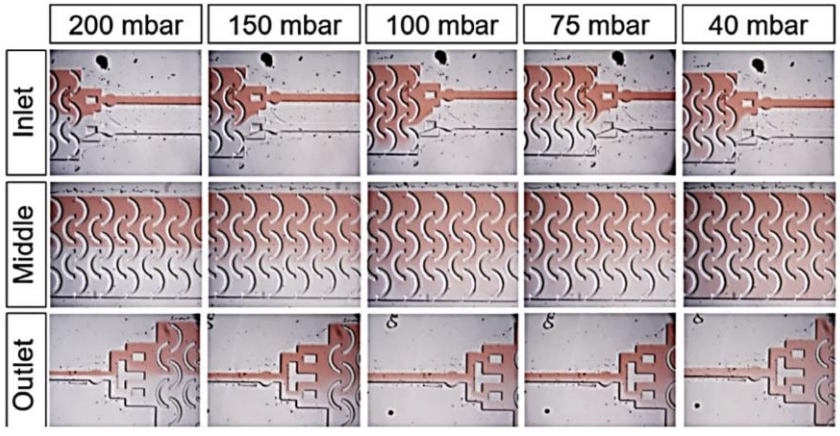

Figure 6.23 Mixing experiment microscopic images (4×) at various pressures [91]

6.6.3 Flow mixing in PVC chips with parallelogram barriers

Experimental set-up contained: a syringe pump with two simultaneous channels, two syringes, PTFE tubing, fittings, holder, connections and digital microscope. Set-up is shown in Figure 6.24.

Figure 6.24 Experimental set-up

Since syringe pump has two simultaneous channels the mixing ratio was 50 % - 50 %. Distillate water was the selected fluid. Water and water-based food dye colorant were mixed with ratio 5:1.

All experiments were recorded with Digital Microscope. More precisely, for every flow rate point, 5 to 10 independent photographs on every 2 s were made. Photographs had resolution of 3648 x 2736 dpi. Mixing in the channel was detected visually and mixing rate is measured graphically in Microsoft Visio®.

Mixing in the channel was detected visually using digital camera and mixing rates were determined in Matlab®. For every flow pressure signal, amplitude, and period, 12 independent photographs during one period of signal were recorded. Photographs had high resolution of 3648 dpi x 2736 dpi. Two examples of the recorded photos are shown in Figure 6.27(a) and (b). All pictures are further processed in Matlab® in order to determine mixing efficiency.

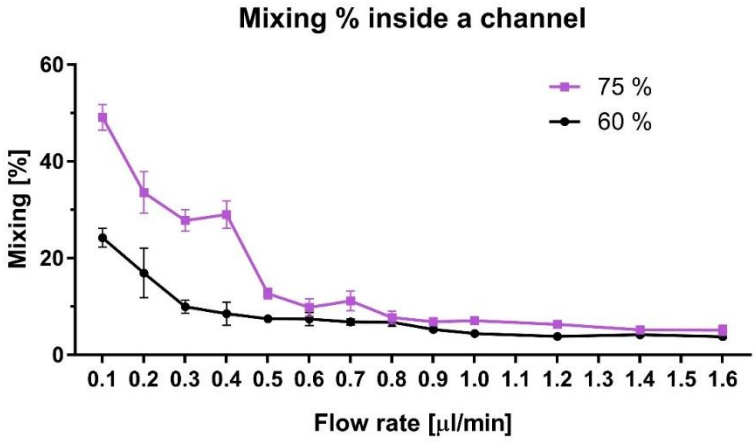

Figure 6.25 Micromixer chip efficiency

Figure 6.25 shows mixing efficiency of this two design fabricated in xurographic technique given with mean values and standard deviations. Observing the results, it can be seen that the best mixing performance is achieved for design with 75 % barrier design during flow rate of 0.1 µl/min and it is 50 % of channel width. As it is expected, increment of flow rate decreases the mixing performance as well as reduction of barrier length.

6.6.4 Flow mixing in SAVA chips with simple channel

In order to verify simulation results, experimental testing has been performed on the fabricated chips. Set-up for conducting the experiment, shown in Figure 6.26, consists of microfluidic flow control system ElveflowOB1, PTFE tubing, fittings, holder, connections and digital microscope.

Figure 6.26 Experimental set-up [92]

Matlab® software was used to isolate the observation field and isolate the pure red and green colour in the image. Because of the equal flows at both inlets, we assume that there is the equal amount of non-mixed red and yellow liquid. In the following step R-red, G-green and B-blue components were determined in order to isolate pixels in the observation field, Figure 6.27(c) and (d).

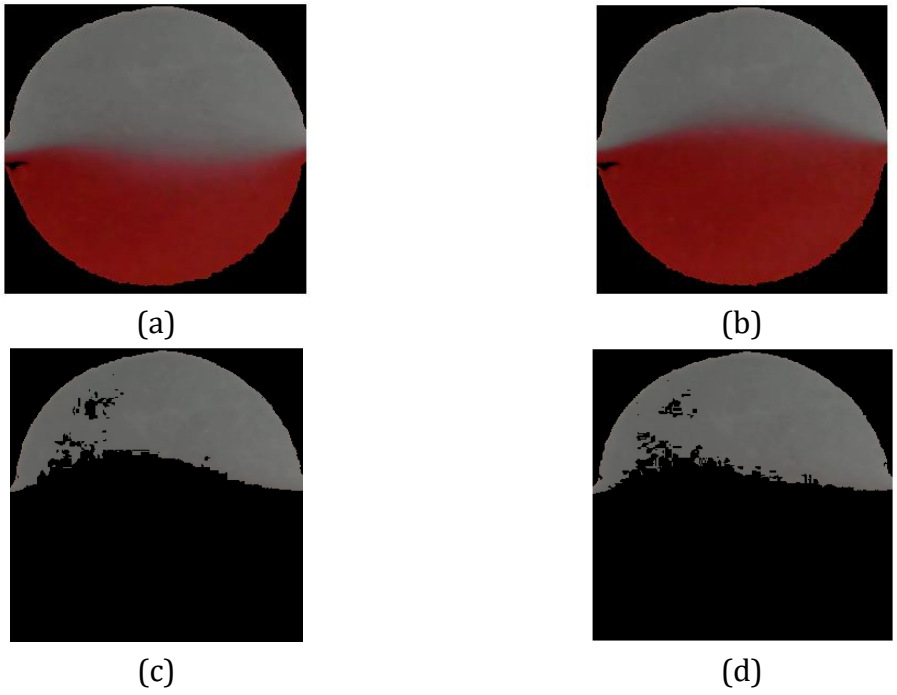

Figure 6.27 Photographs of the observation field after stimulation with: (a) sin, and (b) step signal with amplitude of 50 mbar within the period of 1 s, (c) and (d) isolated pixels of unmixed fluid based on 3 colour channels [92]

Based on that for non-isolating, i.e. non-mixed liquids, pixels were classified and counted. The code is written to count the total number of pixels of the observation field, to take away the number of pure yellow/red, and to calculate the mixing efficiency. These results are presented as heat maps for the different amplitude and periods, after first period of signal. In Figure 6.28 heat map of results is shown in percentage for different pressure, amplitude and period recorded after period of first impulse. As it was expected, better mixing is performed on shorter periods of pulsation, and higher pressures.

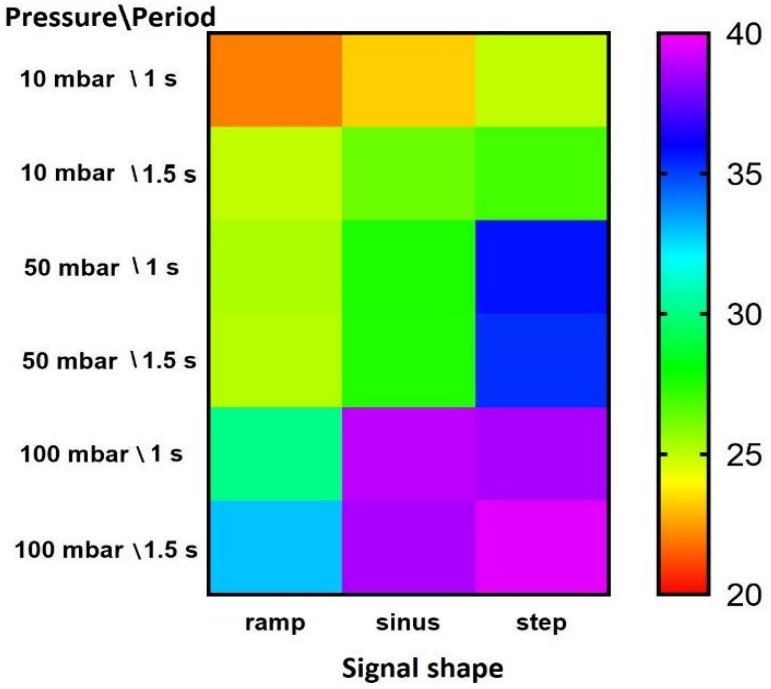

Figure 6.28 Results of the mixing for different pressures, amplitude and period recorded after period of the first impulse [92]

The best mixing occurs for the stimulation with the step signal shape, because of the nature of signal itself, although mixing with sine and ramp signals give almost the same results. With the change of the shape of the signals and their period at the inlets of the microfluidic chips the efficiency of the mixing can be increased for more than 30%.

Chapter VII

Application examples

7.1.1 Analysis of SAVA microfluidic chips for antibacterial solutions delivery in dentistry

Microfluidic properties of two different chlorhexidine (CHX) based mouthwash solutions were analysed, and the chemical composition of the investigated liquids is presented in Table 7.1. Eight SAVA chips were fabricated, they were Y-channel chips without any obstacles inside of the channel, with the input channels set at an angle of 60 °, and the width of 500 - 700 μm (Figure 5.22).

Table 7.1 Composition of investigated mouthwashes

Eludril	**CURASEPT**
Glycerin	Water
Chlorhexidine digluconate (0.1%)	Chlorhexidine digluconate (0.2%)
Water	Xylitol
Alcohol	Propylene glycol
Chlorbutanol	Hydrogenated castor oil

The analysed parameters included the passage, speed and necessary pressure for the laminar flow of solutions. The liquid diffusion was observed with a USB camera (Figure 7.1).

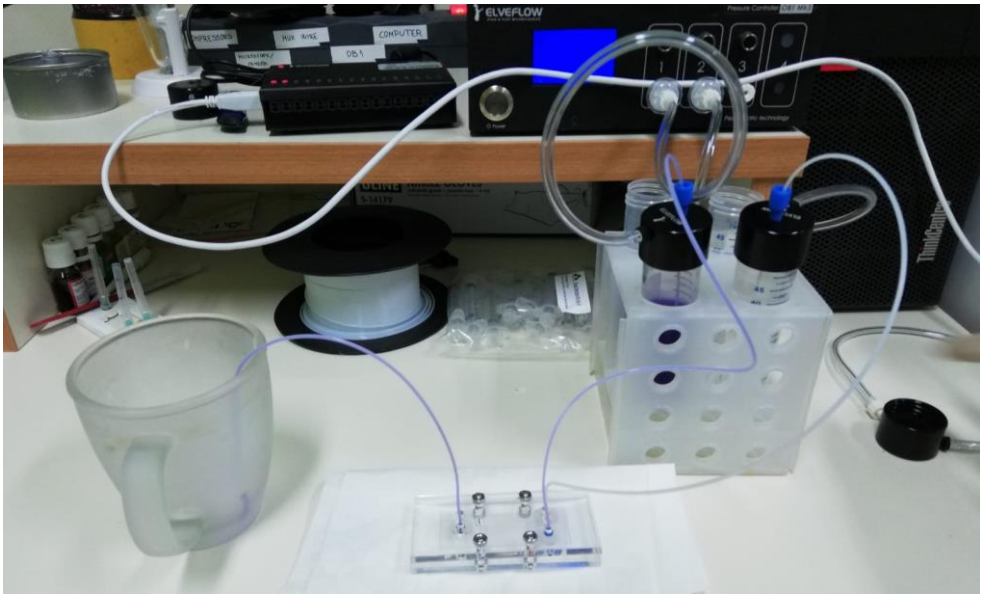

Figure 7.1 Experimental setup for CHX experiments

The microfluidic chip was put into the plexiglas holder to avoid chip movement and flexion. Design and picture of the holder is shown on Figure 7.2(a) and (b).

(a) (b)

Figure 7.2 Holder for PVC and SAVA fabricated microfluidic chips (a) design, (b) picture

For the visualization purposes, tested fluids were painted with gentian violet (Figure 7.3). Laser cutter and Plotter cutter was used to cut the Ceramtape (200 μm) and PVC foils (125 μm), respectively in order to manufacture the microfluidic chips with parameters from Table 5.2. Experimental and setup parameters were used in chapter 6.6.4 above, where for the realization of the microfluidic chips, the SAVA technique was used. In order to examine what pressure in the channel is needed for laminar flow of liquid, the fluid pressure at the inlet was changed.

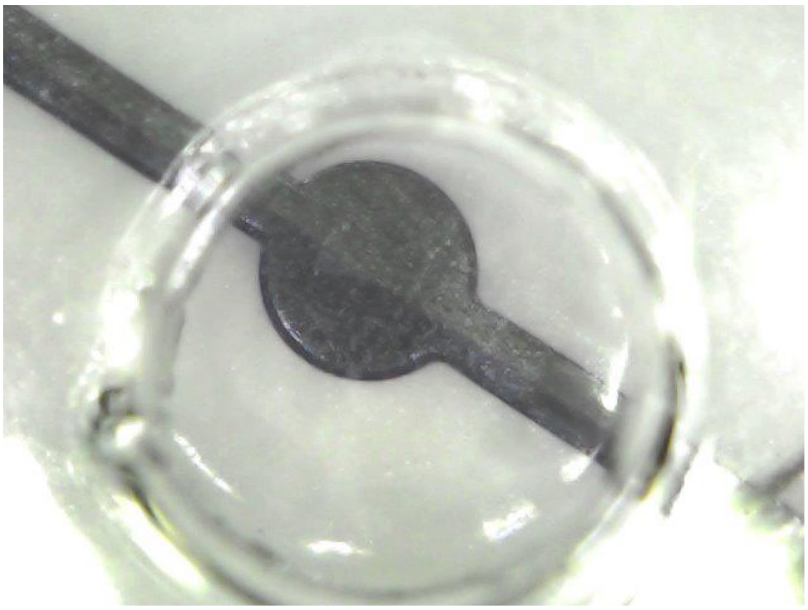

Figure 7.3 Observation field in the holder

This application example was conducted in order to assess the possibilities of integration of salivary diagnostics within the microfluidic systems. This experiment investigates the possibilities of designing optimal microfluidic system for salivary theranostics based on economic and easily fabricated SAVA technology, following the criteria set for contemporary medical devices, and defined as ASSURED by WHO [93], that suggested that appliances used for routine procedures in general health monitoring need to be affordable, sensitive, specific, user-friendly, rapid and robust, without the use of complex equipment.

For more than forty years CHX have been used in preventive, prophylactic and therapeutical procedures in dentistry, and its efficiency has been attributed to a high potency, moderate side effects and the lack of bacterial resistance formation [94]. In the experiment, two commercially available CHX solutions, Eludril and Curasept were chosen for integration into microfluidic system. Controlled release devices, for a prolonged treatment have already been developed and clinically tested within polymer-based systems and with different effects [94], and mainly for the use in periodontal disease treatment. However, the use of CHX based solutions is not limited to the periodontal pocket treatment, since the local delivery of antiseptic agents to hard dental tissues and oral mucosa has a lot of indications, comprising dental plaque accumulation prevention, both bacterial and fungal infections, oral ulcers and various types of stomatitis. In addition, during several past decades, the researchers and clinicians search for a therapeutic option employing the device to be placed in the oral cavity, with the possibility of adherence to hard dental tissues, intraoral appliance or oral mucosa, with the aim of treating surgical wounds, as well as wounds that are

caused by mechanical, physical or chemical trauma, and other types of oral ulcerations [95], which is for the most part important in the therapy of children experiencing oral and dental trauma, or persons with disabilities, whose non-acceptance behaviour makes problematic to put on dressings or local medications.

The expansion of microfluidic setups for salivary diagnostics, controlled drug delivery, possibility for incorporation into intraoral appliances offers significant advantages such as minimal risk of infectivity with no emotional and physical pain together with mechanization, combination, ability for multiple and simultaneous biomarker analysis. This approach offers opportunity for rapid testing using small samples amounts and requires minimal training for final user. Even though the significant academic interest in microfluidics has been observed, together with the increased interest in salivary diagnostics and intraoral route of drug delivery, the commercial applications have not progressed at a similar rate.

Most of the materials currently used in microfluidic research and experimental setups, such as polydimethylsiloxane (PDMS) has not translated over to production well due to matters with manufacturability and scaling. In contrast to that, the lack of research data with respect to other, alternative materials that can be used for microfluidic chip fabrication, such as glass and thermoplastic polymers has been observed, and this is recognized as the major obstacle for rapid transfer of these technologies from experimental laboratories to industry and finally, to everyday clinical practice. On top of that, salivary theranostics carries its own limits, criteria and prerequisites that must be met before actual clinical application. That is the reason why the PVC chips with simple design were fabricated and tested against the commonly used antibacterial agent in the present investigation. There is evident size match between microfluidics and salivary constituents, investigated metabolites and diagnostic analytes. Active drug formulation particles sizes are also in the micrometre scale range. This overlap in dimensions will certainly facilitate application of microfluidic setups in salivary theranostics and justify the need for incorporation of these appliances within intraoral devices. The present study defined the criteria for several basic experimental parameters when it comes to behaviour of two similar, but not identical solutions within the microfluidic systems, revealing the fact that every different specimen requires different experimental parameters. This suggests that future applications require specific chip designs, controlled canals dimension, adequate pressure and sophisticated analytical and control mechanism.

The obtained data indicate that controlled drug delivery for routine use in dental clinical practice utilizing microfluidic setups require additional preclinical confirmation, calibration of all relevant parameters and the improvement of merge of existing medical and engineering technologies.

7.1.2 Viscosity and mixing properties of artificial saliva and four different mouthwashes

In this application example, the analyses of carboxymethyl cellulose-based artificial saliva (labelled as S) were made according to the prescription of the Belgrade Pharmacy Institution, with four mouthwashes: 0.1% chlorhexidine solution (labelled as C) medium concentration (2000 ppm), fluoride solution (labelled as F), zinc-hydroxyapatite (labelled as ZM) and a casein-phosphopeptide amorphous calcium phosphate (labelled as CPP-ACP).

In order to simulate flow and mixing during the experiment microfluidic chips produced in SAVA technology (described in detail in chapter 5.3.3 above) were used. The chip was a Y-channel chip without any obstacles (Figure 5.3) with the inlet channels set at a sixty-degree angle, with the width of 600 nm and the diameter of both inlets and outlet of 2 mm.

All experiments were performed using two systems – the syringe pump and pressure controller. Syringe pump set-up was prepared as follows: mechanical pressure had been exerted on the syringe with the tested solution resulting in a displacement of a commensurate volume with the applied pressure. Before the experiment started, the dimensions (diameter and volume) of the syringe were defined, while the speed was automatically regulated by adjusting the flow rate of the pump. The pressure controller works in a very similar way, with little difference – the flow of fluid is made possible by the injection of air by the compressor into the chambers containing the fluid. In this way, the fluid is displaced under equal pressure under which the air is introduced. The main difference between the two methods is the parameter we want to monitor, in the syringe pump experiments we always know the exact fluid flow through the chip, while in the experiments using pressure controller, we know the exact pressure. The value of the used pressure matches the flow rate generated with the syringe pump. In the syringe pump experiment, a flow rate of 10 μL/min was used and a pressure of 80 mbar was used on the pressure controller.

To determine the proportion of solutions mixing, an image processing algorithm in Matlab program was used [96]. The experiments were first recorded with a microscope equipped with camera employing the magnification up to 10X. Artificial saliva was stained with blue colour (Figure 4.1) for simpler examination during the process of solutions mixing. The obtained raw images were then processed as follows: for each of the two solutions, the pixel values before liquids mixing and the number of pixels of the observation field were defined. Each colour is uniquely determined by three components, red, green and blue (Figure 7.4). After mixing, the observational field

images were processed by the MATLAB algorithm to define the number of liquid pixels whose values did not change at all during the process of mixing. That was the part that remained unmixed (Figure 7.5). Subsequently that value was deducted from the total number of pixels and the quantity portion of the rest, mixed solutions was computed. Because of the thickness, the CPP-ACP paste had been assessed in experimental setups dispersed in 1:3 distilled water.

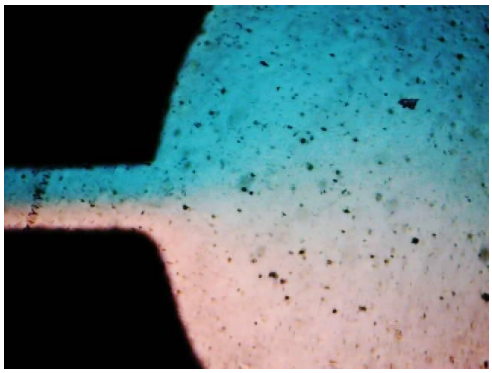

Figure 7.4 Visualisation of solutions mixing within the microfluidic chip

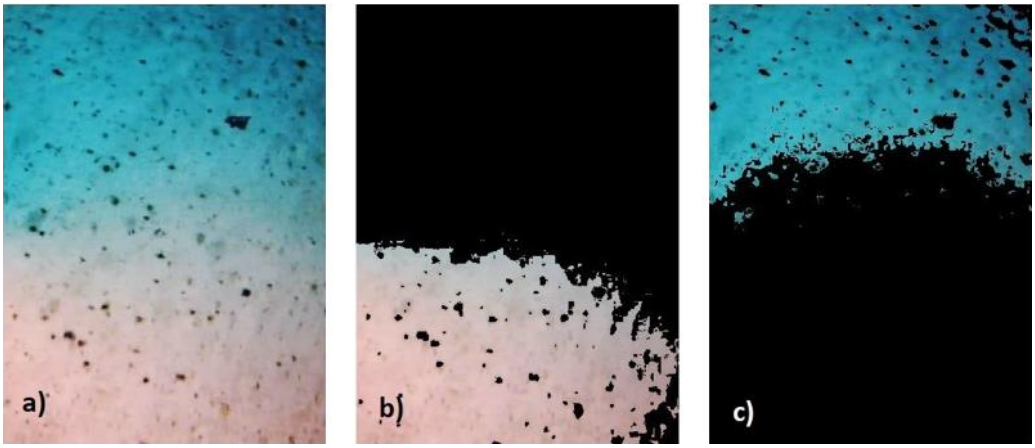

Figure 7.5 (a), (b), (c). Analysis of solution mixing using MATLAB

The RheolabQC rotary viscometer was used to measure the viscosity of the solution individually as well as the mixture with artificial saliva.

Viscosity was measured at two temperatures, room temperature (25.0 °C) and body temperature (36.6 °C). Two viscometer tools were also used, cylindrical (CC27) recommended for viscous solutions and double gap (DG42) recommended for less viscous solutions. Due to its consistency, the CPP-ACP paste could only be tested with a cylindrical tool.

Within the descriptive statistics, the data were presented in the form of mean values and standard deviation. To evaluate how far data were from normality, Shapiro Wilk

test was used. At the level of inferential statistics, due to disturbed distribution normality, the significance of the difference between the examined research groups was tested by the Wilcoxon rank-sum test. For comparing multiple treatments (temperature) and devices (viscometer head) a multiple comparison test had been use Repeated measures ANOVA, non-parametric with Durbin Conover pairwise comparison test). The Statistical Package for Social Sciences (SPSS 20.0) was used for all statistical calculations (SPSS nc., Chicago, IL, USA) together with Jamovi software (version 0.9.2.8).

The mixing results obtained in Figure 7.6 support incomplete mixing of all solutions with artificial saliva, in the range of 23.29% for zinc-hidroxyapatite solutions up to 43.65% for fluoride solutions. Also, the results indicate a higher percentage of mixing using the pressure controller than the syringe pump.

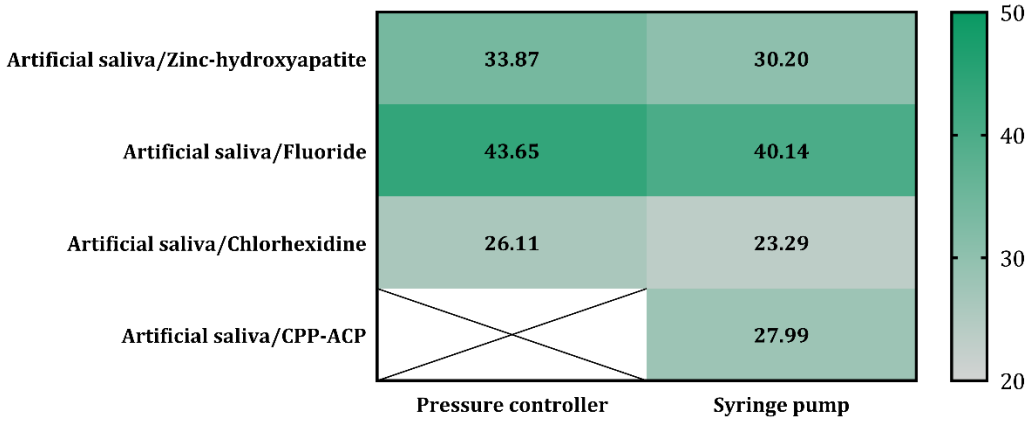

Figure 7.6 Heat map showing the proportion of liquid mixing using 2 different experimental setups

The results of viscosity measurements on the viscometer are shown inTable 7.2, Figure 7.7, Figure 7.8, and Figure 7.9.

Table 7.2 Mean values (± SD) of evaluated solutions and their mixtures with artificial saliva in two different temperatures using 2 different viscometers

	ZM				ZMS			
	CC27/25	**DG42/25**	**CC27/36**	**DG42/36**	**CC27/25**	**DG42/25**	**CC27/36**	**DG42/36**
Mean	26.161	25.925	15.124	16.244	12.222	12.510	4.3200	5.2900
SD	3.1256	0.79560	1.9859	0.72208	2.6805	1.4245	1.2601	0.29301
	F				**FS**			
	CC27/25	**DG42/25**	**CC27/36**	**DG42/36**	**CC27/25**	**DG42/25**	**CC27/36**	**DG42/36**
Mean	2.4920	1.1651	0.64194	0.70253	3.9889	2.8473	2.2710	1.7831
SD	0.65816	0.24813	0.78124	0.17319	1.1228	0.64210	0.74914	0.39287
	H				**HS**			
	CC27/25	**DG42/25**	**CC27/36**	**DG42/36**	**CC27/25**	**DG42/25**	**CC27/36**	**DG42/36**

Mean	9.0965	7.6245	4.7425	5.0298	8.5753	7.0140	4.5649	4.8253
SD	1.3934	0.92256	0.58845	0.83869	1.3723	1.0048	0.85560	0.83833
	S							
	CC27/25	**DG42/25**	**CC27/36**	**DG42/36**				
Mean	7.5726	5.8901	5.9244	3.6589				
SD	1.2221	0.41206	1.6974	0.37683				
	C				**CS**			
	CC27/25	**DG42/25**	**CC27/36**	**DG42/36**	**CC27/25**	**DG42/25**	**CC27/36**	**DG42/36**
Mean	16201		2995.3		1694.3		12926	
SD	16889		7463.2		1089.4		13004	
Shapiro-Wilk p	< .001	< .001	< .001	< .001	< .001	< .001	< .001	< .001

N = 5 specimens for all solutions, N1 = 100 measurements per solution

The obtained results indicate different viscosity of all the test solutions with each other, as well as with the artificial saliva, where the viscosity increases from fluoride solutions (2.44 mPa s), via chlorhexidine (8.64 mPa s) and zinc hydroxyapatite solution (26.16 mPa s), to CPP-ACP paste (7500.43 mPa s). The viscosity of mixtures of these solutions and artificial saliva are in all measurements within the range of viscosity of the artificial saliva and the solution individually. Also, the viscosity of all solutions as well as the mixture with artificial saliva significantly decreases at higher temperatures. The highest viscosity change at different temperatures was observed with fluoride solutions. An analysis was performed, Wilcoxon rank-sum test comparing the obtained values at two different temperatures (25.0 °C and 36.6 °C), but also at two different apparatus (CC27 and DG42) and statistically significant differences were presented in the Table 7.3.

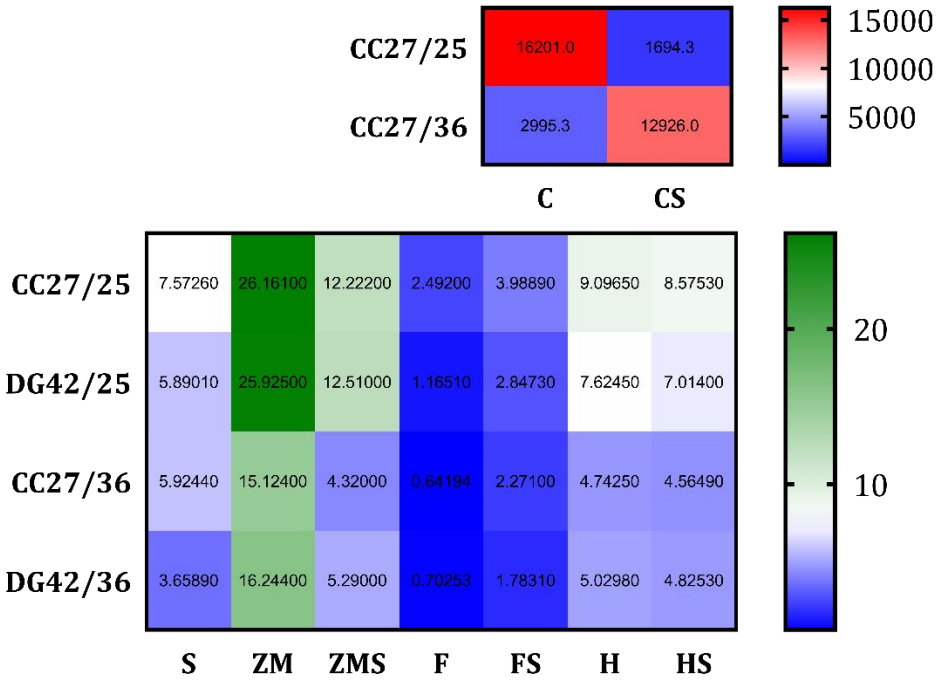

Figure 7.7 Heat map showing mean values of viscosities for evaluated solutions and their mixtures with artificial saliva in two different temperatures using 2 different viscometers

A multiple comparison test (Repeated measures ANOVA, with Durbin Conover pairwise comparison test) revealed statistically significant differences in all pairs of solutions with respect to temperature (25.0 °C and 36.6 °C) and different apparatus (CC27 and DG42) except for the ZMS solution tested with CC27 and DG42 at the temperature of 25 °C, where the difference was not statistically significant.

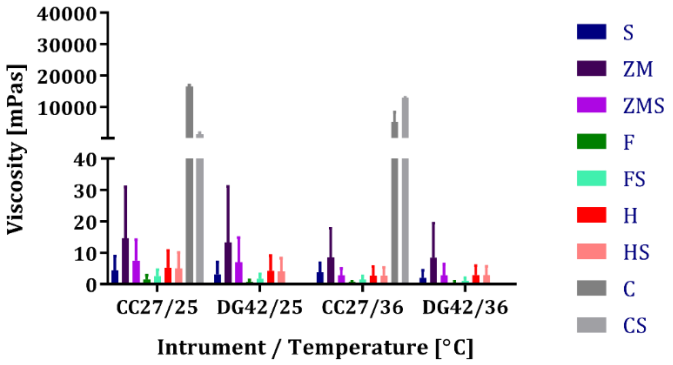

Figure 7.8 Histogram showing mean values with standard deviation of evaluated solutions and their mixtures with artificial saliva in two different temperatures using 2 different viscometers

The aim of this experimental study was to determine how the use of chlorhexidine, fluoride solutions and CPP-ACP paste affects the physical properties of artificial saliva, namely viscosity, and therefore the protective effect of artificial saliva, which depends on these properties. In our previous research, a microfluidic system based on a syringe pump only was used and the possibility of mixing human saliva obtained from 5 healthy volunteers with the help of Matlab software was analysed. In the present investigation, another microfluidic system was included, artificial saliva was used instead of human saliva and the complete set of experiments including viscosity measurements have been performed [96].

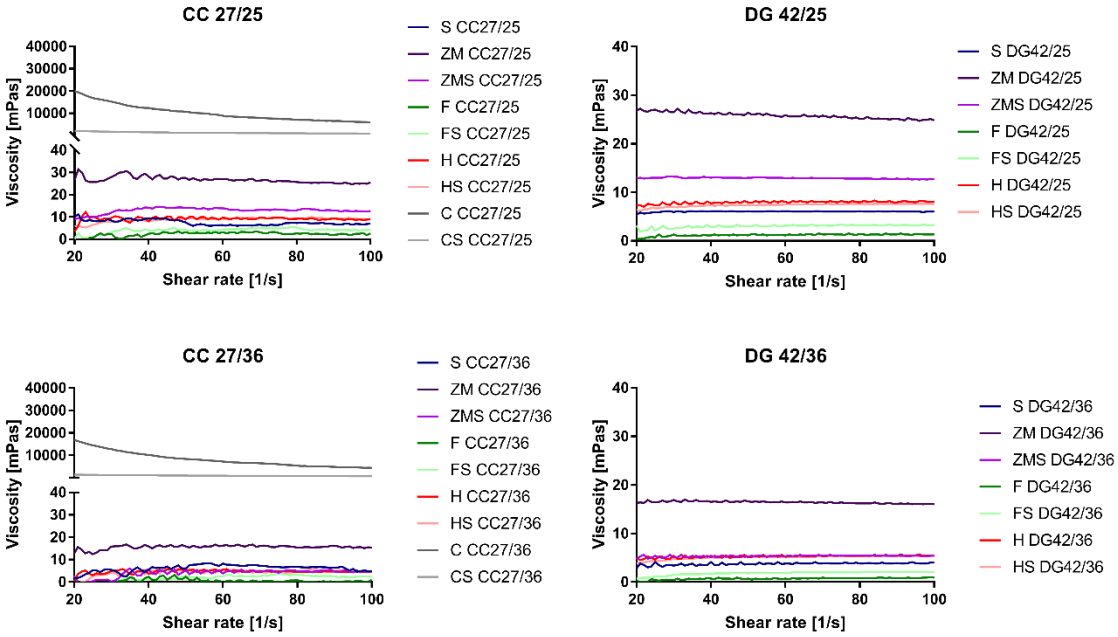

Figure 7.9 The viscosity of investigated solutions in shear rate range up to 100 s (−1) using CC27 measuring system (upper and lower left) and DG42 (upper and lower right) on 25.0 °C (up) and 36.6 °C (down)

It has been observed that it is difficult to select an in vitro model to best represent human saliva, in terms of simulating key characteristics and features, and numerous studies had been conducted investigating multiple factors including, pH, buffering capacity and surface tension. In addition, viscosity is analysed in many studies [97-101]. The present study presents our attempt to extend our knowledge and transfer the salivary diagnostic using microfluidic approach and mathematical models.

The viscosity of human saliva, both stimulated and unstimulated had been extensively analysed in the literature, and the reported values range from 1.5 mPa s over shear rate of 1–300 s^{-1}, over 3–8 mPa s at a shear rate of 90 s^{-1}, up to 100 mPa s at a shear rate of 0.02 s^{-1} [102]. Research groups used different shear rates, temperatures and types of

rheometer and often small sample sizes. This research aims to address these issues by using physiological temperature and assessing viscosity across a range of shear rates anticipated to occur during the action of mouthrinsing. The results from the present investigation obtained for artificial saliva, whose viscosity ranged from 3.6 mPa s to 7.57 mPa s are completely comparable with the viscosity of human saliva reported by Rantonen and coworkers [99].

Table 7.3 Wilcoxon rank-sum test

95% Confidence interval					
		Statistic	***P***	**Lower**	**Upper**
ZM CC27/25	ZM DG42/25	3212.00	< .001	0.40007	0.85000
ZM CC27/25	ZM CC27/36	4005.00	< .001	10.50000	11.20008
ZM CC27/25	ZMS CC27/25	4095.00	< .001	13.19999	13.84995
ZM DG42/25	ZM DG42/36	4371.00	< .001	9.45000	9.75008
ZMS CC27/25	ZMS DG42/25	1954.00	**0.581**	-0.54997	0.35000
ZMS CC27/36	ZMS DG42/36	106.00	< .001	-1.00007	-0.60002
F CC27/25	F DG42/25	2763.00	< .001	1.29993	1.54997
F CC27/25	F CC27/36	1875.50	< .001	1.70002	2.40008
F CC27/25	F CC27/36	1875.50	< .001	1.70002	2.40008
F DG42/25	F DG42/36	3079.00	< .001	0.44999	0.49997
FSCC27/25	FSCC27/36	2329.00	< .001	1.54999	1.94997
FS DG42/25	FS DG42/36	3478.50	< .001	1.00001	1.10007
H CC27/25	H CC27/36	3233.00	< .001	4.34997	4.60006
H CC27/25	H DG42/25	3581.00	< .001	1.24995	1.60004
H CC27/25	H CC27/36	3233.00	< .001	4.34997	4.60006
H DG42/25	H DG42/36	4465.00	< .001	2.59998	2.65001
HS DG42/25	HS CC27/36	3003.00	< .001	2.19999	2.54995
HS DG42/25	HS DG42/36	4186.00	< .001	2.19995	2.25000
S CC27/25	S DG42/25	4084.50	< .001	1.35003	1.90002
S CC27/25	S CC27/36	3112.50	< .001	1.09999	2.14998
S DG42/36	S CC27/36	121.50	< .001	-2.75002	-2.10003
C CC27/25	CS CC27/25	5050.00	< .001	9124.44995	12454.60004
C CC27/25	C CC27/36	5050.00	< .001	9247.04996	12282.45003
CS CC27/25	CS CC27/36	0.00	< .001	-10074.05000	-7106.99999

Viscosity is the resistance by which individual layers of fluid resist the movement of one relative to the other, that is, a type of internal friction that causes fluid to flow at a constant rate. Flow resistance is the result of several factors, including intermolecular interactions, shape and size of molecules [103]. Rheology deals with the deformation of materials exposed to stresses or forces. Newtonian viscous fluids are defined by the

property that stress is linearly related to load rate. These models adequately represent the behaviour of different materials, such as metals, air, water, and oils, for a wide variety of movements [104]. However, there is a large group of materials and biomaterials, such as saliva, that cannot be described by a simple elastic or viscous rheological model. In fact, they exhibit both viscous and elastic properties, and there are no mathematical functions to fully explain their behaviour during the demanding and complex movements to which they are exposed.

The rheological properties of saliva result from many factors and it has shown to behave as a nonNewtonian fluid whose viscosity decreases with increasing shear rate [105]. Since natural saliva is a non-Newtonian fluid, its viscosity varies with the shear rate. The viscosity of saliva at rest and when the shear rate is in the range of 0.1–1 s^{-1} is much higher than the viscosity during chewing and speech when the shear rate is about 60 and 160 s^{-1} [106]. There are recommendations in the literature that higher values of shear rate (as for chewing is 160 s^{-1}) should be tested [100]. In defining the range, the intention was to mimic real clinical situation as much as possible, following the presumption that during the action of mouth rinsing anticipated values should be substantially lower compared to chewing. The followed the reports from the literature that state that, the exact magnitude of the applied shear rates in the mouth is not known; estimates range from 0.1 or 10 to 1000 s^{-1} [99]. In addition, it has been reported that shear rates appear to be modulated by the substance texture and they changed during oral processing [107]. Also it has been pointed to the fact that probably a wide range of shear rates are involved, and different shear rates may be present simultaneously in the mouth, e.g., the bite pouched in the cheek is at a shear rate of zero [108].

Finally, in the report published by Bonda et co-workers [109] the majority research had been summarized and in the majority of the studies shear rates did not exceed 100 s^{-1}, making our findings applicable for possible data comparison.

There is no uniform information in the literature about the role of viscosity of the mouth rinses in their erosive potential. Saliva substitutes and mouthwashes enter the complex processes present in the oral cavity, forming specific connections at the mucosa–liquid and enamel–liquid interfaces. As a result, more viscous agents can affect the ion exchange rate at the enamel–liquid interface, compromising both demineralization and remineralisation processes, which should not be expected from the solutions whose main task is to promote remineralisation and decrease the extent of demineralisation. And the recent clinical reports go in line with that, suggesting that increasing the viscosity of the mouthwash solutions reduced enamel loss by erosion; however, this effect was small and only observed when the solutions were applied only

once a day. There are attempts to neutralize the erosive potential of commercially available mouthwashes with adding of various viscosity increasing substances [110].

This experiment suggests that the potential of mouthwash erosion and enamel wear requires further examination, both in vitro and in vivo, as some physicochemical factors, such as salivary flow and buffering capacity, may influence their overall impact on the dental enamel [111, 112].

In this experiment 2 microfluidic setups were used to simulate mixing of artificial saliva and different mouthwashes. Microfluidics has been developed quickly in last two decades offering countless applications in biomedical research. This so called microfluidics revolution arose due to some advantages offered by system miniaturization, the high analytical throughput, enhanced sensitivity and improved analytical performance. When it comes to salivary in vitro investigation its applicability has been definitely confirmed.

Data acquisition and analysis in salivary in vitro experiments frequently employ image processing tools such as Matlab [113, 114]. Image segmentation is state-of-art method widely used in many different branches of research today. It is efficient, quick and primarily low cost way to extract needed information. In this experiment, rate of mixed and unmixed fluids could be unequivocally determined under certain conditions. Conditions that needed to be fulfilled were that source of light around microfluidic chip and position of camera were constant and unchanged throughout whole experiment. Having this provided, it was enough to film each fluid separately, before conducting an experiment and then to film experiment itself with enough images. From images where fluids were separated, ranges of pixel values could easily be determined by taking minimum and maximum value for each of three channels of colour (red, green and blue).

The results of the research show that there is no linear, defined and predictable change in the viscosity of saliva substitutes and local antiseptic solutions, and that the degree of mixing depends on both the flow of liquid substances and the pressures to which liquids are exposed. Viscosity changes and the degree of solution mixing can significantly affect the properties of saliva, as well as the physicochemical properties of the active substances in antiseptic solutions, thereby modifying the expected preventive ones, prophylactic and therapeutic effect.

Local intraoral administration of various mouthwashes results in incomplete mixing with artificial saliva. Mixing them changes the originally measured viscosities of both saliva and the mouthwash itself. Also, at the temperature of the body, which governs that in the oral cavity, the viscosity of both saliva and artificial saliva and their mixtures

decreases significantly. These changes can have a significant impact on the effects of saliva and solution, and therefore on oral health.

7.1.3 Filtration of pollen particles

In order to show application diversity, a solution for the rapid prototyping of microfluidic elements using combination of laser micromachining and xurographic technique, without using expensive clean-room facility was presented. The complete optical, dielectric, temperature and mechanical characterization of the fabricated chip was performed. To demonstrate the applicability of the proposed technology concept, the 3D microfluidic chip for pollen filtration that combine a mixer, filtration unit, and serpentine was fabricated and tested.

The 3D multi-layered chip that comprises five layers, Figure 7.10(a), was fabricated using combination of laser micromachining and PVC lamination processes. The Layers 2-4 were realized using the Ceramtapes, while Layer 1 and Layer 5 are realized using plastic foils. The laser micromachining process has been used for the preparation of tapes and cutting of microfluidic channel, mixer, serpentine and filter. The microfluidic channels are 200 μm wide, while interconnection holes between layers and holes for the inlet and outlet are realized with diameter of 2 mm. In the next step, the Ceramtapes were stacked, and laminated using Uniaxial press Carver 3895CEB under the pressure of 2200 kg and temperature of 80 °C, for 3 min. The Whatman® 1441-150 filter paper with grade of 20 - 25 μm previously cut with laser has been embedded in the Layer 3 during stacking of the layers before lamination. To avoid leakage, the size of the filter is enlarged to 5 mm, whilst the filtration area has been realized with the radius of 2 mm. The filter is integrated into two layers in the sandwich structure. The cutting plotter was used to engrave inlets, outlet and edges in the plastic laminating films used for top and bottom layers. The top and bottom enclosure layers were assembled in the final step using the hot laminator. The layout of the fabricated 3D microfluidic chip is shown in Figure 7.10 (b).

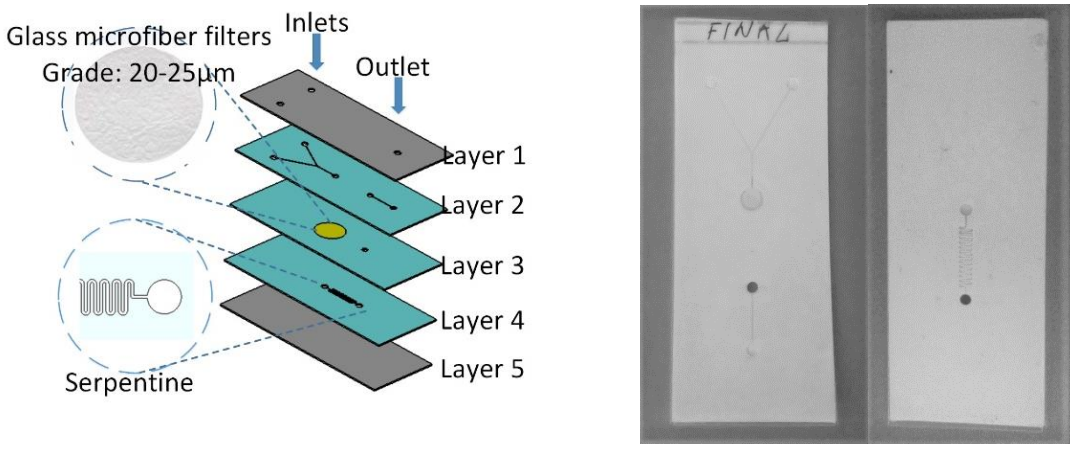

Figure 7.10 (a) Exploded view of multi-layered 3D microfluidic chip, (b) Top and bottom layer of the fabricated 3D microfluidic chip

To test functionality of the chip with filter a custom solution of distillate water and pollen particles (*typha* pollen particles) was made. As experimental set up the same set-up as for determination of the max. flow rate (Figure 6.21 (b)) is used. On two inlets water/pollen mixture was connected with 100 µl/min flow rate and output was kept in the 2.5 ml PMMA cuvette. Figure 7.11 shows three cuvettes left one is water/pollen solution, middle one is pure deionised water (for comparison) and right is filtrated liquid. There can be seen that quantity of pollen particles was significantly reduced. In detail, since *typha* pollen particles have size of 22.7 ± 2.6 µm [115] and filter has grade of 20 - 25 µm all medium and big particles were filtered, only some smaller ones passed through the filter.

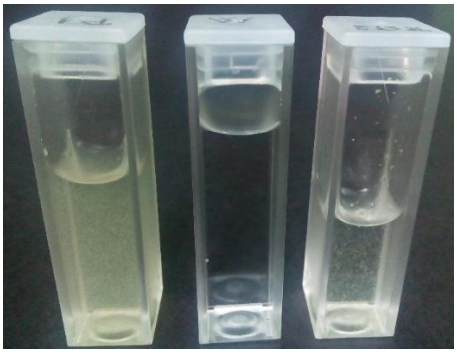

Figure 7.11 Filtration results

Chapter VIII

Conclusion

The scientific area of microfluidic is growing exponentially in the last 20 years. Although massive discoveries and improvements are done there are still countless developments and accomplishments waiting to be found and achieved. In this thesis, as main accomplishments, one novel design of a microfluidic micromixer and one brand new microfluidic chip fabrication technology – SAVA technology are developed. Moreover, several other designs are developed for the testing purpose of SAVA fabrication technology. Furthermore, simulations for three micromixers are conducted to validate design parameters and verify the future fabricated microfluidic chips. The fabrication of the microfluidic chips was done in three different fabrication technologies. The novel established SAVA fabrication technology was profoundly tested. The various microfluidic tests have been performed to examine the performance of the new design and to compare the efficiency and behaviour of different experimental set-ups as well as to confirm the competence of the SAVA technology. In addition, for the application in the biomedical area, three different application examples are presented.

The designs are developed for the testing purpose of the SAVA fabrication technology: (1) the simple channels with different widths – to determine the minimal channel width, (2) the round and square chambers to determine minimal and maximal chamber size, (3) the standard Y channel, (4) the micromixer with parallelogram barriers – to compare the new technology with others in the market, (5) the serpentine – to test the agility of the design, and (6) the novel design never seen before – to achieve precise tuning of mixing for drug delivery experiments.

The simulations for the three micromixers are conducted, (1) for the micromixer with parallelogram barriers for xurographic technique, (2) for the micromixer with parallelogram barriers for SAVA fabrication technology, and (3) for the novel micromixer design. Mixing is one of the most common actions in the microfluidic chip. This is the reason why this was tested in all three fabrication technologies. The summary of all the tests through technologies was as follows:

- PDMS – had the finest tuning but the lowest mixing range,
- PVC – had lowest mixing properties as a consequence of dimension precision limitation,
- SAVA – had average tuning but could achieve full mixing in the channel.

The microfluidic chips are fabricated in three technologies: (1) PDMS moulding, (2) xurography, and (3) SAVA technology. The fabrication parameters are intensely tested and optimised as well as documented in detail, especially for the SAVA technology, as a reference for future research in the field.

In order of characteristics assessment for SAVA fabrication technology, numerous characterisations are performed: (1) the optical transmission – to confirm that performance of this technology are comparable with PDMS and FlexDym meaning that this technology can be used with the optical detection of microfluidic chip reading, (2) the dielectric properties – to confirm that this technology can also be used with microstrip technology – as one of the non-optical representatives of obtaining the results from the microfluidic chip, (3) SEM and optical microscopy – to present the "inside view" for the easier understanding of technology behaviour, (4) mechanical characterisation – to prove that Ceramtape can be used in hybrid fabrication without serious degradation of mechanical characteristics of a microfluidic chip, and (5) temperature exposing – to estimate the range of applicable temperatures.

In order to test and prove the microfluidic characteristics of the chips fabricated for this thesis, four different microfluidic experiments were performed. The main point of the first was to detect the maximum flow rate of the chips fabricated in SAVA technology. The obtained results gave a very interesting fact that the weakest point was not in the chip but the connection to the tubing and that under the same experimental set-up and conditions the chips fabricated in SAVA technology could sustain a 3000 times higher flow rate than exactly the same chips produced in xurographic technique. Further, in three different designs conducted in three different fabrication technologies mixing efficiency was discussed to clarify possible application areas.

In the end, two applications in the dentistry area and one in biology are explained in detail all three for the chips fabricated in SAVA technology as final confirmation of this technology scientific future.

Author's publications†

M21a

[1] Wagle, S.R., Kovacevic, B., Walker, D., Ionescu, C.M., Shah, U., Stojanovic, G., **Kojic, S**., Mooranian, A., Al-Salami, H., 2020. Alginate-based drug oral targeting using bio-micro/nano encapsulation technologies. Expert Opin Drug Deliv 17, 1361–1376. https://doi.org/10.1080/17425247.2020.1789587

[2] Radović, M., Dubourg, G., **Kojić, S.,** Dohčević-Mitrović, Z., Stojadinović, B., Bokorov, M., Crnojević-Bengin, V., 2018. Laser sintering of screen-printed TiO2 nanoparticles for improvement of mechanical and electrical properties. Ceramics International 44, 10975–10983. https://doi.org/10.1016/j.ceramint.2018.03.181

M21

[3] Mooranian, A., Ionescu, C.M., Wagle, S.R., Kovacevic, B., Walker, D., Jones, M., Chester, J., Foster, T., Johnston, E., **Kojic, S.,** Stojanovic, G., Mikov, M., Al-Salami, H., 2021. Polyelectrolytes Formulated with Primary Unconjugated Bile Acid Optimised Pharmacology of Bio-Engineered Implant. Pharmaceutics 13, 1713. https://doi.org/10.3390/pharmaceutics13101713

[4] Wagle, S.R., Kovacevic, B., Walker, D., Ionescu, C.M., Jones, M., Stojanovic, G., **Kojic, S.**, Mooranian, A., Al-Salami, H., 2020. Pharmacological and Advanced Cell Respiration Effects, Enhanced by Toxic Human-Bile Nano-Pharmaceuticals of Probucol Cell-Targeting Formulations. Pharmaceutics 12, E708. https://doi.org/10.3390/pharmaceutics12080708

[5] Stefanović, S., Petrović, B., Porčić, M., Penezić, K., Pendić, J., Dimitrijević, V., Živaljević, I., Vuković, S., Jovanović, J., **Kojić, S**., Starović, A., Blagojević, T., 2019. Bone spoons for prehistoric babies: Detection of human teeth marks on the Neolithic artefacts from the site Grad-Starčevo (Serbia). PLOS ONE 14, e0225713. https://doi.org/10.1371/journal.pone.0225713

† Papers marked with * are closely related to this thesis

[6] ***Kojic, S.P.**, Stojanovic, G.M., Radonic, V., 2019. Novel Cost-Effective Microfluidic Chip Based on Hybrid Fabrication and Its Comprehensive Characterization. Sensors 19, 1719. https://doi.org/10.3390/s19071719

[7] Jovanovic, N., Petrovic, B., **Kojic, S.,** Sipovac, M., Markovic, D., Stefanovic, S., Stojanovic, G., 2019. Primary Teeth Bite Marks Analysis on Various Materials: A Possible Tool in Children Health Risk Analysis and Safety Assessment. Int J Environ Res Public Health 16, 2434. https://doi.org/10.3390/ijerph16132434

M22

[8] *Podunavac, I., Hinić, S., **Kojić, S.**, Jelenčiakova, N., Radonić, V., Petrović, B., Stojanović, G.M., 2021. Microfluidic Platform for Examination of Effect of Chewing Xylitol Gum on Salivary pH, O2, and CO2. Applied Sciences 11, 2049. https://doi.org/10.3390/app11052049

[9] *Samae, M., Ritmetee, P., Chirasatitsin, S., **Kojić, S.**, Kojić, T., Jevremov, J., Stojanović, G., Al Salami, H., 2020. Precise Manufacturing and Performance Validation of Paper-Based Passive Microfluidic Micromixers. Int. J. Precis. Eng. Manuf. 21, 499–508. https://doi.org/10.1007/s12541-019-00272-0

[10] ***Kojić, S.**, Birgermajer, S., Radonić, V., Podunavac, I., Jevremov, J., Petrović, B., Marković, E., Stojanović, G.M., 2020. Optimization of hybrid microfluidic chip fabrication methods for biomedical application. Microfluid Nanofluid 24, 66. https://doi.org/10.1007/s10404-020-02372-0

[11] Stojanović, G., Pojić, M., **Kojić, S.,** Mišan, A., Vasiljević, D., 2019. Mechanical properties of edible biofilm as a substrate for printed electronics. Appl. Phys. A 125, 576. https://doi.org/10.1007/s00339-019-2881-5

[12] Radovanovic, M., **Kojic, S.,** Vasiljevic, D., Stojanovic, G., 2018. Characterization of LC sensor structures realized by PCB and LTCC technology for determining moisture in building materials. PAC 12, 13–20. https://doi.org/10.2298/PAC1801013R

[13] Vukmirović, J., Tripković, Đ., Bajac, B., **Kojić, S.,** Stojanović, G.M., Srdić, V.V., 2015. Comparison of barium titanate thin films prepared by inkjet printing and spin coating. Processing and Application of Ceramics 9, 151–156. https://doi.org/10.2298/PAC1801013R

M23

[14] *Podunavac, I., Hinić, S., **Kojić, S.**, Jelenčiakova, N., Radonić, V., Petrović, B., Stojanović, G., 2021. Microfluidic Approach for Measurements of pH, O2, and CO2 in Saliva. Sensors and Materials 33, 1037. https://doi.org/10.18494/SAM.2021.3219

[15] *Hinic, S., Petrovic, B., **Kojic, S.**, Omerovic, N., Jevremov, J., Jelenciakova, N., Stojanovic, G., 2020. Viscosity and mixing properties of artificial saliva and four different mouthwashes. Biorheology 57, 87–100. https://doi.org/10.3233/BIR-201008

[16] Sipovac, M., Petrovic, B., **Kojic, S**., Pantelinac, J., Penezic, K., Capo, I., Stefanovic, S., 2021. Crown Formation Times of Deciduous Teeth and Age at Death in Neolithic

Newborns. Int. J. Morphol. 39, 780–784. https://doi.org/10.4067/S0717-95022021000300780

[17] Petrovic, B.B., **Kojić, S.,** Perić, T.O., Šipovac, M., Lazarević, J., Stefanović, S., Stojanović, G., 2019. Surface characterization of the raw and cooked bovine cortical metatarsal bone. Acta Bioeng Biomech 21, 13–21. https://doi.org/10.5277/ABB-01197-2018-02

[18] Markovic, D.L., Petrovic, B.B., Peric, T.O., Trisic, D., **Kojic, S.,** Kuljic, B.L., Stojanovic, G., 2019. Evaluation of Sealant Penetration in Relation to Fissure Morphology, Enamel Surface Preparation Protocol and Sealing Material. Oral Health Prev Dent 17, 349–355. https://doi.org/10.3290/j.ohpd.a42689

[19] Petrović, B., Marković, Đ., **Kojić, S.,** Perić, D., G, D., M, D., Stojanović, G., 2019. Characterization of glass ionomer cements stored in various solutions. Materiali in Tehnologije. https://doi.org/10.17222/mit.2018.159

[20] Stojanović, G.M., Lečić, N., **Kojić, S.,** Vasiljević, D., 2018. Characterization of customized ferrite cores for a compact six-phase coupled inductor. International Journal of Applied Electromagnetics and Mechanics 57, 19–27. https://doi.org/10.3233/JAE-170031

[21] *Thamphiwatana, S., Phairatana, T., Chirasatitsin, S., Samae, M., Velvé Casquillas, G., Al-Salami, H., **Kojić, S.**, Stojanovic, G.M., 2018. A microfluidic micromixer fabricated using polydimethylsiloxane-based platform for biomedical applications. Informacije MIDEM 48, 173–180.

[22] **Kojić, S.,** Ajkalo, S., Gužvica, M., Vasiljević, D.Z., Radovanović, M., Stojanović, G., 2014. A counter of number of products on the shelf - Influences on capacitance of interdigitated capacitor with application in intelligent packaging. Informacije MIDEM.

M24

[23] *Jelenčiaková, N., Petrović, B., **Kojić, S.**, Jevremov, J., Hinić, S., 2020. Application of mathematical models and microfluidics in the analysis of saliva mixing with antiseptic solutions. Balkan Journal of Dental Medicine 24, 84–90. https://doi.org/10.2478/bjdm-2020-0014

[24] Petrovic, B., Marković, E., Peric, T., **Kojic, S**., 2019. Challenges in Experimental Evaluation of Morphological, Chemo- Mechanical and Adhesive Properties of Glass-ionomer Based Dental Materials. Journal for Technology of Plasticity 44, 25–30. https://doi.org/10.24867/ATM-2019-2-005

References

[1] S. Kojić, S. Birgermajer, V. Radonić, I. Podunavac, J. Jevremov, B. Petrović, E. Marković, and G. M. Stojanović, "Optimization of hybrid microfluidic chip fabrication methods for biomedical application," *Microfluidics and Nanofluidics,* vol. 24, no. 9, pp. 66, 2020/08/03, 2020.

[2] C.-H. D. Tsai, and X.-Y. Lin, "Experimental Study on Microfluidic Mixing with Different Zigzag Angles," *Micromachines,* vol. 10, no. 9, pp. 583, 2019.

[3] E. K. Sackmann, A. L. Fulton, and D. J. Beebe, "The present and future role of microfluidics in biomedical research," *Nature,* vol. 507, pp. 181, 03/12/online, 2014.

[4] B. K. Gale, A. R. Jafek, C. J. Lambert, B. L. Goenner, H. Moghimifam, U. C. Nze, and S. K. Kamarapu, "A Review of Current Methods in Microfluidic Device Fabrication and Future Commercialization Prospects," *Inventions,* vol. 3, no. 3, pp. 60, 2018.

[5] H. Wu, J. Zhu, Y. Huang, D. Wu, and J. Sun, "Microfluidic-Based Single-Cell Study: Current Status and Future Perspective," *Molecules,* vol. 23, no. 9, Sep 13, 2018.

[6] B. Nasseri, N. Soleimani, N. Rabiee, A. Kalbasi, M. Karimi, and M. R. Hamblin, "Point-of-care microfluidic devices for pathogen detection," *Biosens Bioelectron,* vol. 117, pp. 112-128, Oct 15, 2018.

[7] A. Kiss, and A. Gaspar, "Fabrication of a Microfluidic Flame Atomic Emission Spectrometer: a Flame-on-a-Chip," *Anal Chem,* vol. 90, no. 10, pp. 5995-6000, May 15, 2018.

[8] A. P. Emmanuel Roy, Bacem Zribi, Marie-Charlotte Horny, François Damien Delapierre, Andrea Cattoni, Jean Gamby and Anne-Marie Haghiri-Gosnet, "Overview of Materials for Microfluidic Applications, Advances in Microfluidics

- New Applications in Biology, Energy, and Materials Sciences," X.-Y. Yu, ed., IntechOpen, 2016.

[9] E. Finehout, and W.-C. Tian, *Microfluidics for Biological Applications*, 2009.

[10] K. Ren, J. Zhou, and H. Wu, "Materials for microfluidic chip fabrication," *Acc Chem Res,* vol. 46, no. 11, pp. 2396-406, Nov 19, 2013.

[11] X. Hou, Y. S. Zhang, G. T.-d. Santiago, M. M. Alvarez, J. Ribas, S. J. Jonas, P. S. Weiss, A. M. Andrews, J. Aizenberg, and A. Khademhosseini, "Interplay between materials and microfluidics," *Nature Reviews Materials,* vol. 2, pp. 17016, 04/20/online, 2017.

[12] G. M. Whitesides, "The origins and the future of microfluidics," *Nature,* vol. 442, pp. 368, 07/26/online, 2006.

[13] S. P. Kojic, G. M. Stojanovic, and V. Radonic, "Novel Cost-Effective Microfluidic Chip Based on Hybrid Fabrication and Its Comprehensive Characterization," *Sensors,* vol. 19, no. 7, pp. 1719, 2019.

[14] C. D. Ahrberg, A. Manz, and B. G. Chung, "Polymerase chain reaction in microfluidic devices," *Lab on a Chip,* vol. 16, no. 20, pp. 3866-3884, 2016.

[15] Z. Li, Y. Li, S. Sekine, H. Xi, A. Amano, D. Zhang, and Y. Yamaguchi, "Design and fabrication of portable continuous flow PCR microfluidic chip for DNA replication," *Biomedical Microdevices,* vol. 22, no. 1, pp. 5, 2019/12/10, 2019.

[16] S. H. Lee, J. Song, B. Cho, S. Hong, O. Hoxha, T. Kang, D. Kim, and L. P. Lee, "Bubble-free rapid microfluidic PCR," *Biosensors and Bioelectronics,* vol. 126, pp. 725-733, 2019/02/01/, 2019.

[17] A. Shahid, S. Liaghat, and P. Ravi Selvaganapathy, "28 - Microfluidic devices for DNA amplification," *Bioelectronics and Medical Devices*, K. Pal, H.-B. Kraatz, A. Khasnobish, S. Bag, I. Banerjee and U. Kuruganti, eds., pp. 721-763: Woodhead Publishing, 2019.

[18] K. T. L. Trinh, and N. Y. Lee, "A portable microreactor with minimal accessories for polymerase chain reaction: application to the determination of foodborne pathogens," *Microchimica Acta,* vol. 184, no. 11, pp. 4225-4233, 2017/11/01, 2017.

[19] N. Y. Lee, "A review on microscale polymerase chain reaction based methods in molecular diagnosis, and future prospects for the fabrication of fully integrated portable biomedical devices," *Mikrochim Acta,* vol. 185, no. 6, pp. 285, May 8, 2018.

[20] G. Dutta, J. Rainbow, U. Zupancic, S. Papamatthaiou, P. Estrela, and D. Moschou, "Microfluidic Devices for Label-Free DNA Detection," *Chemosensors,* vol. 6, no. 4, pp. 43, 2018.

[21] B. Bruijns, A. van Asten, R. Tiggelaar, and H. Gardeniers, "Microfluidic Devices for Forensic DNA Analysis: A Review," *Biosensors (Basel),* vol. 6, no. 3, Aug 5, 2016.

[22] A. Rakszewska, J. Tel, V. Chokkalingam, and W. T. S. Huck, "One drop at a time: toward droplet microfluidics as a versatile tool for single-cell analysis," *Npg Asia Materials,* vol. 6, pp. e133, 10/03/online, 2014.

[23] K. Malecha, E. Remiszewska, and D. G. Pijanowska, "Technology and application of the LTCC-based microfluidic module for urea determination," *Microelectronics International,* vol. 32, no. 3, pp. 126-132, 2015.

[24] E. Yakhshi-Tafti, H. J. Cho, and R. Kumar, "Diffusive mixing through velocity profile variation in microchannels," *Experiments in Fluids,* vol. 50, pp. 535-545, 2011.

[25] C. Y. Lee, C. L. Chang, Y. N. Wang, and L. M. Fu, "Microfluidic mixing: a review," *Int J Mol Sci,* vol. 12, no. 5, pp. 3263-87, 2011.

[26] K. K. Shuichi Shoji, *Microfluidics: Technologies and Applications*, 2011.

[27] W. Li, L. Zhang, X. Ge, B. Xu, W. Zhang, L. Qu, C. H. Choi, J. Xu, A. Zhang, H. Lee, and D. A. Weitz, "Microfluidic fabrication of microparticles for biomedical applications," *Chem Soc Rev,* vol. 47, no. 15, pp. 5646-5683, Jul 30, 2018.

[28] Y.-N. Wang, and L.-M. Fu, "Micropumps and biomedical applications – A review," *Microelectronic Engineering,* vol. 195, pp. 121-138, 2018/08/05/, 2018.

[29] K. W. Pulsipher, D. A. Hammer, D. Lee, and C. M. Sehgal, "Engineering Theranostic Microbubbles Using Microfluidics for Ultrasound Imaging and Therapy: A Review," *Ultrasound in medicine & biology,* vol. 44, no. 12, pp. 2441-2460, 2018.

[30] M. U. Ahmed, I. Saaem, P. C. Wu, and A. S. Brown, "Personalized diagnostics and biosensors: a review of the biology and technology needed for personalized medicine," *Critical Reviews in Biotechnology,* vol. 34, no. 2, pp. 180-196, 2014/06/01, 2014.

[31] D. J. Beebe, G. A. Mensing, and G. M. Walker, "Physics and applications of microfluidics in biology," *Annu Rev Biomed Eng,* vol. 4, pp. 261-86, 2002.

[32] K. S. Elvira, X. C. i Solvas, R. C. R. Wootton, and A. J. deMello, "The past, present and potential for microfluidic reactor technology in chemical synthesis," *Nature Chemistry,* vol. 5, pp. 905, 10/13/online, 2013.

[33] H. A. Stone, A. D. Stroock, and A. Ajdari, "Engineering Flows in Small Devices: Microfluidics Toward a Lab-on-a-Chip," *Annual Review of Fluid Mechanics,* vol. 36, no. 1, pp. 381-411, 2004/01/21, 2004.

[34] J. C. Jokerst, J. M. Emory, and C. S. Henry, "Advances in microfluidics for environmental analysis," *Analyst,* vol. 137, no. 1, pp. 24-34, 2012.

[35] Y.-C. Tan, J. S. Fisher, A. I. Lee, V. Cristini, and A. P. Lee, "Design of microfluidic channel geometries for the control of droplet volume, chemical concentration, and sorting," *Lab on a Chip,* vol. 4, no. 4, pp. 292-298, 2004.

[36] J. Zhou, P. V. Giridhar, S. Kasper, and I. Papautsky, "Modulation of aspect ratio for complete separation in an inertial microfluidic channel," *Lab on a Chip,* vol. 13, no. 10, pp. 1919, 2013.

[37] S. G. Kandlikar, and G. Library, *Heat transfer and fluid flow in minichannels and microchannels*: Amsterdam, Netherlands ; Boston : Elsevier %@ 978-0-08-044527-4 %U http://archive.org/details/heattransferflui00kand, 2006.

[38] S. Student, M. Milewska, Z. Ostrowski, K. Gut, and I. Wandzik, "Microchamber microfluidics combined with thermogellable glycomicrogels - Platform for single cells study in an artificial cellular microenvironment," *Materials Science & Engineering. C, Materials for Biological Applications,* vol. 119, pp. 111647, 2021.

[39] M. J. Uddin, N. H. Bhuiyan, and J. S. Shim, "Fully integrated rapid microfluidic device translated from conventional 96-well ELISA kit," *Scientific Reports,* vol. 11, no. 1, pp. 1986 %* 2021 The Author(s) %U https://www.nature.com/articles/s41598-021-81433-y, 2021.

[40] K. Malecha, L. J. Golonka, J. Bałdyga, M. Jasińska, and P. Sobieszuk, "Serpentine microfluidic mixer made in LTCC," *Sensors and Actuators B: Chemical,* vol. 143, no. 1, pp. 400-413, 2009/12/04/, 2009.

[41] "Micro & Nano Technologies Series," *Micromixers (Second Edition)*, N.-T. Nguyen, ed., p. ii, Oxford: William Andrew Publishing, 2012.

[42] P. Zhu, and L. Wang, "Passive and active droplet generation with microfluidics: a review," *Lab on a Chip,* vol. 17, no. 1, pp. 34-75, 2017.

[43] J. Noh, H. C. Kim, and T. D. Chung, "Biosensors in Microfluidic Chips," *Microfluidics: Technologies and Applications*, B. Lin, ed., pp. 117-152, Berlin, Heidelberg: Springer Berlin Heidelberg, 2011.

[44] B. Kuswandi, Nuriman, J. Huskens, and W. Verboom, "Optical sensing systems for microfluidic devices: A review," *Analytica Chimica Acta,* vol. 601, no. 2, pp. 141-155, 2007/10/10/, 2007.

[45] C. Roh, J. Lee, and C. Kang, "The Deformation of Polydimethylsiloxane (PDMS) Microfluidic Channels Filled with Embedded Circular Obstacles under Certain Circumstances," *Molecules,* vol. 21, no. 6, pp. 798, 2016.

[46] D. Huh, B. D. Matthews, A. Mammoto, M. Montoya-Zavala, H. Y. Hsin, and D. E. Ingber, "Reconstituting organ-level lung functions on a chip," *Science,* vol. 328, no. 5986, pp. 1662-8, Jun 25, 2010.

[47] C. D. Chin, V. Linder, and S. K. Sia, "Commercialization of microfluidic point-of-care diagnostic devices," *Lab Chip,* vol. 12, no. 12, pp. 2118-34, Jun 21, 2012.

[48] W. Xi, F. Kong, J. C. Yeo, L. Yu, S. Sonam, M. Dao, X. Gong, and C. T. Lim, "Soft tubular microfluidics for 2D and 3D applications," *Proc Natl Acad Sci U S A,* vol. 114, no. 40, pp. 10590-10595, Oct 3, 2017.

[49] M. D. Ville, P. Coquet, P. Brunet, and R. Boukherroub, "Simple and low-cost fabrication of PDMS microfluidic round channels by surface-wetting parameters optimization."

[50] M. Villegas, Z. Cetinic, A. Shakeri, and T. F. Didar, "Fabricating smooth PDMS microfluidic channels from low-resolution 3D printed molds using an omniphobic lubricant-infused coating," *Anal Chim Acta,* vol. 1000, pp. 248-255, Feb 13, 2018.

[51] S. M. Shameli, C. Elbuken, J. Ou, C. L. Ren, and J. Pawliszyn, "Fully integrated PDMS/SU-8/quartz microfluidic chip with a novel macroporous poly dimethylsiloxane (PDMS) membrane for isoelectric focusing of proteins using whole-channel imaging detection," *Electrophoresis,* vol. 32, no. 3-4, pp. 333-9, Feb, 2011.

[52] E. Roy, J.-C. Galas, and T. Veres, "Thermoplastic elastomers for microfluidics: Towards a high-throughput fabrication method of multilayered microfluidic devices," *Lab on a Chip,* vol. 11, no. 18, pp. 3193-3196, 2011.

[53] J. N. Schianti, N. P. N. Cerize, A. M. Oliveira, S. Derenzo, and M. R. Góngora-Rubio, "3-D LTCC microfluidic device as a tool for studying nanoprecipitation," *Journal of Physics: Conference Series,* vol. 421, no. 1, pp. 012012, 2013.

[54] P. Słobodzian, J. Macioszczyk, K. Malecha, and L. Golonka, "A LTCC microwave-microfluidic reactor." pp. 1-4.

[55] G. Fercher, W. Smetana, M. J. Vellekoop, and W. Neustadt, "Contactless Conductivity Detection in Ceramic Technology for On-Chip Electrophoresis."

[56] N. Jankovic, and V. Radonic, "A Microwave Microfluidic Sensor Based on a Dual-Mode Resonator for Dual-Sensing Applications," *Sensors (Basel, Switzerland),* vol. 17, no. 12, pp. 2713, 11/24

[57] R.-C. Ciobanu, C. Schreiner, V. Drug, T. Schreiner, and D. Antal, "Sensors in LTCC-technology with embedded microfluidic features, for medical applications," *2015 IEEE International Symposium on Medical Measurements and Applications (MeMeA) Proceedings*, pp. 407-410, 2015.

[58] K. Malecha, "The utilization of LTCC-PDMS bonding technology for microfluidic system applications – a simple fluorescent sensor," *Microelectronics International,* vol. 33, no. 3, pp. 141-148, 2016.

[59] M. Karol, G. Irena, and J. G. Leszek, "A PDMS/LTCC bonding technique for microfluidic application," *Journal of Micromechanics and Microengineering,* vol. 19, no. 10, pp. 105016, 2009.

[60] J. Luo, T. Dziubla, and R. Eitel, "A low temperature co-fired ceramic based microfluidic Clark-type oxygen sensor for real-time oxygen sensing," *Sensors and Actuators B: Chemical,* vol. 240, no. C, pp. 392-397, 2017.

[61] A. Vasudev, A. Kaushik, K. Jones, and S. Bhansali, "Prospects of low temperature co-fired ceramic (LTCC) based microfluidic systems for point-of-care biosensing and environmental sensing," *Microfluidics and Nanofluidics,* vol. 14, no. 3-4, pp. 683-702, 2013.

[62] R. D. Sochol, E. Sweet, C. C. Glick, S.-Y. Wu, C. Yang, M. Restaino, and L. Lin, "3D printed microfluidics and microelectronics," *Microelectronic Engineering,* vol. 189, pp. 52-68, 2018/04/05/, 2018.

[63] M. Alizadehgiashi, A. Gevorkian, M. Tebbe, M. Seo, E. Prince, and E. Kumacheva, "3D-Printed Microfluidic Devices for Materials Science," *Advanced Materials Technologies,* vol. 3, no. 7, pp. 1800068, 2018.

[64] N. P. Macdonald, J. M. Cabot, P. Smejkal, R. M. Guijt, B. Paull, and M. C. Breadmore, "Comparing Microfluidic Performance of Three-Dimensional (3D) Printing Platforms," *Analytical Chemistry,* vol. 89, no. 7, pp. 3858-3866, 2017/04/04, 2017.

[65] J. F. Rusling, "Developing Microfluidic Sensing Devices Using 3D Printing," *ACS Sensors,* vol. 3, no. 3, pp. 522-526, 2018/03/23, 2018.

[66] V. Radonic, S. Birgermajer, and G. Kitic, "Microfluidic EBG Sensor Based on Phase-Shift Method Realized Using 3D Printing Technology," *Sensors (Basel),* vol. 17, no. 4, Apr 18, 2017.

[67] Q. Ji, J. M. Zhang, Y. Liu, X. Li, P. Lv, D. Jin, and H. Duan, "A Modular Microfluidic Device via Multimaterial 3D Printing for Emulsion Generation," *Sci Rep,* vol. 8, no. 1, pp. 4791, Mar 19, 2018.

[68] Y. Hwang, D. Seo, M. Roy, E. Han, R. N. Candler, and S. Seo, "Capillary Flow in PDMS Cylindrical Microfluidic Channel Using 3-D Printed Mold," *Journal of Microelectromechanical Systems,* vol. 25, no. 2, pp. 238-240, 2016.

[69] D. Hur, M. G. Say, S. E. Diltemiz, F. Duman, A. Ersöz, and R. Say, "3D Micropatterned All-Flexible Microfluidic Platform for Microwave-Assisted Flow Organic Synthesis," *ChemPlusChem,* vol. 83, no. 1, pp. 42-46, 2018.

[70] Y. Hwang, O. H. Paydar, and R. N. Candler, "3D printed molds for non-planar PDMS microfluidic channels," *Sensors and Actuators A: Physical,* vol. 226, pp. 137-142, 2015/05/01/, 2015.

[71] C. Lim, K. Koh, Y. Ren, J. Chin, Y. Shi, and Y. Yan, "Analysis of Liquid–Liquid Droplets Fission and Encapsulation in Single/Two Layer Microfluidic Devices Fabricated by Xurographic Method," *Micromachines,* vol. 8, no. 2, pp. 49, 2017.

[72] D. A. Bartholomeusz, R. W. Boutte, and J. D. Andrade, "Xurography: rapid prototyping of microstructures using a cutting plotter," *Journal of Microelectromechanical Systems,* vol. 14, no. 6, pp. 1364-1374, 2005.

[73] S. Kojic, D. Milicevic, J. Lazarevic, M. Drljaca, and G. Stojanovic, "Design and Testing of Microfluidic Micromixer Fabricated Using Xurographic Technique."

[74] J. Lachaux, C. Alcaine, B. Gómez-Escoda, C. M. Perrault, D. O. Duplan, P.-Y. J. Wu, I. Ochoa, L. Fernandez, O. Mercier, D. Coudreuse, and E. Roy, "Thermoplastic elastomer with advanced hydrophilization and bonding performances for rapid (30 s) and easy molding of microfluidic devices," *Lab on a Chip,* vol. 17, no. 15, pp. 2581-2594, 2017.

[75] A. Bsoul, S. Pan, E. Cretu, B. Stoeber, and K. Walus, "Design, microfabrication, and characterization of a moulded PDMS/SU-8 inkjet dispenser for a Lab-on-a-Printer platform technology with disposable microfluidic chip," *Lab on a Chip,* vol. 16, no. 17, pp. 3351-3361, 2016.

[76] F. Liu, L. Jiang, H. M. Tan, A. Yadav, P. Biswas, J. R. van der Maarel, C. A. Nijhuis, and J. A. van Kan, "Separation of superparamagnetic particles through ratcheted Brownian motion and periodically switching magnetic fields," *Biomicrofluidics,* vol. 10, no. 6, pp. 064105, Nov, 2016.

[77] N.-E. Oyunbaatar, D.-H. Lee, S. Patil, E.-S. Kim, and D.-W. Lee, "Biomechanical Characterization of Cardiomyocyte Using PDMS Pillar with Microgrooves," *Sensors,* vol. 16, no. 8, pp. 1258, 2016.

[78] S. Y. Leigh, A. Tattu, J. S. B. Mitchell, and E. Entcheva, "M3: Microscope-based maskless micropatterning with dry film photoresist," *Biomedical Microdevices,* vol. 13, no. 2, pp. 375-381, 2011/04/01, 2011.

[79] R. M. Guijt, and M. C. Breadmore, "Maskless photolithography using UV LEDs," *Lab on a Chip,* vol. 8, no. 8, pp. 1402-1404, 2008.

[80] BlackHole Lab. "Mold fabrication —Soft lithography," https://www.blackholelab-soft-lithography.com/soft-lithography-for-mold-fabrication.

[81] K. Metwally, L. Robert, R. Salut, and C. Khan-Malek, "SU-8-based rapid tooling for thermal roll embossing," *Microsystem Technologies,* vol. 18, no. 11, pp. 1863-1869, 2012/11/01, 2012.

[82] D. W. Johnsona, J. Goettertb, V. Singhb, and D. Yemaneb, "SUEX Dry Film Resist@ A new Material for High Aspect Ratio Lithography."

[83] S. C. Baskin Engineering University of California. "Nano- and Microscale Fabrication and Characterization, Lithography Process Flow," https://cleanroom.soe.ucsc.edu/lithography.

[84] J. J. Anđela Stojanović, Bojan Petrović, Sanja Kojić, Jovana Lazarević and Goran Stojanović, "Analysis of PVC microfluidic system for antibacterial solutions delivery in dentistry."

[85] S. Thamphiwatana, T. Phairatana, S. Chirasatitsin, M. Samae, G. V. Casquillas, H. Al-Salami, S. Kojić, and G. M. Stojanović, "A microfluidic micromixer fabricated using polydimethylsiloxane-based platform for biomedical applications," *Informacije MIDEM,* vol. 48, no. 3, pp. 173-179, 2018.

[86] C. Multiphysics®. "Microfluidics User's Guide."

[87] A. Duša, I. Podunavac, S. Kojić, and V. Radonić, "Design and Simulation of Microfluidic Micro-Mixer with Parallelogram Barriers."

[88] A. M. Nicolson, and G. F. Ross, "Measurement of the Intrinsic Properties of Materials by Time-Domain Techniques."

[89] J. Baker-Jarvis, Electronics, E. E. L. E. Division, R. G. Geyer, C. A. Grosvenor, C. L. Holloway, M. D. Janezic, R. T. Johk, P. Kabos, and U. S. N. B. o. Standards, *Measuring the Permittivity and Permeability of Lossy Materials: Solids, Liquids, Metals, Building Materials, and Negative-index Materials*: U.S. Department of Commerce, Technology Administration, National Institute of Standards and Technology, 2005.

[90] M. Franz, I. Atassi, A. Maric, B. Balluch, M. Weilguni, W. Smetana, C. P. Kluge, and G. Radosavljevic, "Material characteristics of the LTCC base material CeramTape GC." pp. 276-281.

[91] S. Thamphiwatana, T. Phairatana, S. Chirasatitsin, M. Samae, G. V. Casquillas, H. Al-Salami, S. Kojić, and G. M. Stojanović, "A microfluidic micromixer fabricated using polydimethylsiloxane-based platform for biomedical applications," vol. 48, no. 3, pp. 7, 2018, 2018.

[92] I. P. Jovana Jevremov, Jovana Lazarević, Sanja Kojić, Vasa Radonić, Goran Stojanović, "Performances of Microfluidic Mixing Regulated using Active Pressure Controller."

[93] C. S. Kosack, A.-L. Page, and P. R. Klatser, "A guide to aid the selection of diagnostic tests," *Bulletin of the World Health Organization,* vol. 95, no. 9, pp. 639-645, 2017/09/01/, 2017.

[94] T. Velten, H. Schuck, T. Knoll, O. Scholz, A. Schumacher, T. Göttsche, A. Wolff, B. Z. Beiski, and I. Consortium, "Intelligent intraoral drug delivery microsystem," *Proceedings of the Institution of Mechanical Engineers, Part C: Journal of Mechanical Engineering Science,* vol. 220, no. 11, pp. 1609-1617, 2006/11/01/, 2006.

[95] M. d. S. Silva, N. L. Neto, S. A. da Costa, S. M. da Costa, T. M. Oliveira, R. C. d. Oliveira, and M. A. A. M. Machado, "Biophysical and biological characterization of intraoral multilayer membranes as potential carriers: A new drug delivery system for dentistry," *Materials Science and Engineering: C,* vol. 71, pp. 498-503, 2017/02/01/, 2017.

[96] N. Jelenčiaková, B. Petrović, S. Kojić, J. Jevremov, and S. Hinić, "Application of mathematical models and microfluidics in the analysis of saliva mixing with antiseptic solutions," *Balkan Journal of Dental Medicine,* vol. 24, no. 2, pp. 84-90, 2020, 2020.

[97] A. Aykut-Yetkiner, A. Wiegand, A. Bollhalder, K. Becker, and T. Attin, "Effect of Acidic Solution Viscosity on Enamel Erosion," *Journal of Dental Research,* vol. 92, no. 3, pp. 289-294, 2013.

[98] B. Yuan, C. Ritzoulis, and J. Chen, "Extensional and shear rheology of okra hydrocolloid–saliva mixtures," *Food Research International,* vol. 106, pp. 204-212, 2018.

[99] P. J. F. Rantonen, and J. H. Meurman, "Viscosity of whole saliva," *Acta Odontologica Scandinavica,* vol. 56, no. 4, pp. 210-214, 1998/01/01, 1998.

[100] D. Briedis, M. F. Moutrie, and R. T. Balmer, "A study of the shear viscosity of human whole saliva," *Rheologica Acta,* vol. 19, no. 3, pp. 365-374, 1980/05/01, 1980.

[101] N. L. Stanley, and L. J. Taylor, "Rheological basis of oral characteristics of fluid and semi-solid foods: A review," *Acta Psychologica,* vol. 84, no. 1, pp. 79-92, 1993/10/01/, 1993.

[102] S. Gittings, N. Turnbull, B. Henry, C. J. Roberts, and P. Gershkovich, "Characterisation of human saliva as a platform for oral dissolution medium development," *European Journal of Pharmaceutics and Biopharmaceutics,* vol. 91, pp. 16-24, 2015.

[103] D. S. Viswanath, T. K. Ghosh, D. H. L. Prasad, N. V. K. Dutt, and K. Y. Rani, *Viscosity of Liquids: Theory, Estimation, Experiment, and Data*: Springer Netherlands, 2007.

[104] W. H. Schwarz, "The Rheology of Saliva," *Journal of Dental Research,* vol. 66, no. 1_suppl, pp. 660-666, 1987/02/01, 1987.

[105] J. Mystkowska, M. Jałbrzykowski, and J. R. Dąbrowski, "Tribological Properties of Selected Self-Made Solutions of Synthetic Saliva," *Solid State Phenomena,* vol. 199, pp. 567-572, 2013.

[106] J. R. Stokes, and G. A. Davies, "Viscoelasticity of human whole saliva collected after acid and mechanical stimulation," *Biorheology,* vol. 44, pp. 141-160, 2007.

[107] A. M. Janssen, M. E. J. Terpstra, R. A. De Wijk, and J. F. Prinz, "Relations between rheological properties, saliva-induced structure breakdown and sensory texture attributes of custards," *Journal of Texture Studies,* vol. 38, no. 1, pp. 42-69, 2007.

[108] A. N. Cutler, E. R. Morris, and L. J. Taylor, "Oral perception of viscosity in fluid foods and model systems," *Journal of Texture Studies,* vol. 14, no. 4, pp. 377-395, 1983.

[109] A. Foglio-Bonda, F. Pattarino, and P. Foglio-Bonda, "Kinematic viscosity of unstimulated whole saliva in healthy young adults," *European review for medical and pharmacological sciences,* vol. 18 20, pp. 2988-94, 2014.

[110] L. O. Sakae, S. J. C. Bezerra, S. H. João-Souza, A. B. Borges, I. V. Aoki, A. C. C. Aranha, and T. Scaramucci, "An in vitro study on the influence of viscosity and frequency of application of fluoride/tin solutions on the progression of erosion of bovine enamel," *Archives of Oral Biology,* vol. 89, pp. 26-30, 2018/05/01/, 2018.

[111] W. A. van der Reijden, E. C. I. Veerman, and A. V. Nieuw Amerongen, "Rheological properties of commercially available polysaccharides with potential use in saliva substitutes," *Biorheology,* vol. 31, pp. 631-642, 1994.

[112] B. M. de Souza, L. R. P. Santi, S. H. João-Souza, T. S. Carvalho, and A. C. Magalhães, "Effect of titanium tetrafluoride/sodium fluoride solutions containing chitosan at different viscosities on the protection of enamel erosion in vitro," *Archives of Oral Biology,* vol. 120, pp. 104921, 2020/12/01/, 2020.

[113] A. E. Herr, A. V. Hatch, D. J. Throckmorton, H. M. Tran, J. S. Brennan, W. V. Giannobile, and A. K. Singh, "Microfluidic immunoassays as rapid saliva-based clinical diagnostics," *Proceedings of the National Academy of Sciences,* vol. 104, no. 13, pp. 5268, 2007.

[114] A. Zlotogorski-Hurvitz, B. Z. Dekel, D. Malonek, R. Yahalom, and M. Vered, "FTIR-based spectrum of salivary exosomes coupled with computational-aided discriminating analysis in the diagnosis of oral cancer," *Journal of Cancer Research and Clinical Oncology,* vol. 145, no. 3, pp. 685-694, 2019/03/01, 2019.

[115] S. A. Finkelstein, "Identifying pollen grains of Typha latifolia, Typha angustifolia, and Typha ×glauca," *Canadian Journal of Botany,* vol. 81, no. 9, pp. 985-990, 2003/09/01, 2003.

План третмана података

Назив пројекта/истраживања
Реализација и тестирање микрофлуидних чипова за примене у биомедицини
Назив институције/институција у оквиру којих се спроводи истраживање
Универзитет у Новом Саду, Факултет техничких наука, Департман за енергетику, електронику и телекомуникације, Катедра за електронику
Назив програма у оквиру ког се реализује истраживање
Докторске академнске студије
1. Опис података

1.1 Врста студије

Укратко описати тип студије у оквиру које се подаци прикупљају

Развој нове технологије фабрикације микрофлуидних чипова и њена карактеризација – механичка, оптичка, температурна, и функционална. Контрола квалитета израде пеоизведених чипова.

1.2 Врсте података

а) квантитативни

б) квалитативни

1.3. Начин прикупљања података

а) анкете, упитници, тестови

б) клиничке процене, медицински записи, електронски здравствени записи

в) генотипови: навести врсту _____

г) административни подаци: навести врсту _____

д) узорци ткива: навести врсту_____

ђ) снимци, фотографије: фотографије експерименатата и микроскопских испитивања

е) текст, навести врсту _____

ж) мапа, навести врсту _____

з) остало: подаци са инструкемата за фабрикацију и карактеризацију

1.3 Формат података, употребљене скале, количина података

Формат података је стандардни формат сваког коришћеног инструмента, количина